สภาพหดตัวและสมบัติเชิงทางความร้อนของฟิล์มเป่าพอลิเอทิลีนความหนาแน่นต่ำ/ยางธรรมชาติ

นางสาวสุภัค มหาพราหมณ์

วิทยานิพนธ์นี้เป็นส่วนหนึ่งของการศึกษาตามหลักสูตรปริญญาวิทยาศาสตรมหาบัณฑิต
สาขาวิชาปิโตรเคมีและวิทยาศาสตร์พอลิเมอร์
คณะวิทยาศาสตร์ จุฬาลงกรณ์มหาวิทยาลัย
ปีการศึกษา 2553

SHRINKABILITY AND THERMAL PROPERTY OF NATURAL RUBBER/LOW DENSITY POLYETHYLENE BLOWN FILM

Miss Supak Mahapram

A Thesis Submitted in Partial Fulfillment of the Requirements
for the Degree of Master of Science Program in Petrochemistry and Polymer Science
Faculty of Science
Chulalongkorn University
Academic Year 2010

Thesis Title	SHRINKABILITY AND THERMAL PROPERTY OF NATURAL RUBBER/LOW DENSITY POLY ETHYLENE BLOWN FILM
By	Miss Supak Mahapram
Field of Study	Petrochemistry and Polymer Science
Thesis Advisor	Assistant Professor Sirilux Poompradub, Ph.D.

Accepted by the Faculty of Science, Chulalongkorn University in Partial Fulfillment of the Requirements for the Master's Degree

S. Hannongbua
.... Dean of the Faculty of Science
(Professor Supot Hannongbua, Dr.rer.nat)

THESIS COMMITTEE

....Chairman
(Professor Pattarapan Prasassarakich, Ph.D.)

Sirilux P.
....Thesis Advisor
(Assistant Professor Sirilux Poompradub, Ph.D.)

W. Trakarnpruk
....Examiner
(Associate Professor Wimonrat Trakarnpruk, Ph.D.)

Chanchai Thongpin
....External Examiner
(Assistant Professor Chanchai Thongpin, Ph.D.)

สุภัค มหาพราหมณ์ : สภาพหดตัวและสมบัติเชิงทางความร้อนของฟิล์มเป่าพอลิเอทิลีนความหนาแน่นต่ำผสมกับยางธรรมชาติ (SHRINKABILITY AND THERMAL PROPERTY OF NATURAL RUBBER /LOW DENSITY POLYETHYLENE BLOWN FILM) อ. ที่ปรึกษาวิทยานิพนธ์หลัก : ผศ.ดร.ศิริลักษณ์ พุ่มประดับ, 96 หน้า.

งานวิจัยนี้ฟิล์มหดเตรียมขึ้นมาจากพอลิเอทิลีนความหนาแน่นต่ำผสมกับยางธรรมชาติ โดยเครื่องผสมแบบปิด ศึกษาอิทธิพลของชนิดของยางธรรมชาติ (ยางรีเคลมและน้ำยางธรรมชาติ) และปริมาณยางธรรมชาติต่อสมบัติของฟิล์มหด ผลการทดลองพบว่าการใช้ยางรีเคลมซึ่งได้จากการบดเศษที่นอนยางพารานั้นไม่เหมาะสมในการใช้เป็นฟิล์มหด เนื่องจากพื้นผิวของฟิล์มRR/LDPE นั้น มีความขรุขระ ในขณะที่ฟิล์มNR/LDPE นั้นผิวหน้าเรียบ ศึกษาสมบัติต่างๆ ของฟิล์มNR/LDPE ที่เตรียมได้ ได้แก่สมบัติทางกายภาพ การเกิดผลึก สมบัติทางสัณฐานวิทยา สมบัติเชิงพลวัติ สมบัติเชิงกล สมบัติทางความร้อน และสมบัติการหดตัว ผลการทดลองพบว่าการเพิ่มขึ้นของปริมาณน้ำยางธรรมชาติไม่ส่งผลต่อสมบัติการมองเห็นของฟิล์ม แต่มีผลต่อสีของฟิล์มNR/LDPE อุณหภูมิการก่อผลึกของฟิล์ม NR/LDPE มีค่าต่ำกว่าฟิล์ม LDPE ส่งผลให้ความสามารถในการเกิดผลึกของฟิล์ม NR/LDPE เกิดได้เร็วขึ้น การที่ผลึกเพิ่มขึ้นส่งผลให้การหดตัวของฟิล์มเพิ่มขึ้นด้วย ค่าการทนทานต่อแรงดึงสูงสุดและความแข็งของฟิล์ม NR/LDPE มีค่าลดลงเมื่อปริมาณน้ำยางธรรมชาติเพิ่มขึ้น ขณะที่ความทนต่อแรงกระแทกและความทนทานค่อการฉีกขาด มีค่าเพิ่มขึ้นเมื่อปริมาณของน้ำยางธรรมชาติเพิ่มขึ้นสูงถึง 5 phr และที่ปริมาณการเติมน้ำยางธรรมชาติสูงกว่านี้สมบัติดังกล่าวลดลง เนื่องจากเกิดการแยกเฟสระหว่างพอลิเอทิลีนความหนาแน่นต่ำและน้ำยางธรรมชาติซึ่งสามารถยืนยันผลได้จากการวิเคราะห์สมบัติเชิงพลวัติและลักษณะทางสัณฐานวิทยา

สาขาวิชาปิโตรเคมีและวิทยาศาสตร์พอลิเมอร์ลายมือชื่อนิสิต.....สุภัค มหาพราหมณ์.........
ปีการศึกษา............ 2553...............................ลายมือชื่อ อ.ที่ปรึกษาวิทยานิพนธ์หลัก........

##5073426123: MAJOR PETROCHEMISTRY AND POLYMER SCIENCE

KEYWORDS: LDPE, NATURAL RUBBER, SHRINKABILITY, BLOWN FILM, THERMAL PROPERTY

SUPAK MAHAPRAM: SHRINKABILITY AND THERMAL PROPERTY OF NATURAL RUBBER/LOW DENSITY POLYETHYLENE BLOWN FILM. ADVISOR: ASST. PROF. SIRILUX POOMPRADUB, Ph.D, 96 pp.

In this study, the shrink film based on LDPE and NR (reclaimed rubber (RR) and natural rubber (NR) latex) blends was prepared by internal mixer. The effect of NR types and NR contents to shrink film properties were investigated. The results indicated that the RR was not suitable to use for shrink film because RR/LDPE films were rough surface, while the NR/LDPE films were smooth surface. Various properties of NR/LDPE films i.e., physical, crystallinity, morphology, dynamic mechanical, mechanical, thermal properties and shrinkability were also investigated. The results indicated that the increasing NR latex contents did not affect the clarity but affected the color of NR/LDPE films. The crystallization temperature (T_c) of NR/LDPE films was lower than that of neat LDPE, resulting in the increase ability of crystallization of NR/LDPE film. The increase of crystallinity, the increase of shrinkability of NR/LDPE film was obtained. The tensile strength and hardness of NR/LDPE films showed decreased with increasing NR latex contents. However, the impact resistance and tear strength increased with the increase of NR latex content up to 5 phr and then their values decreased beyond this content. These results indicated that the phase separation was occurred between LDPE and NR in the blend. These results could be confirmed by measuring dynamic mechanical analysis (DMA) and scanning electron microscopy (SEM).

Field of Study: Petrochemistry and Polymer Science Student's Signature ....

Academic Year: ....2010..................................... Advisor's Signature ...Sirilux P....

ACKNOWLEDGEMENTS

I would like to express my sincerest appreciation and deepest thankfulness to my advisor, Assist. Prof. Dr. Sirilux Poompradub for her discerning suggestion encouragement, sacrifice, and forbearance through my course of study. Thanks are also extended to Prof. Dr. Pattarapan Prasassarakich, Assoc. Prof. Dr. Wimonrat Trakarnpruk and Assist. Prof. Dr. Chanchai Thongpin for being members of the thesis committee and for their worthy comments and suggestions.

I gratefully to program of Petrochemistry and Polymer Science, Faculty of science, Chulalongkorn University and Center of Excellence for Petroleum, Petrochemicals, and Advanced Materials, (NCE-PPAM), Chulalongkorn University.

Finally, I would like to express my gratitude to family members for their love, understanding and great support throughout my study. Also, special thanks are expanded to my friends for friendship, encouragements and cheerful moral support.

CONTENTS

Page

Page

LIST OF TABLES

LIST OF FIGURES

Figure Page

Figure Page

LIST OF SCHEMES

Scheme Page

LIST OF ABBREVIATIONS

ASTM	: American Society for Testing and Materials
BUR	: Blow-Up Ratio
cm	: Centimeter
DMA	: Dynamic Mechanical Analysis
DRC	: Dry Rubber Content
DSC	: Differential Scanning Calorimeter
FDA	: Food and Drug Administration
FR	: Forming Ratio
g	: Gram
ISO	: International Standard Organization
kg	: Kilogram
kN	: Kilo Newton
LA-NR	: Low Ammonia Natural Rubber
LDPE	: Low Density Polyethylene
MD	: Machine Direction
MFI	: Melt Flow Index
Min	: Minute
Nm	: Newton meter
NR	: Natural Rubber
^{o}C	: Degree Celsius
phr	: Part per Hundred part of Resin
rpm	: Rotations Per Minute
RR	: Reclaimed Rubber
SC-XRD	: Single Crystal X-Ray Diffractometer

SEM	: Scanning Electron Microscopy
T_c	: Crystallization temperature
TD	: Transverse Direction
T_g	: Glass transition temperature
T_m	: Melting temperature
TUR	: Take-Up Ratio
UTM	: Universal Tensile Machine
X_c	: Degree of crystallinity
μ	: Micron
δ	: Tangent
β	: Beta
ΔH_m	: Heat of fusion
E'	: Storage modulus
E''	: Loss modulus

CHAPTER I

INTRODUCTION

1.1 Statement of Problems

Plastics are used extensively in packaging due to their outstanding physical, mechanical and chemical properties. The use of plastics has grown faster than any other group of materials in the packaging industry. The vigorous growth has been driven by a material substitution trend, the flexibility in design and wide range in product protection [1]. Especially, shrink film has widely been used in plastic industry; i.e, CD, DVD, food and beverage cans. Shrink film can be processed by a blown film extrusion. In this process, the melted polymer is extruded through an annular die to form a continuous tube. Then, the moving tubular film is stretched and inflated by an internal air pressure, slightly higher than the atmospheric pressure, and creates a "bubble". This bubble is cooled by an air jet flowing from an air ring toward its outside surface. Therefore, the polymer is molten between the annular die and the freeze-line, above which it is solidified completely. The crucial factor, which determines physical and mechanical properties of film, including the tensile strength, tear resistance, heat seal and optical characteristics, has been found to be the amount of frozen-in stresses in the film at the freeze-line [2]. The molecules of polymer tend to become aligned in the direction of the orienting force, for orientation of blown film, which is biaxial oriented [3]. After that, shrink wrapping starts with loosely sealing the plastic around the product, followed by passing package through a shrink tunnel, where it is exposed to heat. The materials used to produce shrink film in the market are consisted of two basic categories: polyvinyl chloride (PVC) and polyolefins which was low density polyethylene (LDPE). PVC films are temperature sensitive and they develop a tendency to shatter and split at low temperature. When PVC films run on a sealing system, a build-up carbon char will occur; otherwise the carbon char will interfere with the sealing process. For this problem, the shrink film in the market is dominated by using LDPE. The advantages of LDPE are flexible, sealable, transparent, easy to process, and therefore, use of meet Food and Drug Administration (FDA) requirement for direct to food contact [4]. The LDPE shrink film in the future tends to be increased. For this reason, the developments of high quality of LDPE shrink film are more interest. The aim of the present study is to improve the shrinkability of LDPE shrink film by using natural rubber (NR) i.e., reclaimed rubber (RR) and NR latex and then produced film by using blown film extrusion. The unique properties of NR are elastically, flexible and strain-induced crystallization. These properties are related to shrink film applications. Additionally, the main advantages of using RR/LDPE and NR/LDPE blend as the shrink film in this study was safety because the reclaimed reagent, compatibilizer and curing agent were not required and the blending process was not complicated. The physical, optical, thermal, dynamic mechanical, morphological, mechanical properties and properties shrinkability of blend films were investigated. Finally, the mechanism of strain-induced crystallization during blown NR/LDPE film process was also proposed.

1.2 Objectives

1.2.1 To study shrinkability and thermal properties of NR/LDPE film

1.2.2 To study possibility of NR/LDPE blend without compatibilizer

1.3 Scope of the Investigation

1.3.1 Surveying of the literature

1.3.2 Design and prepare experimental procedure

1.3.3 Preparation of the RR/LDPE blend by mixing the RR with LDPE directly in a beaker. The ratio of RR to mix with LDPE: 0.5, 1, 2 and 5 phr

1.3.4 Preparation of the NR/LDPE blend by mixing the NR latex with LDPE directly in a beaker and dried in circulated oven under the temperature of 80^{o}C for 30 min. The ratio of NR to mix with LDPE: 1, 5 and 7.5 phr

1.3.5 Preparation of NR/LDPE blends by HAAKE internal mixer and varying parameters as follows:

a) Time for internal mixing: 7, 8, 9, 10 min

b) Rotor speed 40, 50 rpm

c) Temperature 160, 175, 180^{o}C

1.3.6 Investigation of the compatibility of NR/LDPE compound and NR/LDPE film by Scanning Electron Microscope (SEM)

1.3.7 Preparation of NR/LDPE film by blown film extrusion with parameters as follows:

a) Temperature zone: feed zone 180-190^{o}C, screw zone 210-230^{o}C and die zone 230-240^{o}C

b) Screw speed 60 rpm

c) Drawn speed 200-250%

d) Film width 11 cm

e) Film thickness 30 μm

1.3.8 Study the physical, optical properties (ASTM D1746) and density (ASTM D1622) of NR/LDPE film

1.3.9 Study the crystalinity of NR/LDPE film by X-ray diffraction (XRD)

1.3.10 Study the morphology of NR/LDPE blend compound and NR/LDPE film by SEM

1.3.11 Study the thermal properties of NR/LDPE film by Differential Scanning Calorimeter (DSC)

1.3.12 Study the dynamic mechanical analysis (DMA) of NR/LDPE film

1.3.13 Study the mechanical properties of NR/LDPE film: tensile strength and elongation (ASTM D882), hardness (ASTM D2240), tear strength (ASTM D1938) and impact resistance (ASTM D1709)

1.3.14 Study the heat shrinkability (ISO 1150) of NR/LDPE film by circulate oven

1.3.15 Comparison of the physical, optical, density, crystalinity, morphology, thermal, dynamic mechanical, mechanical properties, and heat shrinkability of NR/LDPE film with neat LDPE film

1.3.16 Summarization and discussion the results

1.3.17 Writing the thesis

CHAPTER II

THEORY AND LITERATURE REVIEWS

2.1 Low Density Polyethylene (LDPE)

LDPE has the general structure as shown in Figure 2.1. Its molecule contains many short and long branch chains. The short branches primarily consist of ethyl and butyl branches, which are often located near each other. LDPE is polydisperse in terms of its molecular weight, long chain branching length and placement and short chain branching.

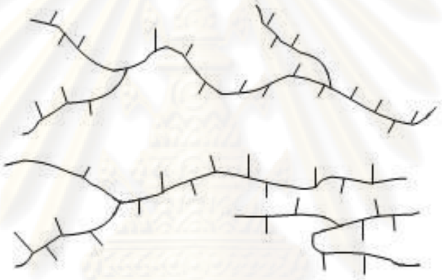

Figure 2.1 Principal variants of LDPE.

LDPE was produced from ethylene monomer in a high pressure reaction via free radical polymerization, which was consisted of the four basic steps as follows: initiation, propagation, chain transfer, and termination. These steps are illustrated in Figure 2.2. In the first step, the initiator creates an active site on the monomer, as indicated by the unpaired electron. During propagation, the active reacts with another monomer, thereby adding the monomer residue to the end of the chain and generating a new active site, causing the chain to grow. Chain growth is terminated when the active site becomes deactivated. A chain transfer is an alternate reaction of the active site. In this process, an active site transfers to another molecule creating one terminated species and new activated species [5].

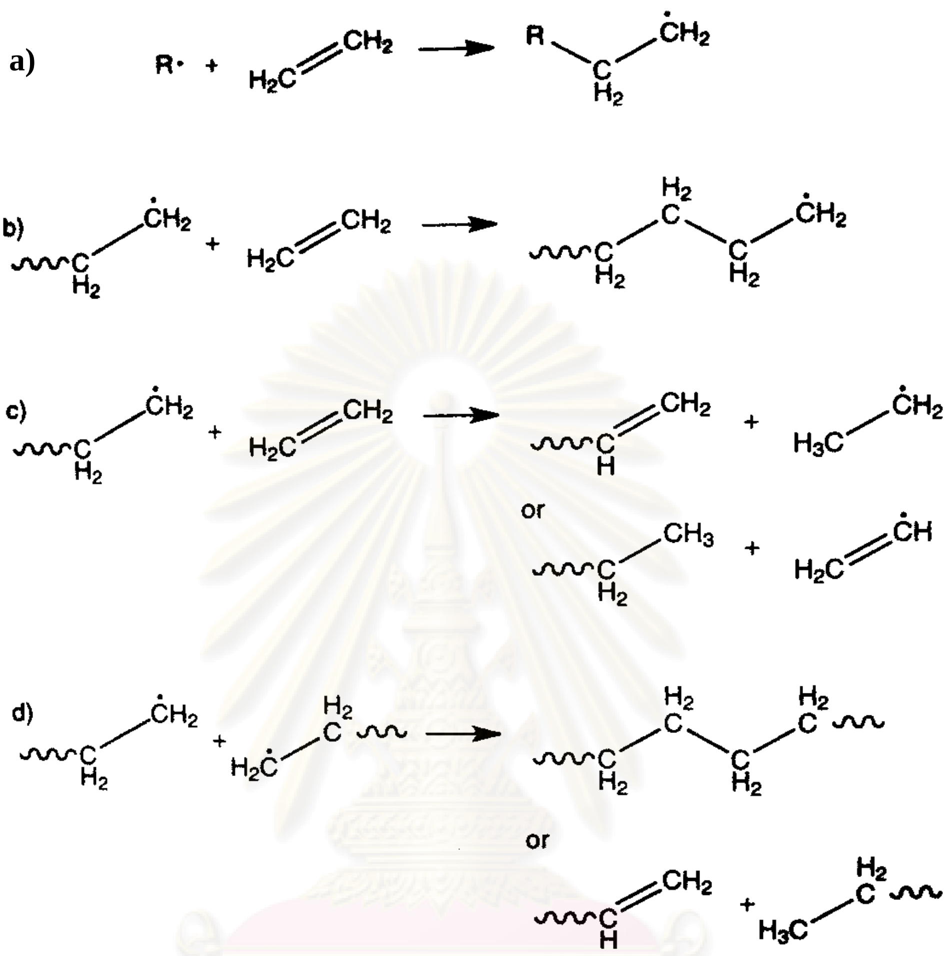

Figure 2.2 Chain growth polymerization exemplified by free radical polymerization of polyethylene.

2.1.1 Properties of LDPE

LDPE is a branched thermoplastic polyethylene with melt flow index (MFI) between 0.2 and 20 g/10 min. The high levels of branching found in LDPE disrupt its ability to crystallize, which limits its density in the solid state to approximately 0.915 to 0.942 g/cm^3, which equates to crystallinity levels ranging from approximately 30 to 55%. The highly branched nature of LDPE and its broad molecular weight distribution give it high melt strength and good shear thinning properties, which are desirable processing characteristics. Chain-branching yields desirable characteristics such as clarity, flexibility, sealability, and ease of processing. LDPE has modest stiffness and moderately high tear and impact resistance. Films made from LDPE are relative transparent, because their spherulites are generally significantly smaller than the wavelength of light. Due to its rheological characteristics, LDPE can be processed by blown film extrusion, cast film extrusion, extrusion coating, extrusion molding, or blow molding. Film is the single largest production from of LDPE; in the U.S.A., 55 percent of the total LDPE produced is made into films with thickness under 12 mils (300 microns). LDPE has a low melting temperature range (98 to 115^{o}C) and, therefore, is an easily sealable material a property of great value in flexible packaging. When compared with other plastics, LDPE provides an excellent barrier to water. On the other hand, it shows one of the highest permeability values for oxygen, carbon dioxide, and organic vapors. Containers, bags for food and clothing, industrial liners, vapors barriers, agricultural films, household products, and shrink- and stretch-wrap films are commonly fabricated from LDPE [1].

Table 2.1 Properties of LDPE

Properties	
Density, g/cc	0.91 to 0.925
Yield, $in^2/lb.mil\ x10^{-3}$	30
Tensile strength, kpsi	1.2 to 2.5
Elongation at break, %	225 to 600
Impact strength, kg.cm	7 to 11
Elmendorf tear strength, g/mil	100 to 400
WVTR, g.mil/100 in^2· day @ 100 °F and 90% RH	1.2
Oxygen transmission rate, cm^3· mil/100 in^2· day ·atm @77 °F and 0% RH	250 to 280
CO_2 permeability, cm^3· mil/100 in^2· day· atm @ 77°F and 0% RH	500 to 5000
Resistance to grease and oil	Varies
Dimensional change at high RH, %	0
Haze, %	4 to 10
Light transmission, %	65
Heat-seal temperature range, °F	150 -350
Service temperature range, °F	-70 to 180
Tensile modulus, 1% secant, kpsi	20 to 40

2.2 Reclaimed Rubber (RR) [6]

RR is manufactured from waste rubber products like scrap tires and tubes. RR is mostly used in making tires, rubber sheets, tiles, mats and tubeless tires. With the rapidly growing rubber industry, rubber wastage is also increasing. However, the rubber industry has found the innovative way of making and using RR in a variety of applications.

2.2.1 Uses of RR

RR is used in different proportions for producing various rubber products. Application of RR is seen in the making of following industrial products.

- Automotive tires
- Tire flaps
- V belts & conveyor belts
- Different types & sizes of mats
- Extruded & molded rubber goods
- Tire inner liners
- Cable compound
- Cycle tubes
- Two, three & four wheeler auto tubes
- Bicycle tires
- Battery containers
- Shoe soles
- Rubber sheets
- Butyl inner tubes
- Adhesives
- Sound dampers
- Automobile parts

2.2.2 RR Manufacturing Processes

There are a number of manufacturing processes for RR.

2.2.2.1 Thermal processes

2.2.2.2 Thermo-mechanical processes

2.2.2.3 Mechano-chemical methods

2.2.2.4 Microwave recycling

2.2.2.5 Ultrasound recycling

2.2.2.6 Biotechnological processes

2.2.2.7 Devulcanization in supercritical carbon dioxide

The most widely used rubber reclamation process includes shredding of tires and other rubber wastes to suitable size with the help of tire shredder and other RR machinery. The fibers are then mechanically removed from the cracked tires. Comparatively fiber-free scrap is ground to finer mesh size and further mixed with chemical agents in a reclaimator which is again a RR machinery. The temperature in the reclaimator is kept in the range of 204-260 °C for the desirable time for de-vulcanization. Reclaimed material is then mixed and blended with small proportions of reinforcing and processing agents.

2.2.3 Advantages of RR

- Excellent aging properties
- Minimum reversion
- Reduced compound cost
- Shorter breakdown in mixing time
- Reduced power consumption
- Lower processing temperature
- Fast and uniform processing
- Improved dimensional stability

2.3 Natural Rubber (NR)

The most important source of NR latex is the *Heavea brasiliensis trees*, now grown in plantations in many tropical parts of the world. The white sap of the common milkweed and dandelion is rubber latex. It owes its colloid stability to the presence of adsorbed proteins at the surface of the rubber particles. These absorbed proteins are in the anionic state so that the rubber particles carry negative charges at their surfaces. NR latexes can be preserved by the addition of ammonia or caustic alkali, but its low rubber content and high non-rubber solids content severely limits the usefulness of preserved field latex [6]. This naturally occurring polymer is known chemically as *cis*-1,4-polyisoprene (Figure 2.3)

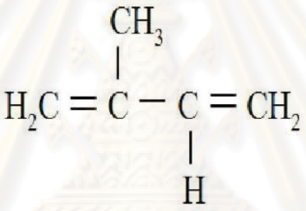

$$H_2C=\overset{\overset{\displaystyle CH_3}{|}}{C}-\underset{\underset{\displaystyle H}{|}}{C}=CH_2$$

Figure 2.3 Isoprene structure.

The possibility that the NR molecule might contain a mixture of *cis*- and *tran*- groups was considered to be unlikely because such a mixed polymer would have an irregular structure and be unable to crystallize in the manner of NR. Infrared studies have certainly shown that NR was at least 97 percent *cis*-1,4-polyisoprene and the other were 1,2-structure and 3,4-structure [7]. Raw NR latex consists of particles of rubber hydrocarbon and non rubbers suspended in an aqueous serum phase. The average dry-rubber content of latex may range between 30 percent and 45 percent. A typical composition of fresh latex is shown in Table 2.1 [8].

Table 2.2 Typical composition of fresh latex and dry rubber

Latex composition	Latex, %	Dry rubber, %
Rubber hydrocarbon	36.0	93.7
Protein	1.4	2.2
Carbohydrates	1.6	0.4
Neutral lipids	1.0	2.4
Glycolipids + Phospholipids	0.6	1.0
Inorganic constitutuents	0.5	0.2
Other	0.4	0.1
Water	58.5	-

2.3.1 Processing of NR

NR is usually considered to have good processing properties. Although it is tough and "navy" at temperatures well below 100 °C, it breaks down easily to a useable plasticity. The efficiency of mastication is lowest at around 100 °C. Mastication is best carried out below 80 °C (well-cooled open mill) or above 120 °C (internal mixer). The processability of NR cannot be predicted by any single parameter, viscosity still remains the most widely used measure of processing quality. During mixing, good control of compound viscosity within fairly narrow limits is essential to insure smooth operation during further processing, such as extrusion and injection molding. For NR, a relatively good correlation exists between mixed-batch viscosity and raw-rubber viscosity if the viscosities are not too low or too high. Unvulcanized compounds of NR have super superior green strength and building tack compared to other elastomers.

The aim of the present study is using NR latex to improve the shrinkability of LDPE shrink film. The unique properties of NR latex are elastically, flexible and strain-induced crystallization. These properties are related to shrink film applications especially strain-induced crystallization of NR, more crystallinity is more shrinkability of film. Additionally, the main advantage of using NR/LDPE blend as the shrink film in this study was safety because the compatibilizer and curing agent were not required and the blending process was not complicated.

2.4 Blending Process [9]

Processes for blending vary from simplest to sophisticated high speed machine. In most cases it is necessary to achieve both good distribution and good dispersion for satisfactory product.

2.4.1 Blend Formation

Polymer blends can be produced by mixing two polymers (as melts, lattices, or in solution) or by in situ polymerization of a monomer in the presence of a dissolved polymer. All processes have advantages and disadvantages with respect to the process, the properties of blends, and economic.

Melt Mixing. The energy taken up during melt mixing is used for flow processes and the generation of surfaces of new micro domains. After some time, a steady state is established and the domain size becomes constant. The high shear fields create some polymer degradation. The resulting polymer radicals lead to graft polymers that provide some anchoring of domains. No macroscopic demixing occurs because of the show diffusion resulting from the high viscosities.

Latex Blending consists of two aqueous polymer dispersions. Far lower temperatures and shear fields are employed than in melt blending. The good mixing of the latex particles remains after coagulation. The domain size is, however, restricted to the size of the latex particle themselves; it is not altered by subsequent melting of the coagulated. No grafting occurs; the blends have low impact strengths.

Solution Blending involved the mixing of a solution of polymer 2 in solvent 1 with a solution of polymer 3 in the same solvent. Solutions of immiscible polymers remix, however, at very low concentrations, sometimes under fractionation with respect to molar masses. Domains grow further on solvent removal by distillation or freeze-drying. Solutions of thermodynamically miscible polymer 2 and 3 deliver one-phase blends if no two-phase regions are passed through over the whole concentration and temperature range during the solvent removal. In such systems, miscible polymers can be blended to domain of molecular sizes.

***In situ* Polymerization** involves solutions or gels of polymers in monomers which are subsequently polymerized. Three processes can be distinguished. In process a non-crosslinkable polymer is dissolved in a non-crosslinkable monomer that is subsequently polymerize. The industrially most important process involved a graft able and crosslinkable rubber in a monomer that will convert to a thermoplastic on polymerization. Process utilizes an already crosslinked polymer in a crosslinkable monomer this process produces inter- penetrating networks.

2.4.2 Influence of Processing Methods on Morphology [10]

2.4.2.1 Internal Mixer

The internal mixer has been used especially for making rubber-based blends, but it is also a useful laboratory tool for blending a wide range of thermoplastics, since it allows for the mixing of small quantities and for the monitoring of torque, which is governed by viscosity. It is a batch mixer consisting of counter rotating rotors turning at difference speeds. The degree of mixing is related to the rotor speed and the time to mixing. The mixer is characterized by high-shear stress zones where dispersive mixing or homogenization takes place.

2.4.2.2 Single- and Twin-Screw Extrusion

1. Single-Screw Extruder

The single-screw extruder remains a very common tool for blending polymers, because of its wide - spread availability. It is, however, a relatively poor mixing device, owing to its low shear and poor distributive mixing.

2. Twin-Screw Extruder

Co-rotating and counter rotating twin-screw extruder is high-intensity mixing devices consisting of two screws with a kneading section for intensive mixing. The entire screw configuration can be built to fit a particular requirement. e.g., high shear, through the addition of kneading blocks.

2.4.2.3 Injection Molding

Injection molding is characterized by complex and nonisothermal flow into a closed and cooled mold cavity. This process generally results in an isotropic skin-core structure. The filling of the mold cavity occurs through fountain flow. During molding, the polymer in contact with the cooled mold wall freezes immediately to form the skin, where the shear will be a maximum. Dispersed, deformable particles will be elongated in the direction of flow. The hot core will be less deformed and has sufficient time to relax. The final result of this complex process is the so-called skin-core structure. Another major complication associated with multigated injection molding of polymer blends is that subsequent failure usually occurs at the weld line of the piece.

2.4.3 Morphology Characterization of Blends by Microscopy Technique [10,11]

Microscopy is uniquely suited to characterize these microstructural variations. Historically, microscopic studies have been largely qualitative, focused primarily on the identification and description of the various internal phases. More recently, there has been a demand to better qualify critical structural parameters in order to define more precisely the effect of composition and processing history on the microscopic properties and appearance of material. The microscopic study of polymer blends is to develop adequate contrast between the phases of interest. Sometimes, this contrast occurs naturally, because of differences in reflective index, chemical composition, or cutting characteristics. Most often, however, it must be enhanced by staining, etching or extraction.

2.4.3.1 Transmission Electron Microscopy (TEM)

In transmission electron microscopy (TEM), a sample is bombarded with electrons and the number of electrons which travel through the sample is measured as a function of position. The number of electrons that pass through the sample is proportional to the sample thickness and the electron density.

2.4.3.2 Scanning Electron Microscopy (SEM)

The large depth of field of the SEM makes it ideally suited to the examination of samples with a high degree of surface relief. This feature, together with the ease with which fractured surfaces can be prepared, has led to the wide spread use of fractography to study the internal structure of polymer blends. The best results have been obtained when the internal phase(s) are poorly bonded and the matrix undergoes brittle failure. These conditions produce surfaces having an assortment of debonded particles and cavities, which are often used to make crude assessments of particle-size distributions and adhesion. Micrographs obtained in this way are more commonly over interpreted than are any other micrographs.

2.4.3.3 Optical Microscopy (OM)

The use of optical microscopy in the analysis of polymer blends is often limited by the small size of typical dispersions. As a result many researchers routinely defer to higher magnification techniques such as SEM and TEM. Nonetheless, the ease with which optical observations can be carried out remains a significant advantage, and by combining various types of illumination, it is sometimes possible to produce information that is not readily available by other methods such as TEM, SEM.

2.4.4 Properties of Blends [5]

Though both miscible and immiscible blends are composite materials, their properties are very different. A miscible blend will exhibit a single glass transition temperature that is intermediate between those of the individual polymers. In addition, the physical properties of the blends will also exhibit this intermediate behavior. Immiscible blends, on the other hand, still contain discrete phases of both polymers. This means that they have two glass transition temperatures and that each represents one of the two components of the blend. (A caveat must be added here in that two materials that are immiscible with very small domain size will also show a single, intermediate value for T_g). In addition, the physical properties are often a mixed bag based on the relative composition of the two phases, the form of the polymer in the phase, and the connectivity between the two materials.

2.5 Blown Film Extrusion

Blown film extrusion is a continuous process in which the polymer melted, the melt is forced through an annular die and the resulting tube is inflated with air into the "bubble" and cooled. Air is always blown on the outside of the bubble to cool the film; to increase production rates, internal bubble cooling can also be used. The film is stretched in the longitudinal and circumferential directions during production, resulting in biaxial orientation of the film. The amount and relative degree of stretching determine the degree of orientation. The circumferential stretching is inherent in the blowing process. Longitudinal stretching is imparted by drawing of the film between the extruder and the nip rolls.

The principal polymers used in blown film production are polyolefins, although other polymers can also be used. The major applications are those that require biaxial strength, and include bags of all kinds, as well as agricultural and construction film. In food packaging, coextruded structures with three to five layers, or even more, are common, with major markets including packaging for cereal, meat, snacks, and frozen foods.

The properties of the film are determined by the blow-up ratio and the linear line speed. The blow-up ratio is the ratio between the diameter of the final tube of film and that of the die. The internal air pressure that expands the tube into the bubble is typically supplied through a port into the mandrel, the interior part of the die. Once the process is running steadily, little air is usually lost, so make-up requirements are small. When internal bubble cooling is used, air is constantly being exchanged inside the bubble [13].

2.5.1 The Machinery of Blown Film Extrusion

The machinery of blown film extrusion can into 2 systems; extruder and blow film systems

2.5.1.1. Extruder Systems [14]

The purpose of extruder is to feed a die with a homogeneous material at constant temperature and pressure. This definition highlights three primary responsibilities that the extruder must accomplish while delivering material to a shaping die. First, it must homogenize, or satisfactorily mix, the material. Second, the material entering the die must have minimal temperature variation with respect to both time and position within the melt stream. Third, there must be minimal melt pressure variation with time. It is important that the design and operation of an extrusion system consider all three of these objectives to produce a quality product. Components of the extruder can be categorized into five systems (Figure 2.4).

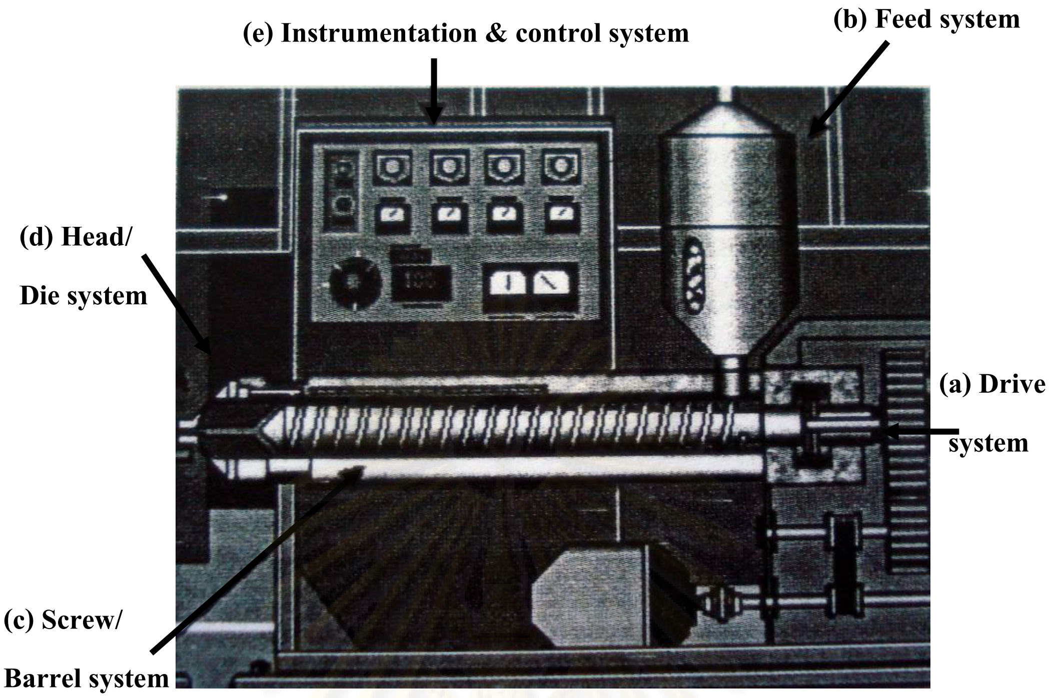

Figure 2.4 The five extruder hardware systems: (a) Drive system, (b) Feed system, (c) Screw/barrel system, (d) Head/die system, (e) Instrumentation and control system.

2.5.1.2. Blown Film Systems

Blown film systems cover hardware specific to blown film extrusion. It is organized by the order in which material flows through the extrusion line, beginning upstream of the extruder and proceeding through wind up. The major sections are in this system as shown in Scheme 1.

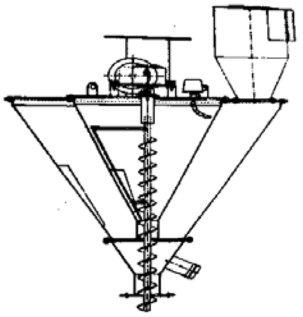

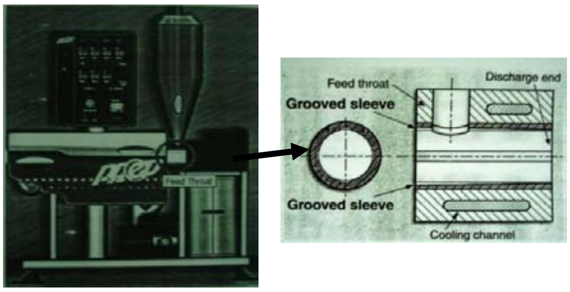

(a) Upstream components

(b) Grooved feed throat

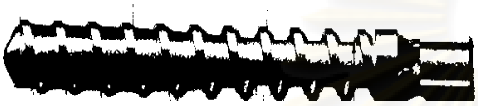

(c) Screws for blown film extrusion

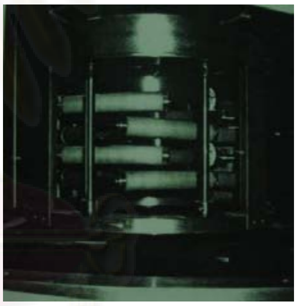

(e) Collapsing frames

(f) Bubble stabilization

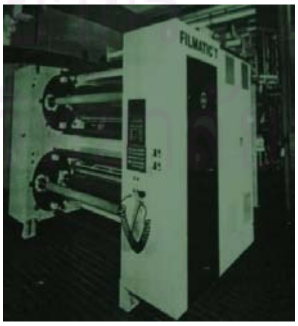

(g) Haul-off

(h) Winders

Scheme 1 Schematic illustrate of blown film systems.

2.5.2 Processing of Blown Film Extrusion

Blown film extrusion offers excellent manufacturing flexibility because of the ease with which product geometry (such as film thickness and/or lay flat width) can be changed without a need to change hardware. Perhaps the most important processing characteristic, however, is the ability to impart biaxial orientation (the alignment of the long, chainlike molecules) into the film in a cost effective manner. Proper molecular orientation in the film is one of the most important objectives of this process. For example, adequate impact strength or puncture resistance in a film can be obtained one or two ways, by creating suitable orientation or by increasing the film thickness significantly. As one would expect, every manufacturer would choose the former over the much more expensive latter, every time.

Biaxial orientation means that polymer molecules are aligned in the plane of the film, i.e., in both the machine direction (MD, along the long axis of the bubble) and the transverse direction (TD, around the hoop direction of the bubble). The result is a tough film that resists tearing in either direction (a kind of “rip-stop” effect), as opposed to a film that tears easily in one direction (a so called “splitty” film). This molecular structure is produced when melt exiting the die is stretched in both MD and TD at the same time. Therefore, the geometry of the bubble and the process conditions yielding the geometry are crucial to proper orientation. As mentioned earlier, these process conditions are highly interdependent. This section provides an overview of the relationships between blown film processing, molecular structure and solid-state film properties. Herein, blown film processing is characterized by bubble geometry, molecular structure by orientation, and film properties primarily by tensile strength and tear strength. This approach provides an effective technique for understanding and applying the fundamental principles involved in these process/structure/property relationships.

2.5.3 Process Variables and Bubble Geometry

In this topic defines the response that increasing each of the four main process variables (nip speed, screw speed, cooling speed, and bubble volume) has on each of the three main bubble geometric variables (film thickness, bubble diameter, and frost-line height). An asterisk identifies the primary response to each increase.

When the nip speed increases, the primary effect is for the melt to be stretched more in MD, making the film thinner. As a result of the film traveling past the cooling air more quickly, the height on the bubble where the temperature has dropped to the point of polymer solidification (the frost line) increases. (It is easy to mistakenly think that the frost-line height always increases). As the frost-line height increases, the small diameter stalk below the frost line lengthens and the air volume in the bubble is displaced more to the top, because the bubble contains a fixed volume of air. This increase in bubble volume above the frost line pushes the bubble outward to a higher diameter, also contributing to film thinning.

An increase in screw speed results in an increase to all three bubble geometry variables. The increase in output from the extruder has the primary effect of increasing film thickness. Also, a greater amount of material results in a greater amount of heat that must be removed from the film. This takes a longer time under constant cooling conditions, thus increasing the frost-line high. Again, as the frost line moves upward, the bubble diameter increase. The slight thinning effect due to an increase in bubble diameter is far outweighed by the thickness increase created by greater output.

Increasing the cooling air speed causes faster heat removal from the bubble. Because the film reaches solidification temperature sooner, the primary effect is a lowering of the frost line. As a result, the bubble diameter decreases from the constant internal air volume being distributed over a greater distance from frost line to nip rollers. Because a low bubble diameter means the film is not stretched as much in TD, the film thickness increase. When more are is inserted into the bubble, bubble volume increase, primarily the diameter increases by stretching more in TD. The increased TD stretching results in thinner film. Thinner film cools more quickly, consequently lowering the frost line.

2.5.4 Process/Structure/Property Relationship

Molecular structure, as imparted by processing, has a significant influence on the physical properties of extruded products. This is known as a process/structure/property relationship. In the case of blown film, the extruder conditions and the bubble geometry influence the molecular structure, which then affects film performance.

While blown film processing can be quantified with take-up ratio (TUR), blow-up ratio (BUR), and forming ratio (FR) as described in the previous section, structure is most readily characterized through molecular orientation. When molecular are oriented, they are deformed from their natural configuration (random coil) into a stretched and frozen configuration (Figure 2.5) on the left, a polymer molecule shown in its preferred, unstressed state called a random coil and on the right, after experiencing stress, in an oriented state. The alignment of long chain molecules in the solid film increase tensile strength in the direction of orientation and improve toughness and impact properties.

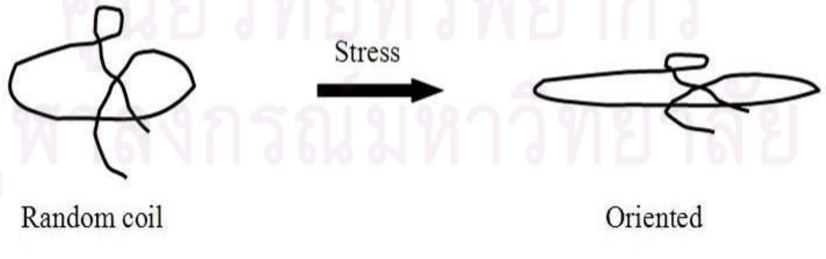

Figure 2.5 The deformation of long chain molecules before (random coil) and after stress (oriented).

Molecular orientation is measured by various techniques. While most of these methods (such as infrared dichroism and x-ray diffraction) are conducted only in research facilities, a method that is readily conducted by the average film processor is the shrinkage test. In this experiment, square specimens of film are placed on hot oil for a short time, allowed to shrink, and removed to cool. The length of the specimen in MD and TD are then measured to determine directional shrinkage, an indication of original orientation in each direction. While this does not provide a direct measure of molecular orientation, the technique has been shown to correlate well with direct measurement methods.

Several important studies have been conducted to obtain direct measurement of molecular structure in blown films [15-21]. In most cases, these studies seek to correlate process conditions to molecular structure, including orientation and crystallinity. Further, an attempt is often made in these types of studies to relate the structure to film physical properties. Many physical properties of blown film are measured to determine fitness for use. The primary mechanical properties of interest are tensile properties (strength, modulus, and elongation) in MD and TD, puncture resistance, impact strength, and MD and TD tear strength. These are all highly dependent on molecular orientation. Other film properties that are measured include brittleness and optical clarity. Generalizations can be made about process/ structure/property relationships that are helpful to the blown film operator. For example, an increase in TUR generally results in an increase in MD orientation (Figure 2.6). Subsequently, MD tensile strength is higher, but MD tear strength is lower because a tear can be more easily propagate through the oriented molecules. When the BUR is increased, TD orientation increases. This leads to higher TD tensile strength, but lower TD tear strength. Finally, when FR approaches one, the MD and TD mechanical properties of the film tend to be balance, i.e., toward isotropy.

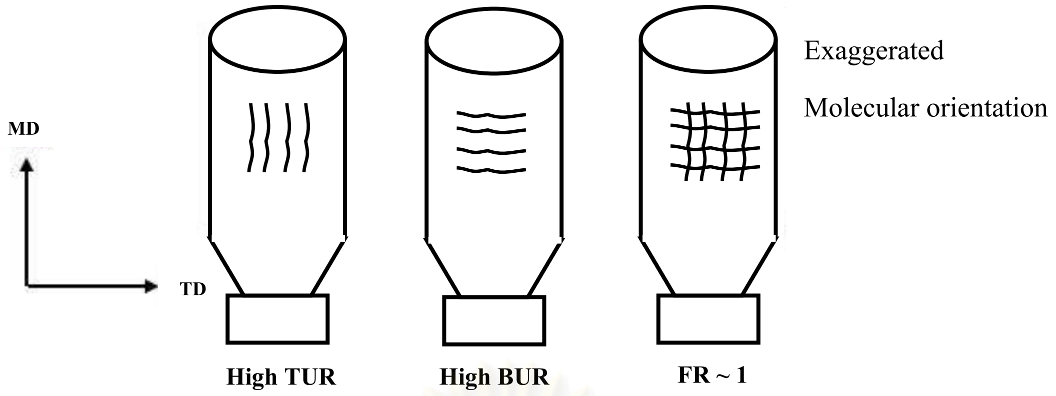

Figure 2.6 The type of molecular orientation in the film depends on the type of processing stress-high TUR yields high MD orientation, high BUR yields high TD orientation, forming ratio approaching 1 yields balanced orientation.

2.5.5 Film Properties

2.5.5.1 Tensile Strength (ASTM D822)

Tensile strength, also known as the highest stress for those materials to be able to sustain stress before breaking, provides data regarding the load carrying capability of the film. It is measured on a universal testing machine (Figure 2.7) that pulls the ends of a rectangular strip at a specified rate in opposite directions until it breaks.

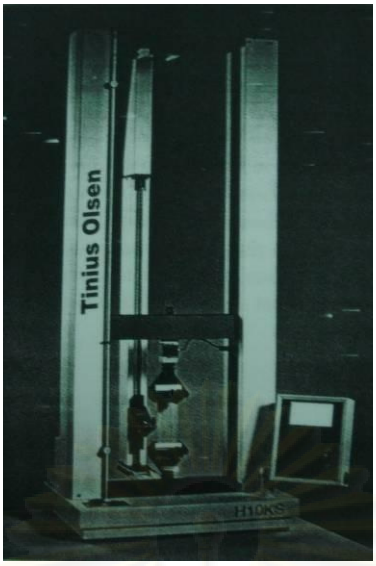

Figure 2.7 A universal testing machine used to measure tensile properties.

2.5.5.2 Elongation (ASTM D822)

Another tensile property covered by the same ASTM method as that for tensile strength is elongation. This property describes the ability of the film to stretch prior to breaking or yielding. A material was stretched significantly prior to the break point is called *a ductile material* while one that breaks after only a small degree of stretching is called a *brittle material*.

2.5.5.3 Tear Strength (ASTM D1004, D1992 and D1938)

Tear strength is an important property measured for quality control by blown film process i.e., process stretching (orientation). There are various methods of measuring tear strength of the film, as seen by the multiple ASTM methods listed above. These focus on the resistance to either the initiation of a tear (rupture) or the propagation of an existing tear.

2.5.5.4 Impact Resistance (ASTM D1709, D3420 and D4272)

In many film applications the product is subjected to puncture or impact loads. These types of loads are applied perpendicular to surface of the film. Therefore, the stresses act biaxially (in both the machine and transverse directions simultaneously) and are not represented well by a uniaxial test. Impact resistant test are designed to biaxially load the film to measure its energy absorbing capability. In popular method (ASTM D 1709), a five-inch diameter circular film specimen is clamped into the base of an apparatus. Then a blunt, metal dart is dropped onto the specimen from a specified height. If the specimen fails, some weight is removed from the dart and the test is repeated with a new specimen. If the specimen does not fail, some weight is added to the dart and the test is repeated. This process continues until a statistically valid number of specimens are tested resulting in the nominal weight to failure. At that point, the impact failure energy can be determined. It has been shown for this procedure that friction between the dart surface and the film specimen has a very strong affect on test result (Figure 2.8).

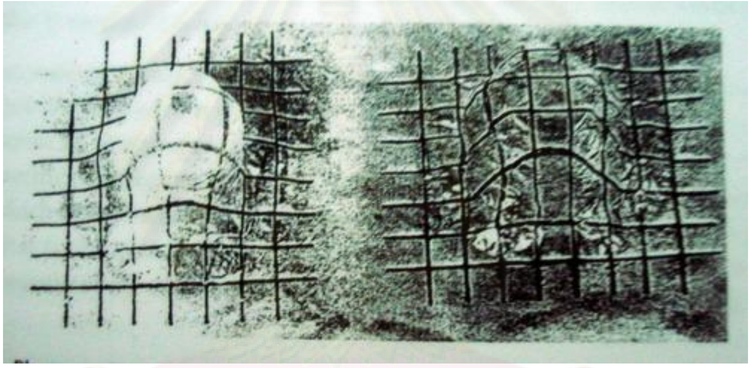

Figure 2.8 Photograph showing how friction affects dart impact test on film. Left side shows film lubricated with powder deforms biaxially, while right side shows a more uniaxial deformation when there is high friction.

2.5.5.5 Transparency (ASTM D1746)

Transparency tests provide a measure of the amount of incident light that passes through a film sample without being scattered. Films with higher values are called transparent; films with lower value are called translucent.

2.5.5.6 Haze (ASTM D1003)

Haze is a measure of the amount of light that is scattered as it passes through a film. In the standard test method, a haze meter is used to measure the amount of light scattered outside of a specified beam angle. The meter utilizes the inside. Surface of a sphere to collect and quantify the amount of scatted light. The greater degree of light scattering is the higher the value of percent haze.

2.6 Shrink Film [13]

A wrap is the simplest form of plastic package, using a flat piece of plastic film that is folded or wound around the packaged item. Wraps are used to an extent foe retail packages, but the larges market is stretch wrap for pellet loads of productions, serving to unitize and stabilize them during distribution. Shrink films, like stretch films, use the tendency of a film to try to return to a smaller dimension after deformation to provide a tight wrap around a packaged object. In shrink film the product is loosely packaged, and when it is exposed to heat, the film shrinks. The resistance of the product on the film provides the holding force.

To make a shrink film, a polymer film can be oriented at an elevated temperature and the orientation "frozen" by rapid cooling. When the film is subsequently heated, the molecular "memory" of the polymer causes it to attempt to return to its original dimensions. Lightly cross-linked materials are often used to increase the tendency to shrink. In that case, electron beam irradiation of the plastic film produces free radicals, which then react to produce cross-links between adjacent molecules. The presence of these cross-links means the material will no longer become liquid and flow at its normal melting temperature. That, in turn, allows the shrink film to be exposed to high temperature, at or above it former melt temperature, without flow, so these elevated temperatures can be used to promote shrinking.

Shrink wrapping starts with loosely sealing the plastic around the product, followed by passing the package through a shrink tunnel, where it is exposed to heat. If the temperature, residence time, and size of the package and product are chosen properly, then a tightly wrapped package comes out of the shrink tunnel. Because exposure to this very brief, even products with some temperature sensitivity can be packaged in this way. Over time, shrink wrap, like stretch wrap, tends to loosen somewhat, due to creep and stress relaxation, with the loss of holding power increasing at higher temperatures. Shrink wrap materials include PE, PP and PVC, among others.

2.6.1 Shrink Film Categories [22]

The shrink film market is comprised of two basic categories; the polyvinyl chloride (PVC) and polyolefin. Shrink polyethylene is not typically included in the competitive polyolefin category; "poly" lacks the clarity, gloss and the tight second skin polyolefin provide. These attributes are critical for retail appeal. The polyolefin "family" consists of film made from polyethylene or polyethylene and polypropylene copolymer resin. PVC shrink films derive their properties from additives, which are primarily plasticizer. As these film ages, the plasticizer migrates and the film reverts to its brittle state, turning to yellowish color. Comparison between polyolefin and PVC film as below;

Polyolefin Film

- Polyolefin film provides superior optical properties, very important attributes for retail appeal.
- During shrinking process, polyolefin films need an air evacuation hole or multiple perforations.
- Polyolefin film must be exposed to the correct temperature for the correct amount of time for proper shrinkage to occur.
- Polyolefin film meet FDA requirement for direct food contact.

PVC Film

- PVC films are temperature sensitive. Develop a tendency to shatter and split at cold temperature and "shrink back" when exposed to high temperature over a period of time.

- During the shrinking process, PVC film does not need “artificially created” air escape holes, due the make-up of PVC, the seal typically is full or small pinholes.
- PVC film requires only heat in order to cut, seal
- When PVC film run on a sealing system, build-up of carbon char will occur, and will need to be cleaned from sealing head; otherwise the carbon will interfere the sealing process.
- PVC film do not meet FDA requirement for direct food contact.

2.6.2 Shrink Wrapping Machines [23]

The machines that accompany these specialty films with their contents all consist of a device to feed the film to a point where it can be wrapped loosely around the product; hot wire sealing devices, which produce a side seam, seal both ends closed and cut off the sealed package; and a so-called “shrink tunnel” through which the loosely wrapped object passes to heat shrink the film tightly around the package. As with conventional box wrappers, shrink wrapping machines range from inexpensive models used sporadically to wrap objects produced one at a time to more costly machines designed to accept uniformly shaped products that are produced rapidly and that must be wrapped equally rapidly, at speeds up to 150 packaged per minute. The simplest and slowest of these machines is the so-called “L-bar sealer”, its name derived from the shape of the bar that produces the seals. Figure 2.9 shows how the L-bar sealer works. Since the L-bar sealer operates with folded film, as shown, the manufacturer must supply his firm product in that form. High speed shrink wrapping machines automate the process, as shown in Figure 2.10, where the shrink tunnel and film supply roll have been omitted for simplicity. To maintain continuous operation, the orbital cross sealing mechanism must travel along with the film for a dwell time sufficient to produce a strong seal and then return to perform the next seal. The arrows above that device in Figure 2.10 illustrate the necessary reciprocal motion.

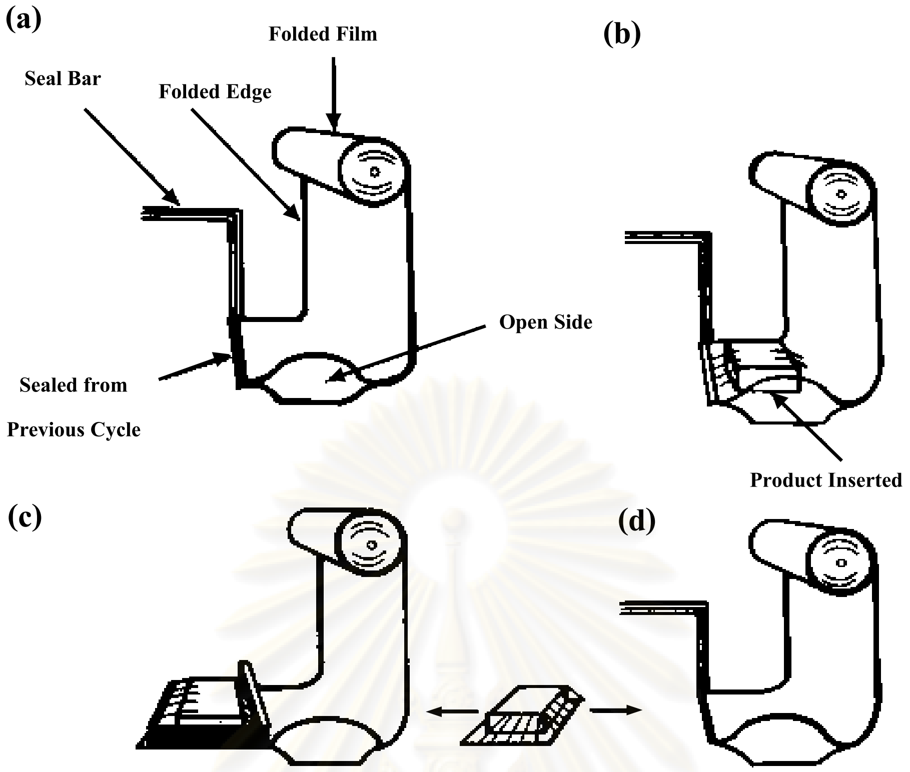

Figure 2.9 The L-bar sealer for shrink film.

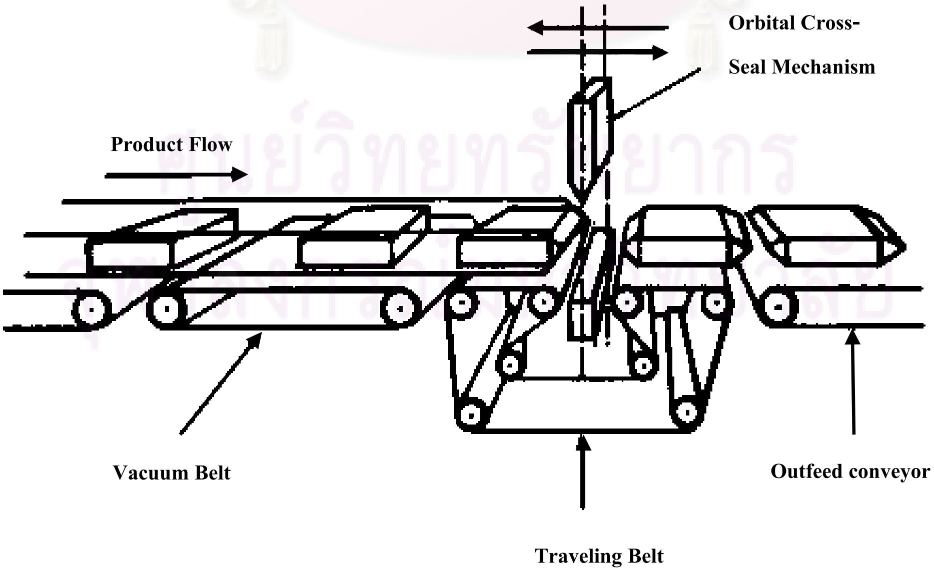

Figure 2.10 An automatic shrink wrapper.

Unbalanced shrink properties are advantageous if the item to be wrapped has an odd shape, but the added cost of the rarely used unbalanced film usually persuades the buyer to settle for a balanced film.

Shrink temperature and *shrink temperature range* are also important. The former should be as low as possible and the latter should be as large as possible to simplify the operation of the shrink tunnel and to prevent heat damage to package contents.

Shrink tension is crucial when delicate or easily distorted items are being shrink wrapped. For example, most commercially available shrink firms exert a shrink force on a tin pad of paper that is so large that the pad tends to curl up into a cylinder after the firm wrap is heat shrunk, rather than lying flat.

The *degree of shrinkage* varies from about 25 to 75 % and is shrink temperature dependent. The degree of shrinkage needed depends on the application. Contour wrapping a highly irregular object requires a high degree of shrinkage to produce a neat package; tightening up a loosely wrapped regularly shaped package requires a must lower degree of shrinkage.

2.7 Literature Reviews

Khonakdar *et al.* [24] studied on the thermal and shrinkage behavior of stretched peroxide-crosslinked high-density polyethylene (HDPE). The compounding process was carried in an internal mixer with speed 50 rpm at 145°C. Crosslinking agent (di-*tert*-butyl cumyl peroxide: BCUP) content was varies in a range of 0.5-3%. The results showed that crosslinking hindered the crystallinzation process by decreasing the melting and crystallization temperature as well as the total degree of crystallinity. The stretching ratio had no significant effect on shrink temperature but rather on ultimate shrinkage. The stretching temperature had relatively significant influence on the shrink temperature. Crosslinked HDPE stretched at above melting point (140 ^{o}C) had higher shrink temperature as compared to those stretched at lower temperature (90 ^{o}C). These effects could be reasonably explained by Hoffman theory and changes in crystallites and total amount of crystallinity.

Dahlan *et al.* [25] studied on the effect of liquid natural rubber (LNR) as a compatibilizer in binary blends of 60/40 NR/linear low-density polyethylene (LLDPE) blends to the morphology and thermal properties. It has been observed that increasing LNR content decreases T_m and ΔH_f which were indicators of the crystalline part of the blends. The decrease reflects a reduction in degree of crystallinity which was due to the interference in the form of NR dissolution into the LLDPE phase. The phenomenon leads to a shift in T_g of the amorphous part of LLDPE to higher temperatures as observed by DMA thermograms. The dissolution effect creates better interactions between the phases leading to improvements in the compatibility of the blends. Further confirmation was obtained through SEM examination.

Haijin *et al.* [26] studied on the influence of molecular architecture and melt rheological characteristic on the optical properties of low density polyethylene (LDPE) blown films. The three commercial LDPE blown film samples used in this study were LD1, LD2 and LD3. Density of LD1, LD2 and LD3 were 0.925, 0.923 and 0.919 g/cm^3 respectively. The three LDPE films to be tested were produced by blown film extrusion at the same conditions. It was found that the LDPE sample with higher haze value exhibits distinctly larger portion of higher molecular weight component, broader molar mass distribution, and significantly higher side chain branch density.

Mishra *et al.* [27] studied on effect of interchain crosslinking on the shrinkability of the blends consisting of grafted LDPE and carboxylated nitrile rubber (XNBR). Two samples had been prepared for this purpose; LDPE/XNBR blends without compatibilizer, and glycidyl acrylate (GA) grafted LDPE was blended with XNBR. The results indicated that interchain crosslinking in the grafted LDPE and XNBR improves the heat shrinkability. Here, crosslinked point between a rubber and plastic molecule served as a memory point during recovery process.

Mishra *et al.* [28] studied on the preparation of a heat shrinkable material from polycaprolactone (PCL) and epoxidized natural rubber (ENR) blend. The mixing formulations are PE5050, PE5050D and PE7030 (ratio as PCL:ENR:DCP). Effect of crosslinking by dicumyl peroxide (DCP) and rubber content on shrinkable behavior of the blends was studied. It was found that the crosslinking enhances the heat shrinkability of the blend, and in the case of uncrosslinked blend containing higher amount of rubber showed greater heat shrinkability.

Ismail *et al.* [29] studied to compare the mechanical and morphological properties of polypropylene (PP)/ NR and polypropylene (PP)/recycled rubber (RR) blends. Thermoplastic elastomers (TPEs) were prepared on brabender mixing was done at 190^{o}C and 50 rpm as various rubber contents in formulas. The results indicated that at a similar rubber content, PP/RR blend have higher, tensile strength and Young's modulus but lower elongation at break and stabilization torque than PP/NR blends. SEM examination of the tensile fracture surface of PP/RR blends indicated that a higher energy was needed to cause catastrophic failure compared to PP/NR blends.

Sirisinha *et al.* [30] studied on the influence of maleated ethylene propylene diene rubber (EPDM-g-MA) as a compatibilizer and a phenol-based antioxidant, on oil and thermal aging resistance in 50/50 chlorinated polyethylene (CPE)/NR blends. The results found that EPDM-g-MA could decrease phase size of the blend system, indicating compatibilizing effect. The optimal concentration of EPDM-g-MA was 1 phr. Beyond this concentration, phase size started to increase. The additions of phenolic antioxidant apparently decreased the phase size in blends. This was probably due to the improvement in the thermal stabilization of NR phase in blend providing by the antioxidant, which led to a reduction in phase coalescence during blending. In addition, the results of oil and thermal aging resistance were in good agreement with the morphological results, indicating that the oil resistance and thermal aging properties based on relative tensile strength in the 50/50 CPE/NR blend were strongly controlled by the size of the NR dispersed phase in CPE matrix. The smaller the dispersed phase size, the higher the resistance to oil and thermal aging.

Chowdhury *et al.* [31] studied on the correlations of structure, shrinkability and thermal properties in blends of ethylene vinyl acetate (EVA) and carboylated nitrile rubber (XNBR). Preparation of samples by dicumyl peroxide (DCP) cured blends of EVA and XNBR. The results indicated that shrinkability of the blends depended on the elastomer content, cure time and temperature. With increase in cure time, the shrinkage was found to decrease. With increase in elastomer content shrinkability increased up to a certain level of elastomer content (50%) and then decreased. High temperature stretched samples showed higher shrinkage than room temperature stretched samples. Blend composition and degree of orientation controlled the thermal stability of the blends. Increase in EVA (plastic) content i.e. crystallinity and increase in orientation of blends increased the thermal stability. The values of heat of fusion were consistent with the values of percent crystallinity.

Nakason *et al.* [32] studied on the effect of compatibilization, blend ratio and curing system to NR/HDPE blends. In this work, an attempt was made to prepare thermoplastic NRs (TPNRs) based on the blending of NR and HDPE via a dynamic vulcanization process. Various types of compatibilizer were studied in this work namely: un-modified: SP-1045, HRJ-10518 and modified phenolic resin: LNR, PhSP-PE and PhHRJ-PE. After suitable types of compatibilizer were found from the experiments, various blend ratios of NR/HDPE were 50/50, 60/40 and 70/30. Furthermore, three vulcanization systems (sulphur, peroxide and mixed curing systems) were used to prepare the thermoplastic vulcanizates (TPVs) via a dynamic vulcanization. The results were found that TPVs with modified phenolic resin compatibilizers showed higher tensile strength and elongation at break than those of the TPVs with un-modified phenolic resin and without compatibilizer. This may be attributed to chroman ring structure from the reaction of NR and phenolic molecules. Therefore, it was found that the TPV with PhHRJ-PE gave a highest tensile strength and elongation at break. Increasing the content of the NR gave an increased trended to elongation at break but decreasing trends in permanent set (expressed as tension set), tensile strength and hardness. Various vulcanization systems were also used to prepare TPV, with a mixed curing system showing the highest shear stress and tensile strength, whilst the sulphur curing system gave the lowest values, and the peroxide curing system exhibited intermediate values.

Radhesh *et al.* [33] studied on the LDPE-based thermoplastic elastomers (TPEs) containing ground tire rubber (GTR) with and without dynamic curing. TPEs composed of LDPE, fresh rubber (EPDM, NR and SBR) and GTR (particle size 0.4-0.7mm) with and without curing. Dynamic vulcanization occurred either by sulphur or by peroxide curatives. Investigation the result on the thermo mechanical and mechanical properties of TPEs, the best performance was achieved by recipes containing GTR^M and EPDM after dynamic vulcanization with sulphur. The ethylene segments of the EPDM were compatible with LDPE. Dynamic curing by sulphur was traced to an interfacial crosslinking via formation of sulphur bridges between the GTR particles and EPDM.

CHAPTER III

EXPERIMENTAL

3.1 Chemicals

3.1.1 LDPE grade D2022, melt flow index 0.25 g/10 min, density 0.92g/cm^2, process temperature 170-230 ^{o}C from TPI polene thailand.

3.1.2 RR powder (recycle NR mattress) from latex systems company

3.1.3 NR latex (60% DRC and low ammonia). The percentage of dry rubber content (% DRC) of LA-NR is 60 from thai rubber latex company

3.2 Apparatus

Apparatus	Brand, model and Country
Differential scanning calorimeter (DSC)	Netzsch model 204F Phoenix, Germany
X-ray diffractometer (XRD)	Bruker model X8APEX , German
Twin screw extruder (single layer)	Pilot scale JSW TEX 30α, Japan
Internal mixer	HAAKE, German
Blown film extrusion	HAAKE polylab OS-torque rheometer
Scanning electron microscopy (SEM)	JEOL model JSM-5410LV, Japan
Circulate oven	Memmert model UWB400, German
Universal tensile machine (UTM)	Instron model 5565,USA
Impact tester (free falling dart)	Instron model DX-8165A, USA
Transparent test	M57 spherical haze meter, UK.
Dynamic mechanical analysis (DMA)	Netzsch model 242, Germany
Hardness test	Instron model 930/250, USA

3.3 Procedures

3.3.1 Preparation of RR/LDPE Blend

The formulations of LDPE and RR powder are also presented in Table 3.1. Then, the blend was subjected to an injection as condition shown in Table 3.1 and the polymer blend was extruded by blown film extrusion single layer system model HAAKE polylab OS-torque rheometer as condition shown in Table 3.2.

Table 3.1 Blend formulations of RR

Blends code	LD0	LD0.5	LD1	LD2	LD5
LDPE (phr)	100	100	100	100	100
RR powder (phr)	0	0.5	1	2	5

Table 3.2 Condition for injection and blown film extrusions

Condition	Injection	Blown film extrusion
Screw speed (rpm)	50	60
Temperature (^{o}C)	Feed zone 190-200, Screw zone 220-240, Die zone 240-250	Feed zone 180-190, Screw zone 210-230, Die zone 230-240
Drawn speed (%)		200-250
Film width (cm)		10
Film thickness (μm)		30

3.3.2 Preparation of NR/LDPE Blend

LDPE and NR latex were directly mixed in a beaker and then ovened in circulated oven under the temperature of 80°C for 30 min. The procedure for preparation of polymer blend and formulations of the blend are also presented in Table 3.3. Then, the obtained product was subjected to an internal mixer and after that the polymer blend was extruded by blown film extrusion single layer system model HAAKE polylab OS-torque rheometer as condition as shown in Table 3.4. The best condition to NR/LDPE blend is a screw speed of 50 rpm at 160 °C for 7 min [28] and maximum torque is 55-83 Nm.

Table 3.3 Blend formulations of NR latex

Blends code	LD0	LD1	LD5	LD7.5
LDPE (phr)	100	100	100	100
NR latex (phr)	0	1	5	7.5

Table 3.4 Condition for internal mixer and blown film extrusion conditions

Condition	Internal mixer	Blown film extrusion
Time for mixing (min)	7,8,9,10	-
Screw speed (rpm)	40, 50	60
Temperature (°C)	160, 175, 180	Feed zone 180-190, Screw zone 210-230, Die zone 230-240
Drawing speed (%)		200-250
Film width (cm)		10
Film thickness (μm)		30

The schematic of blown film extrusion is shown in Scheme 2. The film is stretched in the longitudinal and circumferential directions during production, resulting in biaxial orientation of the film [3].

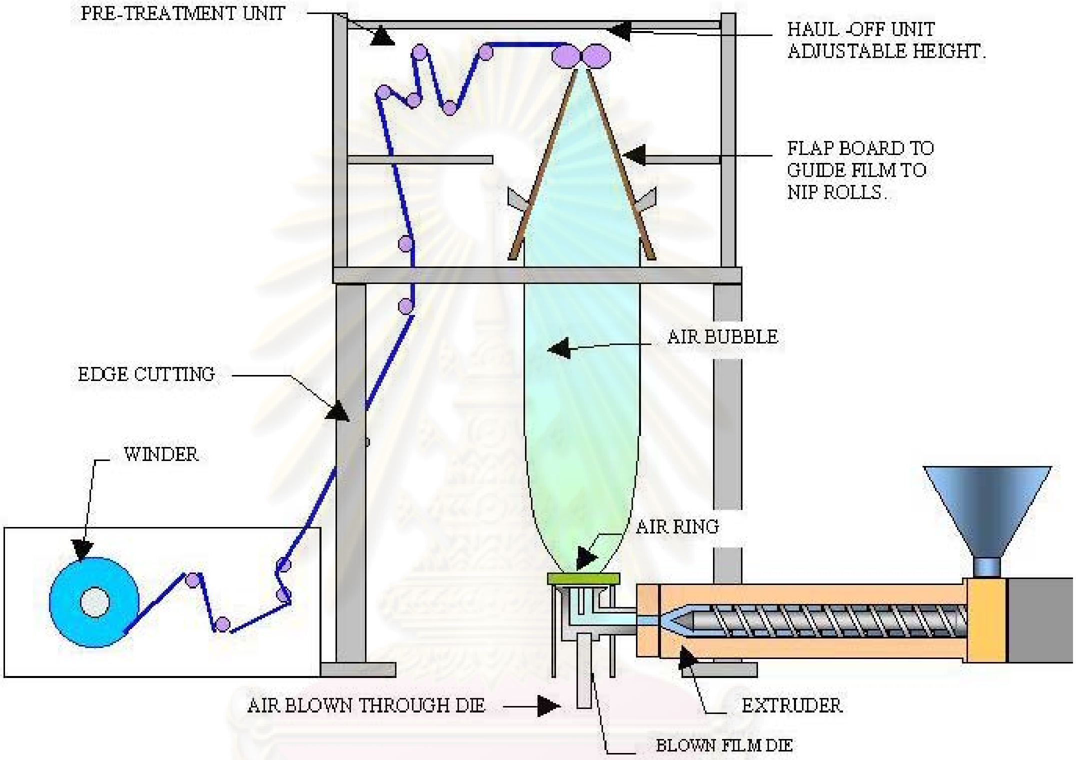

Scheme 2 Schematic of blown film extrusion process.

3.3.3 Physical Properties of NR/LDPE Blown Film

3.3.3.1 Transparency Testing [14]

Transparency provides a measure of the clarity of a film sample. The test provides a measure of the amount of incident light that passes through a film sample without being scattered. The commercial film interest has a range of transparency of about 10 – 90% as measured by this test. Films with higher values are called transparent; films with lower values are called translucent. Transparency is a property that highly depends on the degree of crystallinity in the polymer resin. It is common practice to an attempt to minimize crystallinity, hence improve clarity. In this study, the transparency tests were measured by M57 spherical haze meter. Transparency tests were carried out according to ASTM D1746. The samples used were 50 mm in diameter. The sample shall have substantially plane-parallel surfaces free of dust, grease, scratches, and blemishes. The values reported for each sample were based on an average of fifth measurements.

3.3.4 Density Test [14]

The density of a material is the mass per unit volume. The SI unit of density is kg/m^3. Density test was carried out according to ASTM D1622. The samples used were 5x10^{-6}m^3 in volume. Weight the test specimen on an analytical balance and record. The values reported for each sample were based on an average of five measurements. Calculate the density of sample as follow:

$$D = \frac{W_s}{V} \tag{3.1}$$

where D is density of specimen (kg/m^3), W_s is weight of specimen (kg) and V is volume of specimen (m^3)

3.3.5 X-ray Diffraction (XRD) [34]

XRD is a non-destructive analytical technique which provides detailed information about the internal lattice of crystalline substances, including unit cell dimensions, bond-lengths, bond-angles, and details of site-ordering. Directly related is single-crystal refinement, where the data generated from the X-ray analysis is interpreted and refined to obtain the crystal structure. X-ray diffraction is based on constructive interference of monochromatic X-rays and a crystalline sample. These X-rays are generated by a cathode ray tube, filtered to produce monochromatic radiation, collimated to concentrate, and directed toward the sample. The interaction of the incident rays with the sample produces constructive interference (and a diffracted ray) when conditions satisfy Bragg's Law ($n\lambda=2d\sin\theta$). This law relates the wavelength of electromagnetic radiation to the diffraction angle and the lattice spacing in a crystalline sample. These diffracted X-rays are then detected, processed and counted. By changing the geometry of the incident rays, the orientation of the centered crystal and the detector, all possible diffraction directions of the lattice should be attained. All diffraction methods are based on generation of X-rays in an X-ray tube. These X-rays are directed at the sample, and the diffracted rays are collected. A key component of all diffraction is the angle between the incident and diffracted rays. Powder and SC-diffraction vary in instrumentation beyond this.

In this study, the XRD of shrink films were recorded with a bruker model X8APEX diffractometer using Cu K_α radiation in the angular range 5-45^o (2θ) at an operating voltage 40 kV. The generator current was 40 mA and the scan speed was 0.5 sec/step. SC-XRD study was carried out to get an idea of crystallinity of the blends as affected by rearrangement during blown film extrusion process. The area under the crystalline and amorphous portion was determined in arbitrary units and the degree of crystallinity (X_c) measured using the relation,

$$X_c = \frac{I_c}{I_a + I_c} \qquad (3.2)$$

where I_a and I_c are the integrated intensity corresponding to the amorphous and crystalline phases, respectively.

3.3.6 Morphology Test

3.3.6.1 Scanning Electron Microscopy (SEM) [5]

SEM used to examine the surfaces molded samples, fracture surfaces, or the interior of sample revealed by microtomy. It relies on differences in surface photography to create the image. Smooth samples may be etched to create surface texture representative of the sample, using various forms to radiation, solvents, acids, or bases. Etching tends to remove amorphous regions, leaving crystallites or other more resistant regions standing slightly proud of the surface. In this study, the morphology of fracture surface of NR/LDPE blend compound and NR/LDPE film was examined by SEM, JEOL model JSM 5410LM. The sample was staining with osmium tetraoxide (OsO_4) and sputter coater was used to pre-coat conductive gold onto the fractured surfaces before observing under the micrographs. The acceleration voltage was 15 kV.

3.3.7 Dynamic Mechanical Analysis (DMA) [35]

DMA measures the elastic modulus or storage modulus (E'), viscous modulus or loss modulus (E'') and damping coefficient (tan δ) of a material. The storage modulus depends on the mechanical properties of the material and its dimensions. It is frequently converted to a modulus to enable sample intercomparisons. Damping is expressed in terms of tan δ and is related to the mechanical properties change dramatically when relaxation behavior is observed. DMA yields information about the mechanical properties of a sample placed in minor, usually sinusoidal and oscillating force as illustrate in Figure 3.1. DMA is the most sensitive technique for monitoring relaxation events, such as glass transitions.

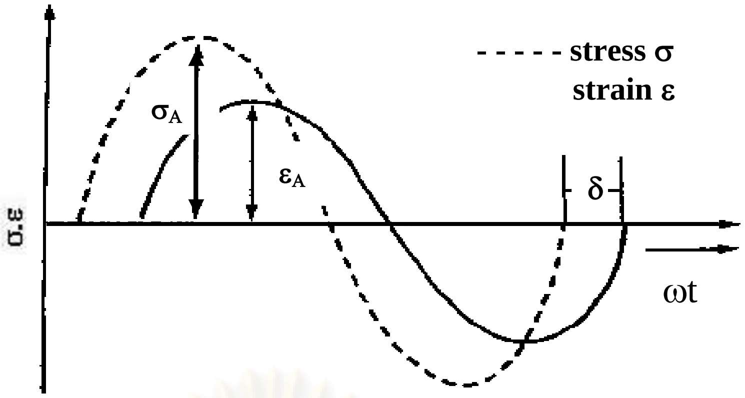

Figure 3.1 Sinusoidal oscillation and reponse of a linear-viscoelastic material; δ=phase angle.

Dynamic mechanical properties of rubber vulcanizates were measured under a tension mode by a dynamic mechanical analyzer GABO (EPLEXOR QC 25). Rectangular sample of 20 x 5 x 2 mm was subjected to sinusoidal loading heated from -120 $^{\circ}$C to 150 $^{\circ}$C at scanning rate, dynamic strain and test frequency of 10 $^{\circ}$C/min, 0.5% and 10 Hz, respectively.

3.3.8 Differential Scanning Calorimetry (DSC) [5]

The thermal studies of NR/LDPE films were examined by a differential scanning calorimeter (DSC), Netzsch model 204F Phoenix (Germany). The 10 mg of sample were weighed exactly and put in an aluminum pan with a cover under nitrogen atmosphere in a temperature range of 0 – 230 $^{\circ}$C at heating rate of 10 k/min. The melting temperature (T_m) was determined as the peak temperature and the enthalpy of fusion (ΔH_m) was determined from the area of DSC endotherm. A computer provides the results as a function of temperature. Thermograms provide information regarding the transitions that polymers pass through in the temperature range of interest. A schematic example of DSC thermogram is shown in Figure 3.2.

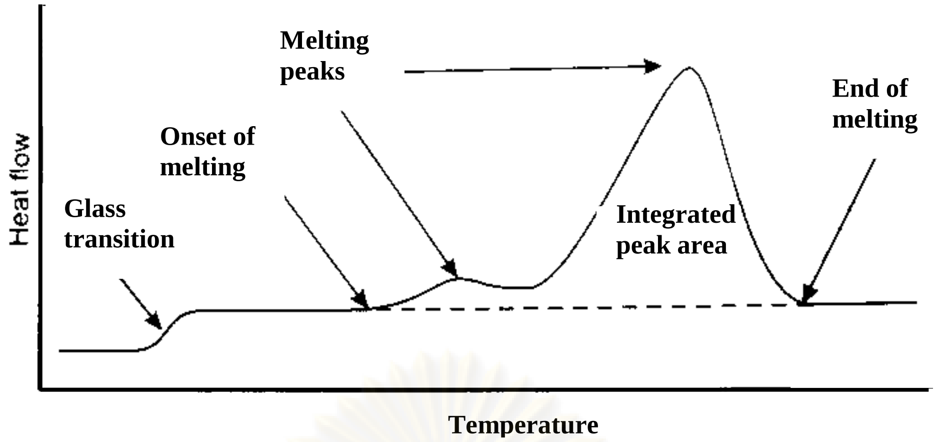

Figure 3.2 Schematic representation of a differential scanning calorimetry thermogram.

The degree of crystallinity was calculated via the total enthalpy method, according to the following equation:

$$X_C = \Delta H_m / \Delta H^{+}_m$$

where X_c is the degree of crystallinity, ΔH_m is the enthalpy of fusion, and ΔH^{+}_m is the enthalpy of fusion for100% crystalline polyethylene. The ΔH^{+}_m value for 100% crystalline polyethylene is taken as 288 kJ/kg.

3.3.9 Mechanical Properties

3.3.9.1 Tensile Testing [36]

Tensile measurement is among the most important indications of strength in a material and the most widely specified properties of plastic materials. Tensile test, in broad sense, is a measurement of the ability of a material to withstand forces that tend to pull it apart and to determine to what extent the material stretches before breaking. The tensile property data are most useful in preferential selection of a particular type of plastic from a large group of plastic materials and such data are of limited use in actual design of the product. In this study, the tensile properties were measured by a Universal Testing Machine (UTM), Instron model 5565. Tensile tests were carried out according to ASTM D 882. The films were conditioned to 23±2 °C and 50±5% relative humidity for 40 h prior to test. The sample was stretched vertically in a symmetric mode. The samples used were 250 mm in gauge length, 50 mm in width and 30 μm in thickness. The crosshead speed was set at 50 mm/min with load cell 5 kN. The test was operated at room temperature. The values reported for each sample were based on an average of fifteen measurements.

3.3.9.2 Hardness [36]

Hardness is defined as the resistance of a material to penetrate, particularly permanent deformation, indentation, or scratching. Hardness is purely a relative term and should not be confused with wear and abrasion resistance of plastic materials. Hardness tests can differentiate the relative hardness of different grades of particular plastic. Many tests have been devised to measure hardness. Because plastic materials vary considerably with respect to hardness, one type of hardness test does not cover the entire range of hardness properties encountered. Two of most commonly used tests for plastics are the rockwell and the durometer hardness test. For softer materials such as flexible PVC, thermoplastic rubber and polyethylene, durometer hardness is measured. In this study, the hardness testing was measured by using an Instron hardness tester shore-type-D (model 930/250) according to ASTM D 2240. The test temperature was carried out at room temperature. The measurements were taken from five different points distributed over the sample and the reported were based on an average of five measurements.

3.3.9.3 Tearing Test [37]

The measurement of the tear strength of a material evaluates the energy absorbed by the sample during tear initiation and/or propagation. The value of tear strength of a film depends on the orientation stretching ratio, and whether the measurement is performed along the machine direction and cross direction using a tensile apparatus. In this study, the tearing tests were measured by an Instron Universal Testing Machine (model 5565) according to ASTM D1938.

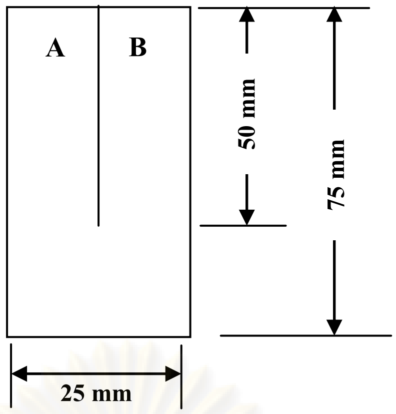

Figure 3.3 Single-tear specimen.

The specimen shape was showed in Figure 3.3. Secure A part (see Figure 3.3) in one grip and B part in the other grip of the constant rate-of-grip separation-testing machine, using an initial grip separation of 50 mm. Align the specimen so that its major axis coincides with an imaginary line joining the centers of the grips. Using a grip-separation speed of 250 mm/min, start the instrument, and record the load versus extension. Continue the test until the tear has propagated through the entire slit 25 mm portion. Mean of the fifteen average tear-propagation determinations.

3.3.9.4 Impact Resistance [36]

The impact properties of the polymeric materials are directly related to the overall toughness of material. Toughness is defined as the ability of the polymer to absorb applied energy. Impact resistance is the ability of a material to resist breaking under a shock loading or the ability to resist the fracture under stress applied at high speed. The theory behind toughness and brittleness of the polymers is very complex and therefore difficult to understand. The molecular flexibility plays an important role in determining the relative brittleness or toughness of material.

In this study, the impact strength tests were measured by dart drop impact machine, Instron model DX-8165A according to ASTM D 1709 (method A). The samples used were 12.7 cm in diameter circular. The film specimen is clamped into the base of an apparatus. Then a blunt, metal dart is dropped onto the specimen from a specified height. If the specimen fails, some weight is removed from the dart and the test is repeated with a new specimen. If the specimen does not fail, some weight is added to the dart and the test is repeated. This process continues until a statistically valid number of specimens are tested resulting in the nominal weight to failure. Calculate the impact failure weight W_F as follows:

$$W_F = W_0 + [\Delta W\,(A/N - 1/2)] \qquad (3.3)$$

where W_F is impact failure weight (g), W_0 is the first of missile weight to failure film, ΔW is uniform weight increment used (g), A is constant value (15), and N is constant value (10).

3.3.10 Shrinkability Test [38]

Shrinkability test is the change in length of an unrestrained film sample subjected to a specific elevated temperature. The shrinkage of the films is based on the relaxation of the orientation stresses introduced in the film during the production of the film. The relaxation causes a good enclosure of the package. In this study, sample of film shall be conditioned for minimum of 2 h in standard atmosphere prior to cutting out and measuring test by circulated oven, memmert model UWB400. The sample shape was showed in Figure 3.4 and cutting the film for test in two directions (MD: machine direction and TD: transverse direction). The test sample is placed in a hot oven and subsequently cooled down to room temperature. MD and TD values are evaluated and reported separately. Units are reported as percentage change from the original dimension (shrinkage). The method and calculation of percentage of shrinkability was measured according to ISO 1150.

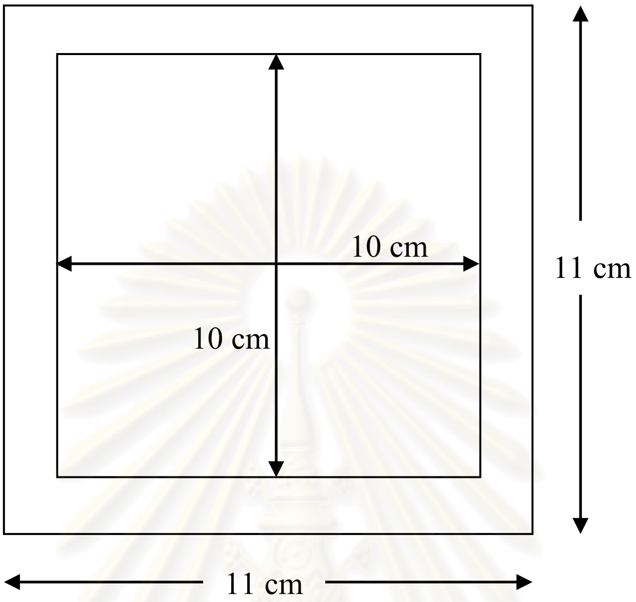

Figure 3.4 Film specimens for shrinkage test.

CHAPTER IV

RESULTS AND DISCUSSION

4.1 The Effect of Rubber Type on the Blown Film Process

4.1.1 Reclaimed Rubber

Figure 4.1 shows the appearance of RR/LDPE blend compounds at various ratios of RR (0.5, 1, 2 and 5 phr) after extruding by using twin screw extruder. The surface of RR/LDPE blend compounds was clearly rough when the RR content is increased. The obtained polymer blend compound was then subjected to the blown film process and the appearance of RR/LDPE film was shown in Figure 4.2. It is clearly seen that the RR particles (bright spot) were well distribute in LDPE matrix. As it can be seen that RR particle could not be dispersed in LDPE matrix, due to the crosslinked structure, these RR in this study was not suitable to use as filler in the shrink film. The crosslink particles are result in rough surface and low transparency, which are needed properties in shrink film production. In order to overcome these problems, NR latex was chosen to replace the RR. The general properties of NR latex are similar to RR, however; for the safety reason, NR latex used in this process was unvulcanized. The excellent properties of NR latex are good elasticity and flexibility material. The advantages of NR latex include the ability to be processed on thermoplastics machinery without requiring vulcanization [39].

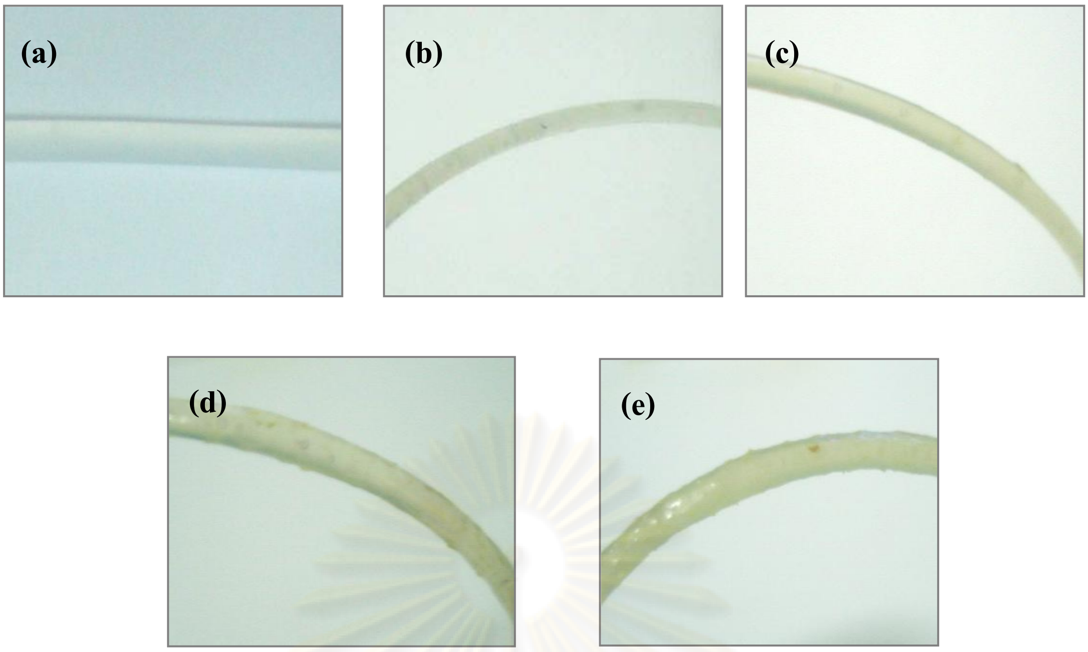

Figure 4.1 The appearance of neat LDPE and RR/LDPE blend compounds: (a) neat LDPE, (b) RR 0.5 phr, (c) RR 1 phr, (d) RR 2 phr and (e) RR5 phr.

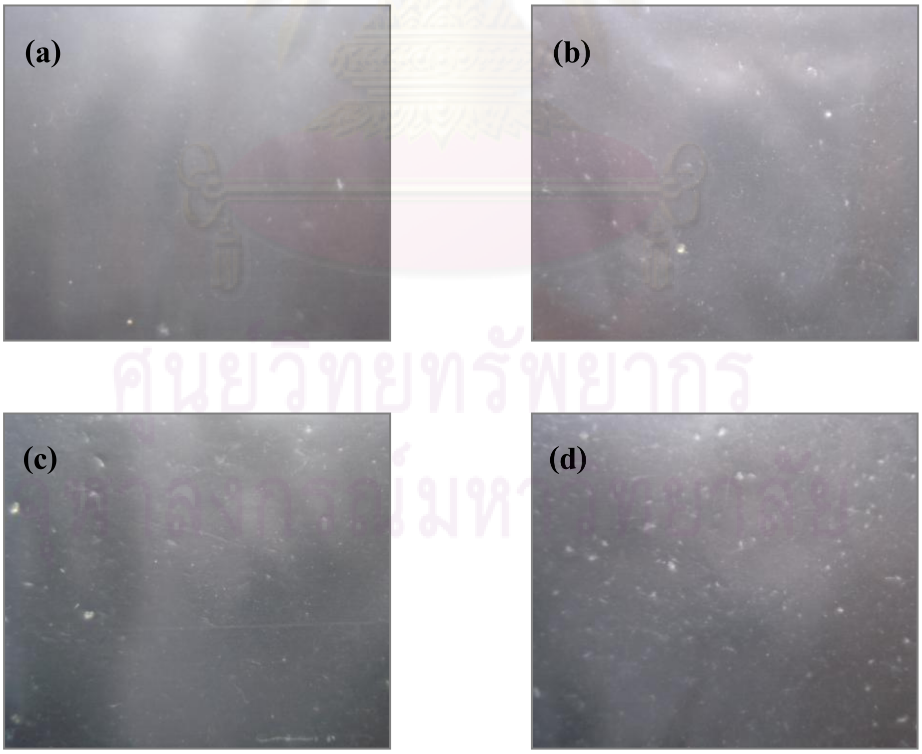

Figure 4.2 The appearance of RR/LDPE films: (a) RR 0.5 phr, (b) RR 1 phr, (c) RR 2 phr and (d) RR 5 phr.

4.1.2 NR Latex

Figure 4.3 shows the appearance of neat LDPE and NR/LDPE blend compounds at various ratios of NR contents (1, 5 and 7.5 phr) after blending in HAAKE internal mixer. It is clearly seen that both components of the compound were compatible and the color of compound become more yellow when the NR latex content was increased. After the NR/LDPE blend, compound was subjected to the blown film process. The appearance of NR/LDPE film was shown in Figure 4.4. The film surface was smooth and the color of film was similar to the NR/LDPE blend compounds. However, the maximum content NR add into LDPE was at 7.5 phr. In this experiment, film can not be blown if NR content was 7.5 phr. Based on this result, we could prepare the good appearance film, i.e., smooth surface and transparent. Additionally, the unmelted NR latex was not observed.

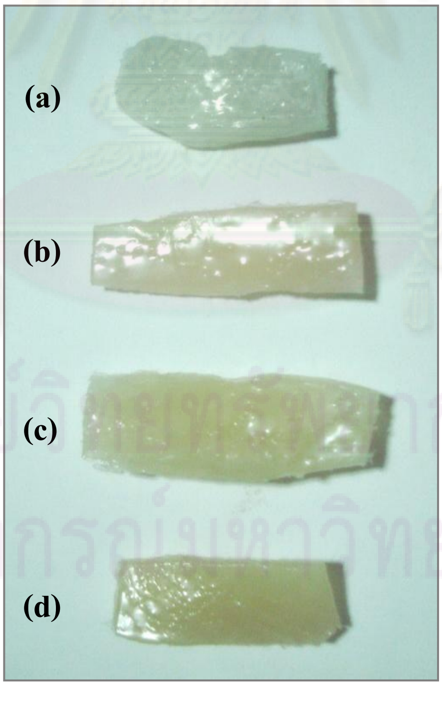

Figure 4.3 The appearance of NR/LDPE blend compounds: (a) neat LDPE, (b) NR 1 phr, (c) NR 5 phr and (d) NR 7.5 phr.

4.2 Morphology of NR/LDPE Blend Compound and NR/LDPE Film

Due to the high temperature (~ 160 °C) for the processing of polymer blend, NR may be degrade during mixing with LDPE. Therefore, the morphologies of NR/LDPE blend compounds before blown film process were investigated by SEM after staining with osmium tetraoxide (OsO_4) and the SEM images was shown in Figure 4.4. The dark area indicated LDPE matrix, which was not active with OsO_4, while the white spots denoted NR particles, which was react with OsO_4. Scheme 3 shows the reaction of OsO_4 with double bond of NR. OsO_4 can react specifically with double bonds of NR in order to form an osmate ester [10].

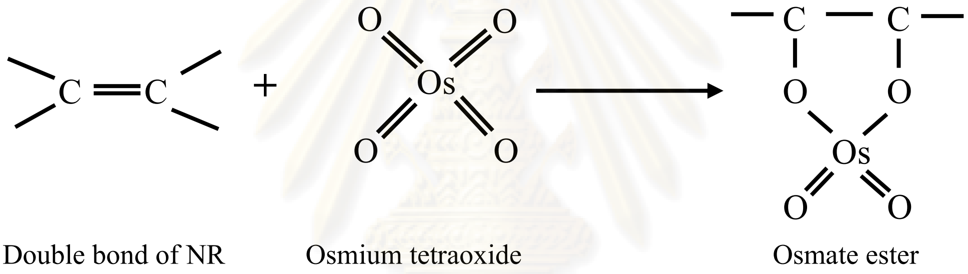

Scheme 3 The reaction of osmium tetraoxide with double bond [10].

From Figure 4.4, the shape of NR was in a regular spherical of small size. For all ratios of NR content in LDPE blend, the white spots increased with increasing NR contents. At small NR contents, the NR particles were well dispersed in LDPE matrix; however, when the NR contents increased, they could be broken in small particle. These observations confirmed that the mixing condition used in this study was suitable for controlling the distribution of NR particles in LDPE matrix.

The SEM images of LDPE and NR/LDPE films are shown in Figure 4.5, The white spots representing NR particles distributed in the LDPE matrix (black area). It is evidence that many NR particles seemed to be covered with LDPE, and the boundary between the NR and LDPE was not so sharp comparing with NR/LDPE compound (Figure 4.4). It is may b due to the degradation of N particles during blown film process. This result was indicated the outer surface of NR particles could insert in LDPE matrix. The NR chains were entanglement and interlog with LDPE chain. Consequently, NR phase was still remaining in the LDPE matrix and NR was able to crystallize during blown film process. The proposed mechanism of strain induced crystallization will be explained in the next section.

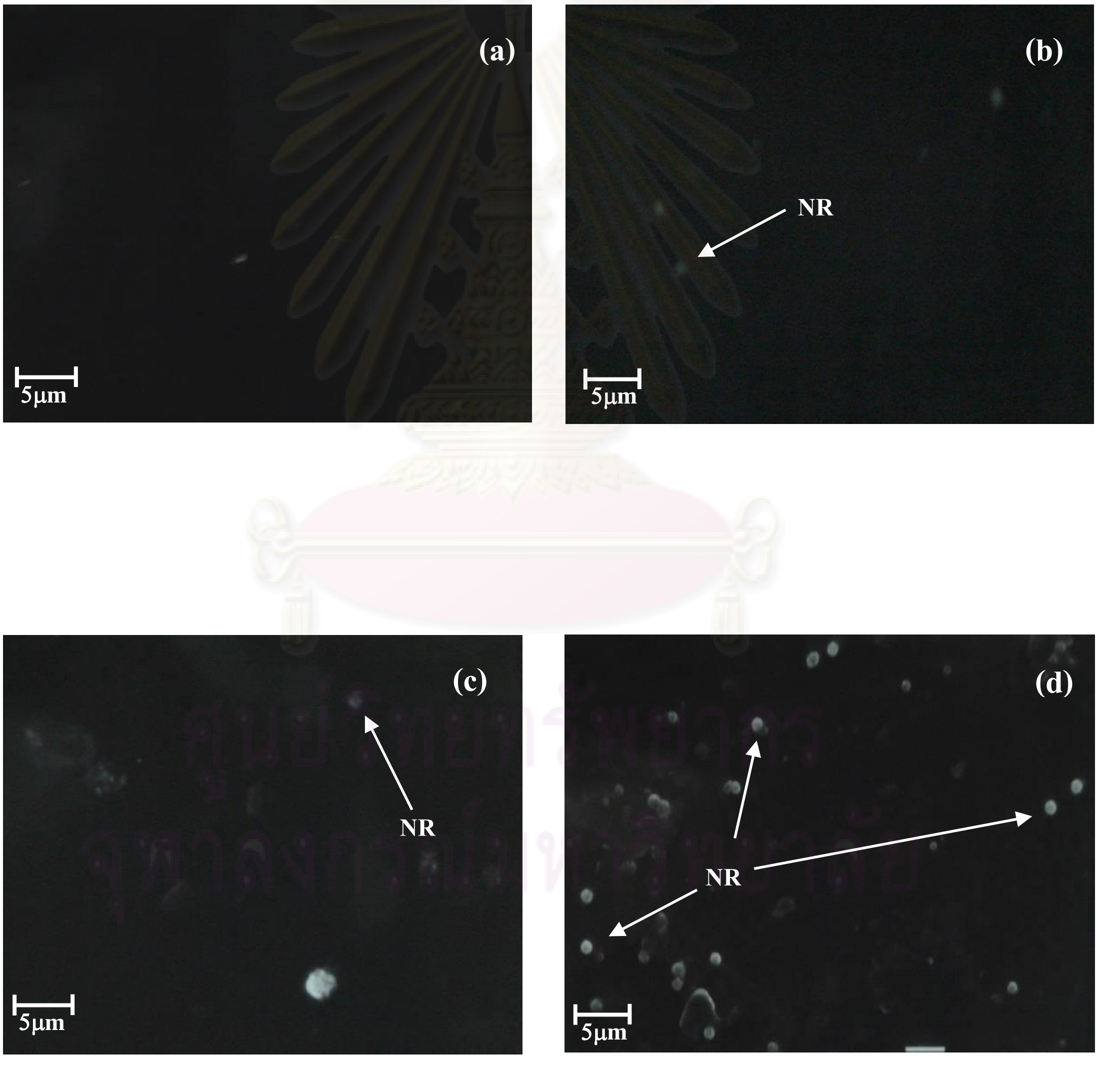

Figure 4.4 The SEM images of NR/LDPE blend compounds staining with vapour of OsO_4 (x 5000 magnification): (a) LD0, (b) LD1, (c) LD5 and (d) LD7.5.

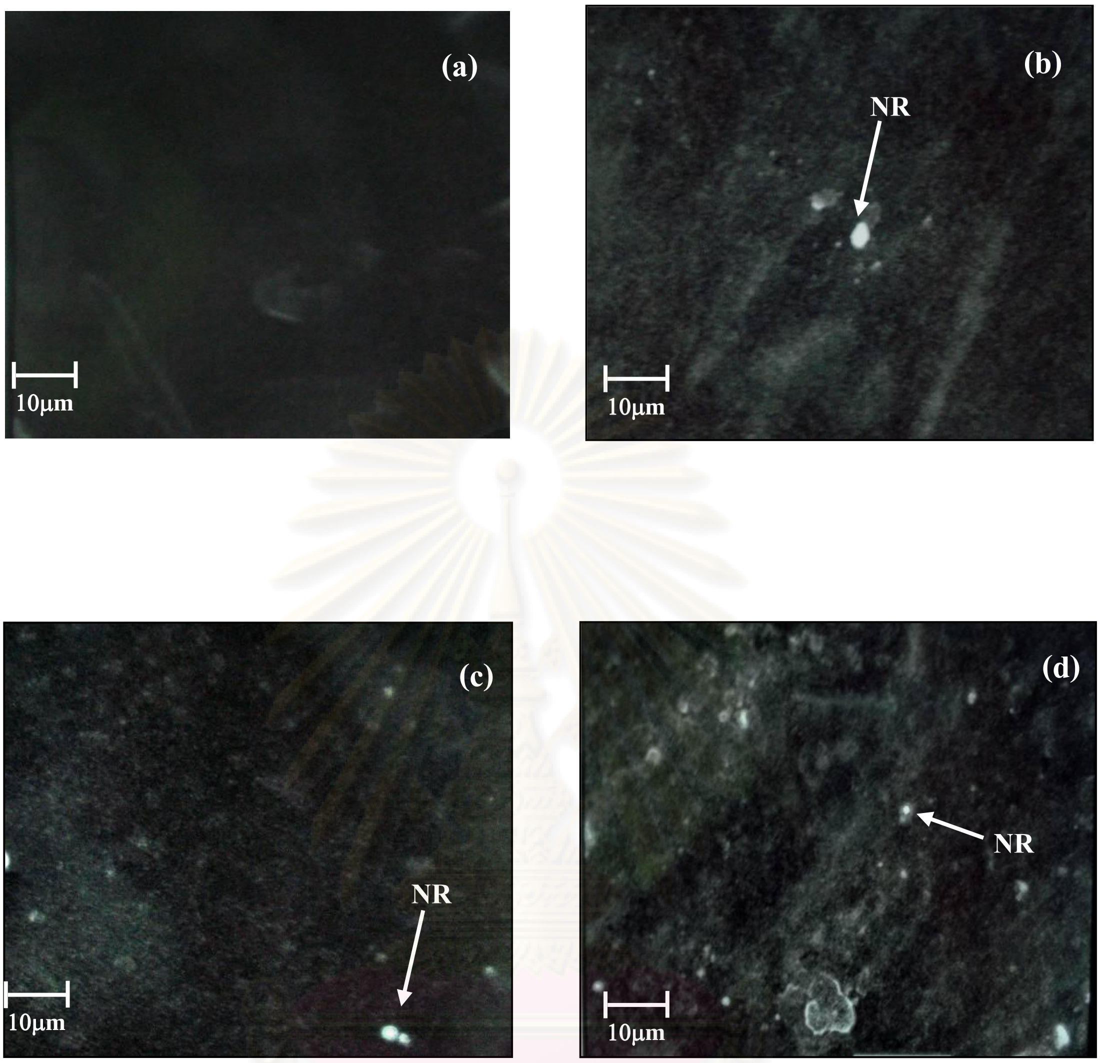

Figure 4.5 The SEM images of NR/LDPE film staining with vapour of OsO_4 for 3 hrs (x 1000 magnification): (a) LD0, (b) LD1, (c) LD5 and (d) LD7.5.

4.3 Physical and Optical Properties of the NR/LDPE Film

The physical and optical properties of NR/LDPE film were summarized in Table 4.1. The percentage of clarity of NR/LDPE films for all samples with and without adding NR latex were about 93%. This result clearly indicated that the addition of NR latex in LDPE matrix was not affected the clarity of film. However, the color of film was slightly changed from colorless to yellow when the NR content was increased as seen in Figure 4.6. This behavior caused the constituent in raw NR latex, hence β-carotene. The β-carotene is the chromatic in NR latex and it indicates the color from pale yellow to brown depending on type of latex tree [40]. The rubber products are generally sensitive to color of finish product that needs to extract the β-carotene in NR latex before use in process via the bleaching agent, i.e., xylyl mercaptan (0.05% wt) or tolyl mercaptan (0.05% wt) and sodium bisulfite (0.5-0.75% wt) [12].

The degree of crystallinity of NR/LDPE film was summarized in Table 4.1. The degree of crystallinity of NR/LDPE film increased with increasing NR contents. In the blowing film process, the orientation of polymer chains occurred in the melt state as the result of shear stress in the die as well as of stretching during the film blowing. The film was stretched in the longitudinal and circumferential directions during the production, resulting in a biaxial orientation of the film. Biaxial orientation means that polymer chains were aligned in the plane of the film in both the machine direction (MD) and the transverse direction (TD) [14]. Virtually, all thermoplastics can be oriented to some extent, but one can orient amorphous materials more readily than crystalline one [25]. The stretching process frequently induces the crystallization of NR and increases the crystallization of LDPE [3]. Additionally, the role of deformation on the crystallization has been rationalized in terms of enthalpic and entropic differences between deformed and undeformed melt. Both the enthalpy and entropy of a polymer melt are altered by the application of a large orienting deformation [41].

In this study, both LDPE and NR can be oriented in the direction of applied stress. During the stretching process, the orientation behaviour of LDPE can be divided into three stages: elasticity (% strain = 0 to 15), strain softening (% strain = 15 to 40) and plastic stage (% strain = 40 to 110), respectively. The plastic stage implies that the degree of crystallization increases, owing to the orientation of chains and molecules [42].

NR has been extensively studied not only as a unique elastic material but also as a crystalline polymer. NR tends to crystallize spontaneously when it is keep at low temperature [43] or when it is stretched at high deformation [44]. Luch *et al.* [45] studied the morphology of strain-induced crystallization of uncrosslinked NR by using electron microscopy. It was found that when stretched uncrosslinked NR film to elongation grater than about 200%, the NR film showed distinct fibrillar morphology at room temperature.

As polymer melt extruded from annular die and consequently blown exceeding to the frozen line, LDPE chains were elongated, both in MD and TD. At the same time NR chains were also extended. After the frozen line, LDPE molecule was cooled down to room temperature and subsequently frozen. At this stage, NR chains were immobilized, under stretched, by interpenetrated through LDPE chain at some certain extent around rubber particles, the boundary between the NR and LDPE was blur. This result corresponding to the SEM images of NR/LDPE films are shown in Figure 4.5. Accordingly, we tried to propose the mechanism of strain-induced crystalline in NR/LDPE film during a blown film process as seen in Figure 4.7. Under the condition at blown film process used in this study the NR/LDPE film was drawn over than 40% elongation, resulting in the LDPE crystallization started firstly. With the increase of strain, the equilibrium distribution of chain conformations was perturbed under the stress, making it possible to achieve the low energy conformations. These results in chain orientation were extension and then a sufficient number of chains were aligned. Both NR and LDPE were able to produce the crystalline during stretching process. Further extension, the LDPE crystallines were acting as nuclei to induce the crystallization of neighbor NR molecules for starting the crystal growth. Accordingly, when the NR content increased, the degree of crystallinity was also increased as seen in Table 4.1.

Table 4.1 Physical, optical properties and degree of crystallinity of NR/LDPE film

Properties of film	LD0	LD1	LD5	LD7.5
Clarity (%)	93.4±0.2	93.2±0.2	93.5±0.2	93.1±0.2
Color	colorless	Pale yellow	Pale yellow	Yellow
Degree of crystallinity[1] (%)	9.6	20.1	23.6	31.2
Density (g/cm^3)	0.922	0.922	0.923	0.922

[1] from XRD measurement

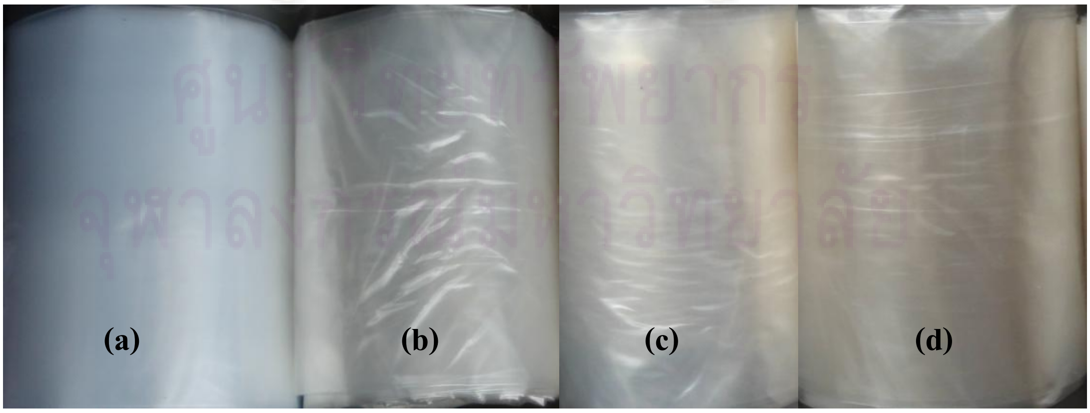

Figure 4.6 The appearance of neat LDPE and NR/LDPE films:(a) LD0, (b) LD1, (c) LD5 and (d) LD7.5.

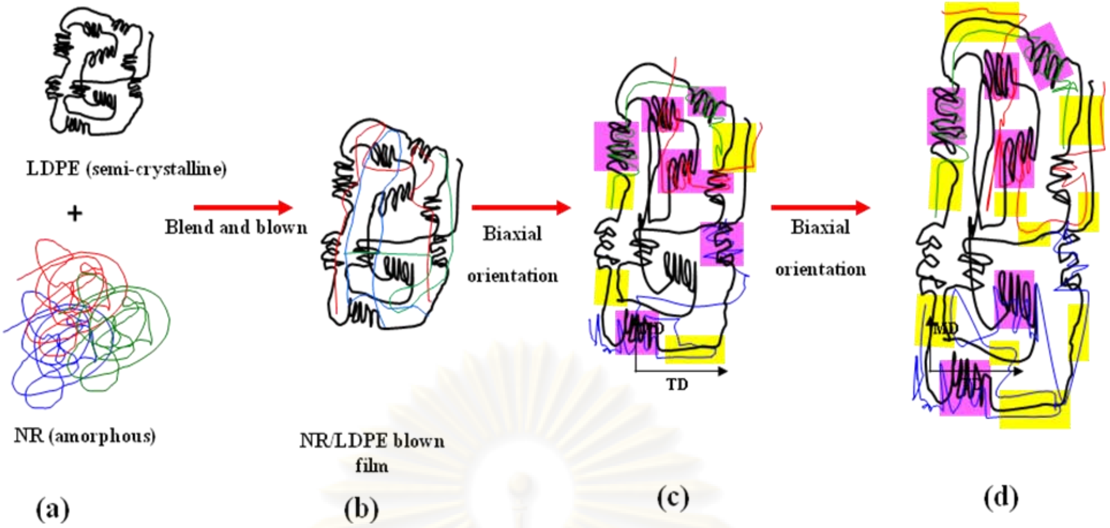

Figure 4.7 Proposed mechanism of stain-induced crystallization in NR/LDPE film during a blown film process: (a) before stretching, (b) the interpenetration between LDPE and NR in NR/LDPE film and (c) the extension more than 40%, stretched chains of LDPE acting as the nucleus of crystallites (yellow part) and LDPE crystallites induced crystallization of NR (pink part) and (d) the extension range more than 200%, (MD: machine direction, TD: transverse direction).

4.4 Dynamics Mechanical Analysis of NR/LDPE Film

The viscoelastic behavior of NR/LDPE film was examined by using DMA. Figure 4.8 shows the dynamic mechanical properties a function of temperature for neat LDPE and NR/LDPE film. The E' is not only a measurement of the energy stored during the deformation (elastic behavior) but also the stiffness of the materials, while E'' is a measure of the energy stored during the deformation, usually as heat (viscous behaviour) [46] and can define the phase separation of polymer. The tan δ is a fraction of mechanical energy dissipated as heat during loading per unloading cycle [47]. Figure 4.8 (a) it is clearly seen that E' values at any given temperature of neat LDPE (LD0) showed the highest values when compared with the E' values of NR/LDPE films. The E' values of NR/LDPE film trended to be decreased with increasing NR contents. This result indicated that LD0 was stiffer than NR/LDPE film due to the LDPE as the semicrystalline material [48].

From Figure 4.8 (b), it is clearly seen that LD0 shows a peak around -6.7 °C whereas NR/LDPE films (LD1 and LD5) showed two transition peaks around -15 °C and -60 °C and only one strong broad peak at -57 °C was appeared I LD7.5 du to the long time for relaxation. This result indicated that the immiscibility and incompatibility between the LDPE and NR phases.

As seen in Figure 4.8(c) the maximum peak of tan δ of LD0, LD1 and LD5 show only one peak, while tan δ of LD7.5 was presented two peaks at -60 and 100 °C. This result indicated that the phase separation occurred in the polymer blend. The maximum peak at -60 °C was related the T_g of NR [49].

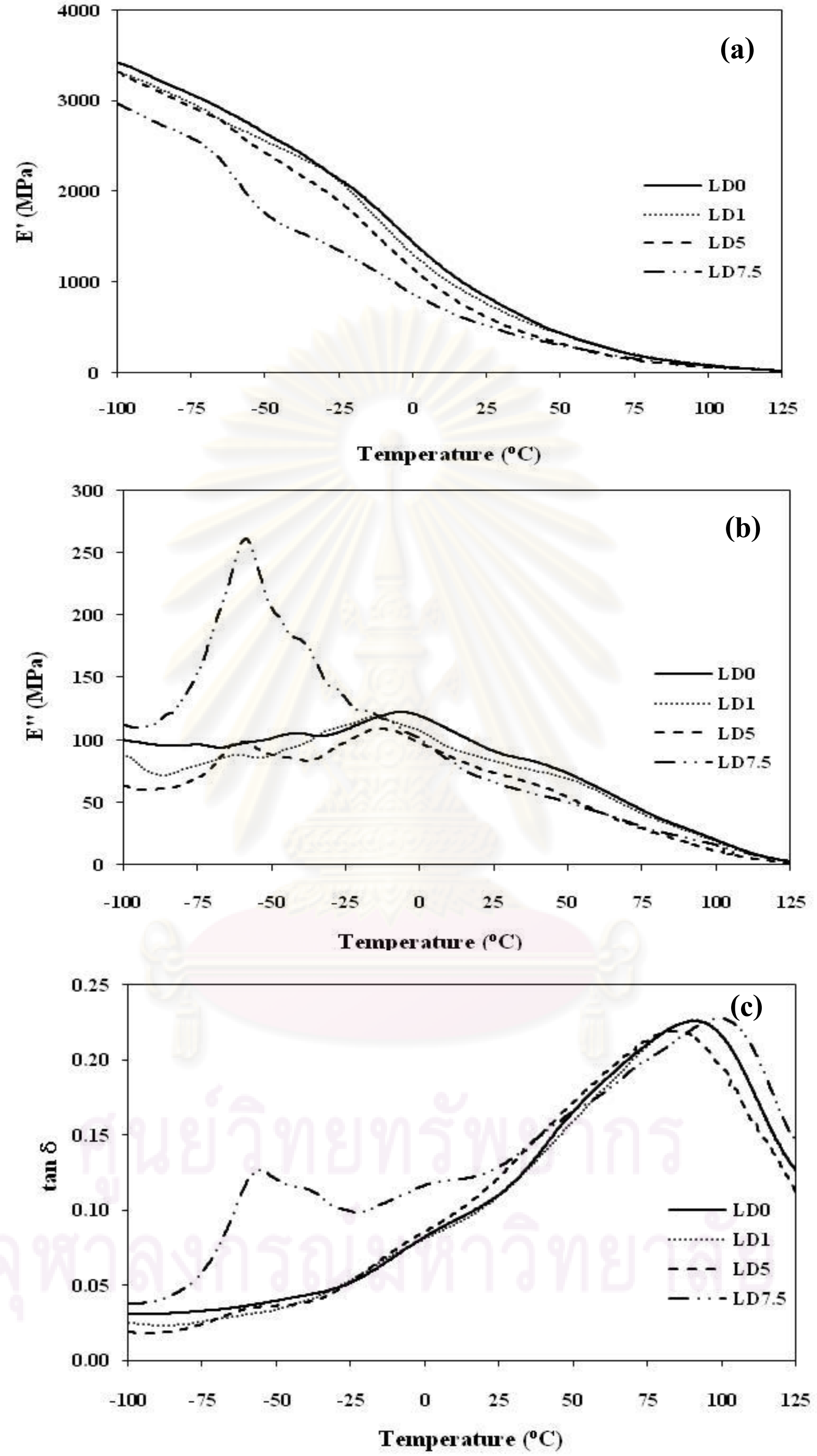

Figure 4.8 Dynamic mechanical properties of neat LDPE and NR/LDPE films (a) storage modulus (E′), (b) loss modulus (E″) and (c) tan δ.

4.5 Mechanical Properties of NR/LDPE Film

Figure 4.9 shows the effect of NR content on the mechanical properties in term of tensile strength (T_B), elongation, hardness, impact resistance and tear strength of NR/LDPE film. The T_B and hardness of NR/LDPE films tend to decreased with increasing the NR contents due to the increase of soft segment (NR) in polymer blend [50-52]. The elongation at break (E_B) of NR/LDPE film with various NR content as seen in Figure 4.9c trended to decrease with increasing NR contents until 5 phr and then E_B was significantly increased. Normally, elastomer is the flexible segment, when the elastomer content increases, it makes elongation increase, too. Contrary, our results showed that the addition of NR result the decrease of E_B. It may be due to the incompatibility between NR and LDPE. During elongation, NR and LDPE phases tend to be separated. As seen in Figure 4.10, with high NR contents in NR/LDPE blend, the phase separation between both was observed. Due to the large deformation by tensile testing, we could clearly observe the phase separation of NR and LDPE started from 5 phr compared with the small deformation of DMA, which could observed when 7.5 phr NR was blend with LDPE matrix.

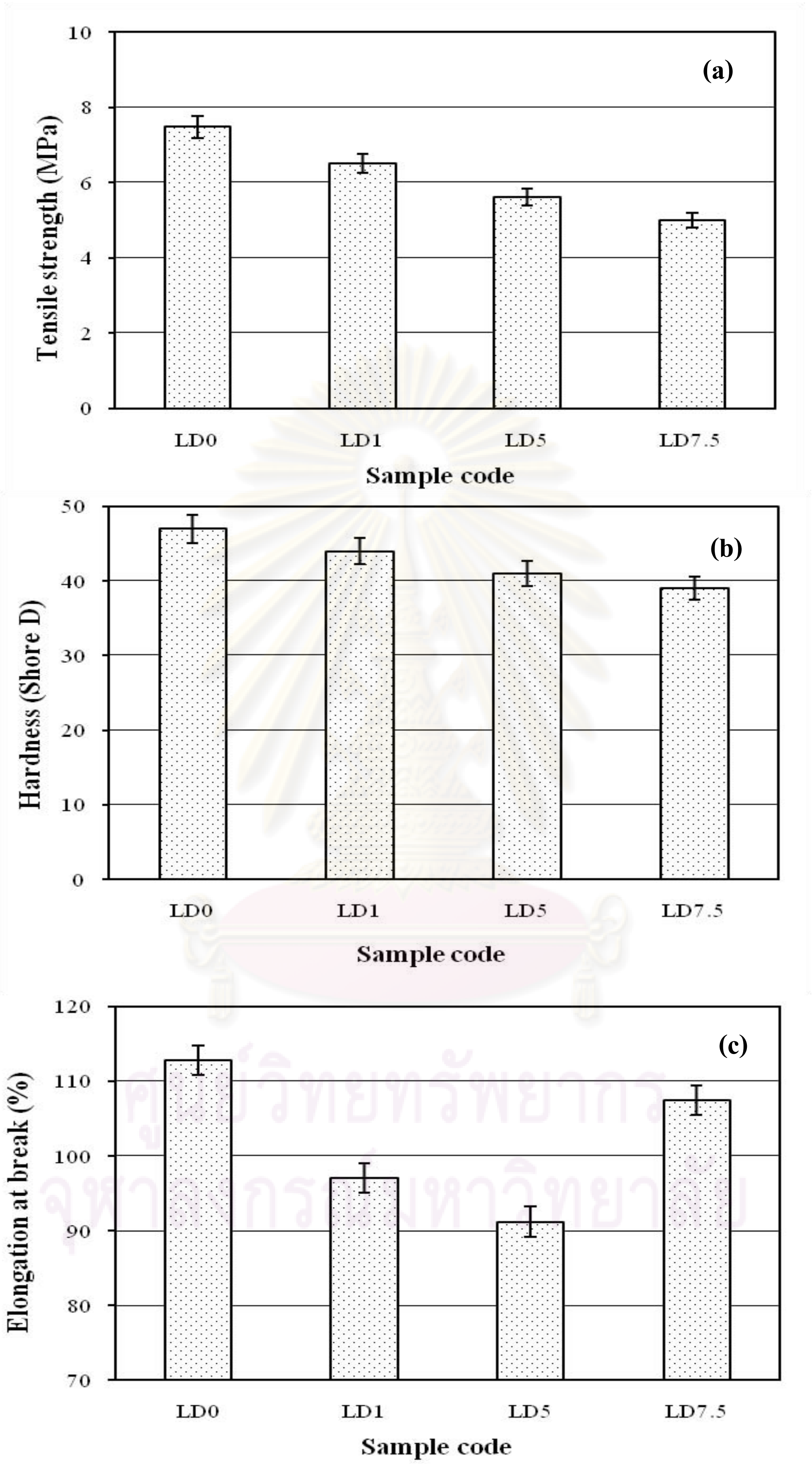

Figure 4.9 Effect of NR content on the mechanical properties of NR/LDPE films (a) tensile strength (b) elongation and (c) hardness.

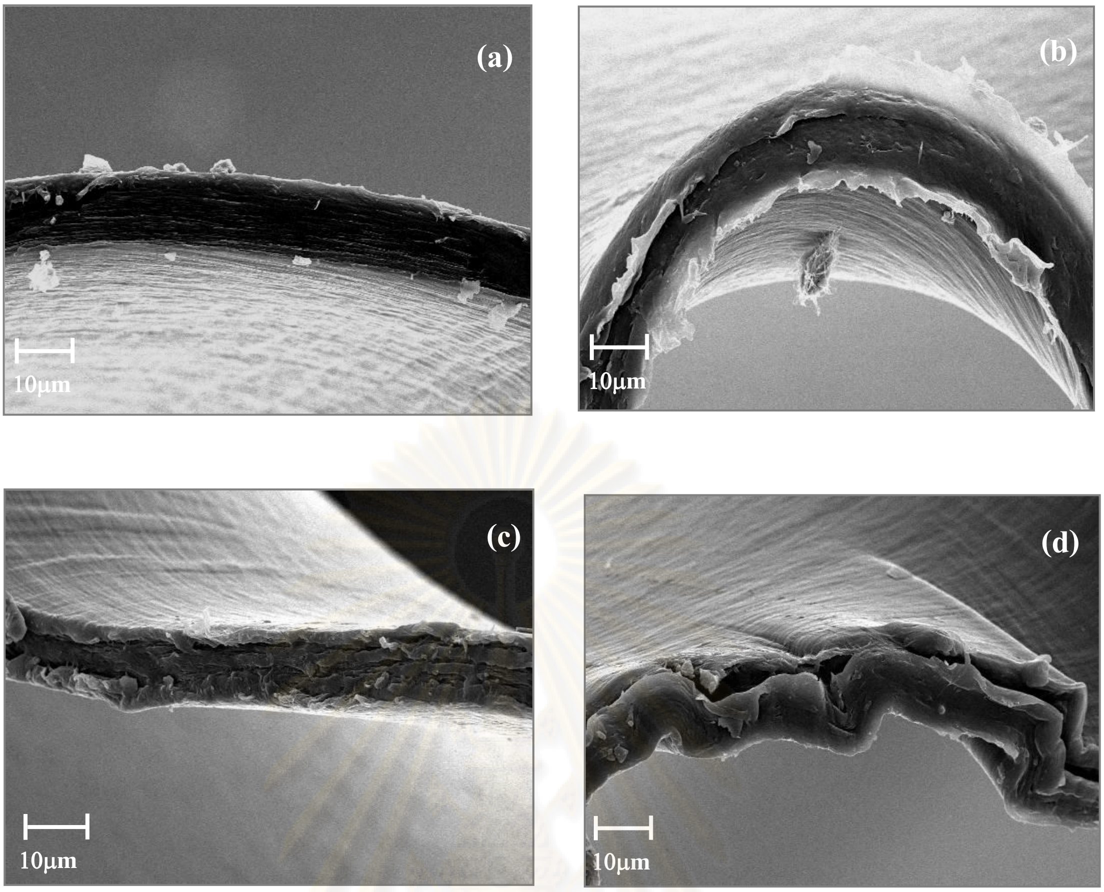

Figure 4.10 The SEM images of fracture surface of NR/LDPE films after tensile test: (a) LD0, (b) LD1, (c) LD5 and (d) LD7.5 (x 1000 magnification).

Figure 4.11 shows the effect of NR content on the tear strength and impact resistance of NR/LDPE film. The tear strength and impact resistance tend to be increased with increasing NR contents up to 5 phr after that both properties were decreased. According to the DMA result, the phase separation between NR and LDPE film was occurred when the LDPE blended with NR at 7.5 phr. We try to confirm this result again by investigating SEM photographs of fracture surface of NR/LDPE film after tension test in Figure 4.10. For NR/LDPE blend, the NR component form droplets in continuous glassy matrix (Figure 4.4-4.5) and this result in a composition of enhanced toughness. The NR particles behave almost like cavities in the LDPE matrix, these blends is the large increase in the number of site for yielding or crazing. The NR particles were absorbed energy and retard breaking process. The result is a somewhat lower breaking stress but a greatly increased extension before breaking occurs, so that the energy required to cause breakage is greatly increased [53].

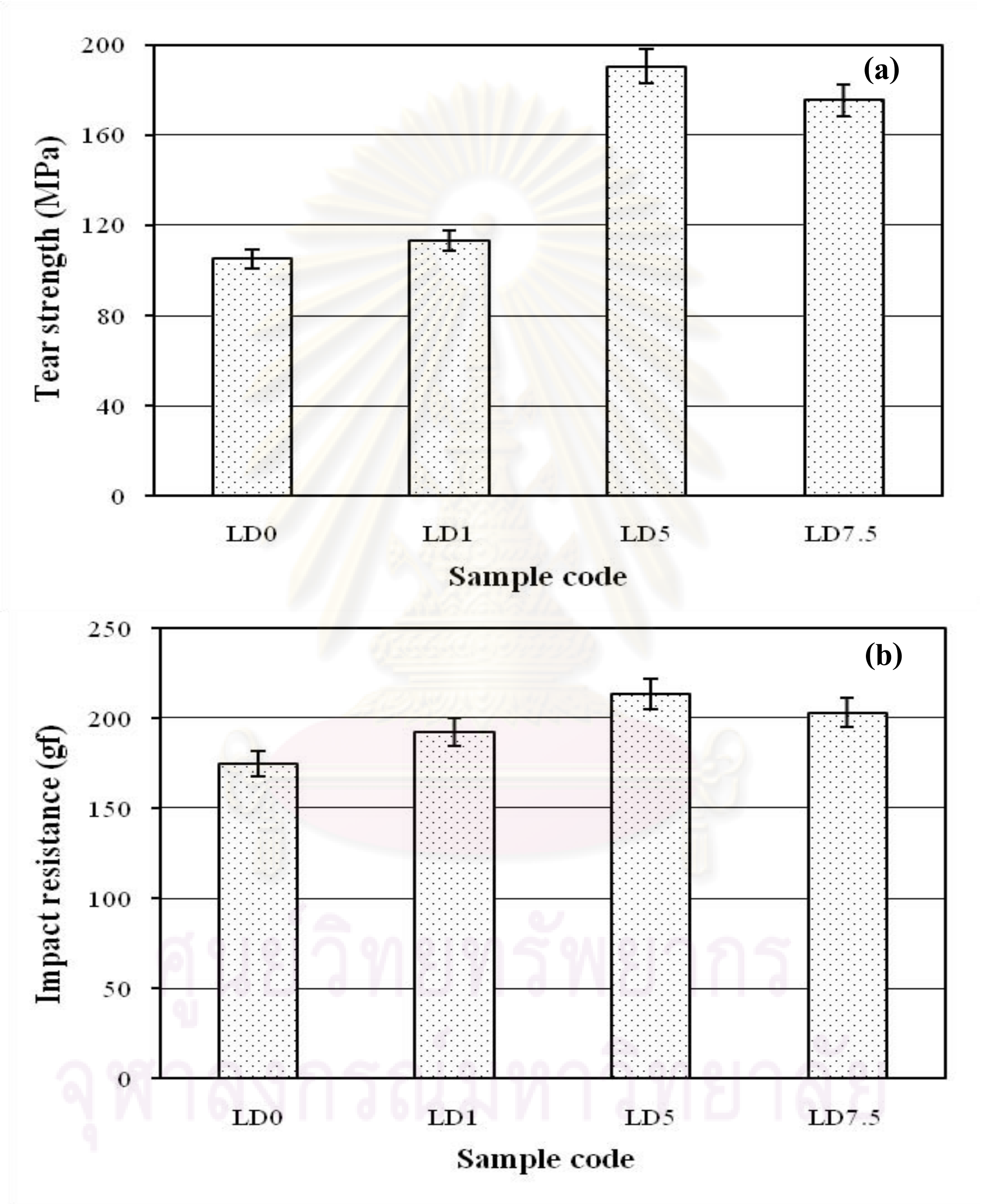

Figure 4.11 Effect of NR content on the mechanical properties of NR/LDPE films (a) tear strength (b) impact resistance.

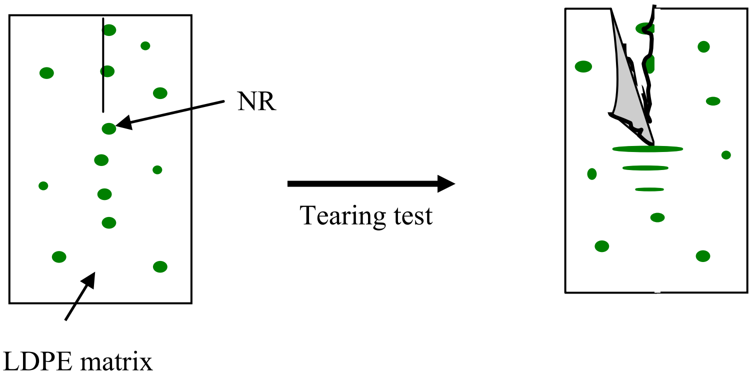

Figure 4.12 Rubber particles standing in LDPE matrix during tearing test.

Figure 4.12 show the mechanism of rubber particle in LDPE matrix during crack process. During crack the fractured surfaces tend to separated and rubber particles became extended in tension. This extension of rubber particle absorbed energy and resisted further crack growth.

4.6 Thermal Properties

Thermal properties of NR/LDPE films were determined by using DSC and the results were summarized in Table 4.2. It is clearly observed that the crystalline melting temperature (T_m) for all samples (with and without NR latex) was independent of NR content and it was almost constant (110 ^oC), except LD1. T_m is making the transition from solid to liquid, and characterized by an uptake in energy while the temperature remain constant, until all the solid material has become liquid. This result is related to rearrangement of crystalline polymer. The NR particles were inserted to crystalline LDPE. This phenomenon indicated the loose pack of crystalline therefore T_m of LD1 was decreased. Generally, the properties of polymer blend were dominated to the major component. The T_m of semicrystalline LDPE was about 110 ^oC, while the T_m of NR was about 28 ^oC. Unfortunately, there is no effect of NR content on the T_m of NR/LDPE film. In addition, there is another effect on the change of T_m of polymer material, which is the density of the polymer blend. Zhu *et al*. reported the effect of density of LDPE on the T_m. They found that T_m increased when the polymer density increased [9]. However, the density of NR/LDPE film in this study was almost constant (0.9 g/cm^3).

The crystalline temperature (T_c) of NR/LDPE film was shown in Table 4.2. T_c of NR/LDPE film was lower than that of neat LDPE (the difference was about 2 ^oC). This result can explained that crystal could be grown from the concentrated molten state. The polymer molecule in this case severely entangled and any polymer molecules added to a specific crystal surface simultaneously [54]. When NR latex was added into LDPE film, NR molecules interfered the crystallization of LDPE, resulting in the shift of T_c of polymer at lower temperature. Then, the crystallization of polymer blend can start lower than the neat LDPE film. The crystallization goes on from the time the proper temperature is reached for it to commence, until the energy level have dropped enough that molecules no longer have enough energy to rearrange themselves into crystallites [13]. In this process, the polymer chains were more flexibility and flavored molecular reorganization, resulting in the increase of crystallization rate or degree of crystallinity [5]. The heat of fusion (ΔH_m), hence the energy used for changing the solid state of crystalline to melting state, related to crystallinity of polymer. More crystallinity of polymer were required more ΔH_m as shown in Table 4.2. This result is in agreement with the degree of crystallinity (X_c) increase with increasing NR content and the X_c calculated by DSC was nearly comparable to the X_c calculated from XRD (Table 4.1).

Table 4.2 Thermal properties of neat LDPE and NR/LDPE films

Sample code	Thermal properties of neat LDPE and NR/LDPE films			
	$T_m{}^1$ (°C)	$T_c{}^2$ (°C)	$\Delta H_m{}^3$ (J/g)	$X_c{}^4$ (%)
LD0	110.8	99.6	27.7	9.6
LD1	108.1	97.2	21.8	7.5
LD5	110.4	97.2	65.0	22.4
LD7.5	110.1	97.3	100.6	34.7

[1] Crystalline melting temperature, [2] Crystallization temperature, [3] Heat of fusion of the blend, [4] Degree of crystallinity calculated from equation 3.1.

4.7 Shrinkability Test

It is well known that the stretching decreases the entropy of the system. If heating is imposed on the stretched sample (without any mechanical force), the material shrinks [28]. The results of the shrinkage of NR/LDPE film at various conditions in both MD and TD direction are shown in Figure 4.13 and the raw data was summarized in Appendix D. The shrinkability of neat LDPE and NR/LDPE film was increased with increasing shrink temperature in both directions. The shrink temperature is increased, resulting in the decrease of shrink time. More shrinkability was clearly observed at the temperature, which was higher than T_m of NR/LDPE blend (~110 °C). The shrinkability of all samples at above T_m (condition B-E) in MD direction was higher than that of blend films in TD direction as seen in Figure 4.13. The maximum shrinkage was obtained about 80 - 85%. The appearance of NR/LDPE film after heating at 150 °C for 1 min was shown in Figure 4.14. Additionally, the shrinkability of NR/LDPE films increased with increasing of NR contents. As the NR content becomes higher, the concentration and orientation of the oriented amorphous materials should be increased during stretching NR films. Thus, the tendency of extended state to revert to a randomly coiled conformation would be more, resulting in the increase of shrinkage. The potential energy stored in the extended molecules is the so-called elastic memory, characteristic of oriented; that is, when the material is reheated to the orientation temperature, the molecules tend to return to their original size and spatial arrangement. For NR/LDPE film, an amorphous part of NR has more entropy so after heated it preferred to original stage (high entropy) that like the springs after remove force. This is result corresponding to the work of Khonakdar *et al.* They studied the thermal and shrinkage behavior of heat shrinkage material. The results showed that crosslinking effect to thermal properties and stretching temperature influence on the shrink temperature [24]. Chattopadhyay *et al.* studied heat shrinkability of EVA/LDPE blend film and the result found that heat shrinkage was increased with the increase in percent crystallinity [55]. For the application of using shrink film for packaging process, we tried to use the NR/LDPE film covered the glass dish. The appearance of NR/LDPE film after heating at 150 ^{o}C for 1 min and taking off to cool at room temperature was shown in Figure 4.15. The NR/LDPE film could be covered and sealed the glass dish. When increasing the NR content can tightly wrapped the glass dish because after heated molecule of NR is immediately revert to original form (high entropy) which is individual propertied of NR.

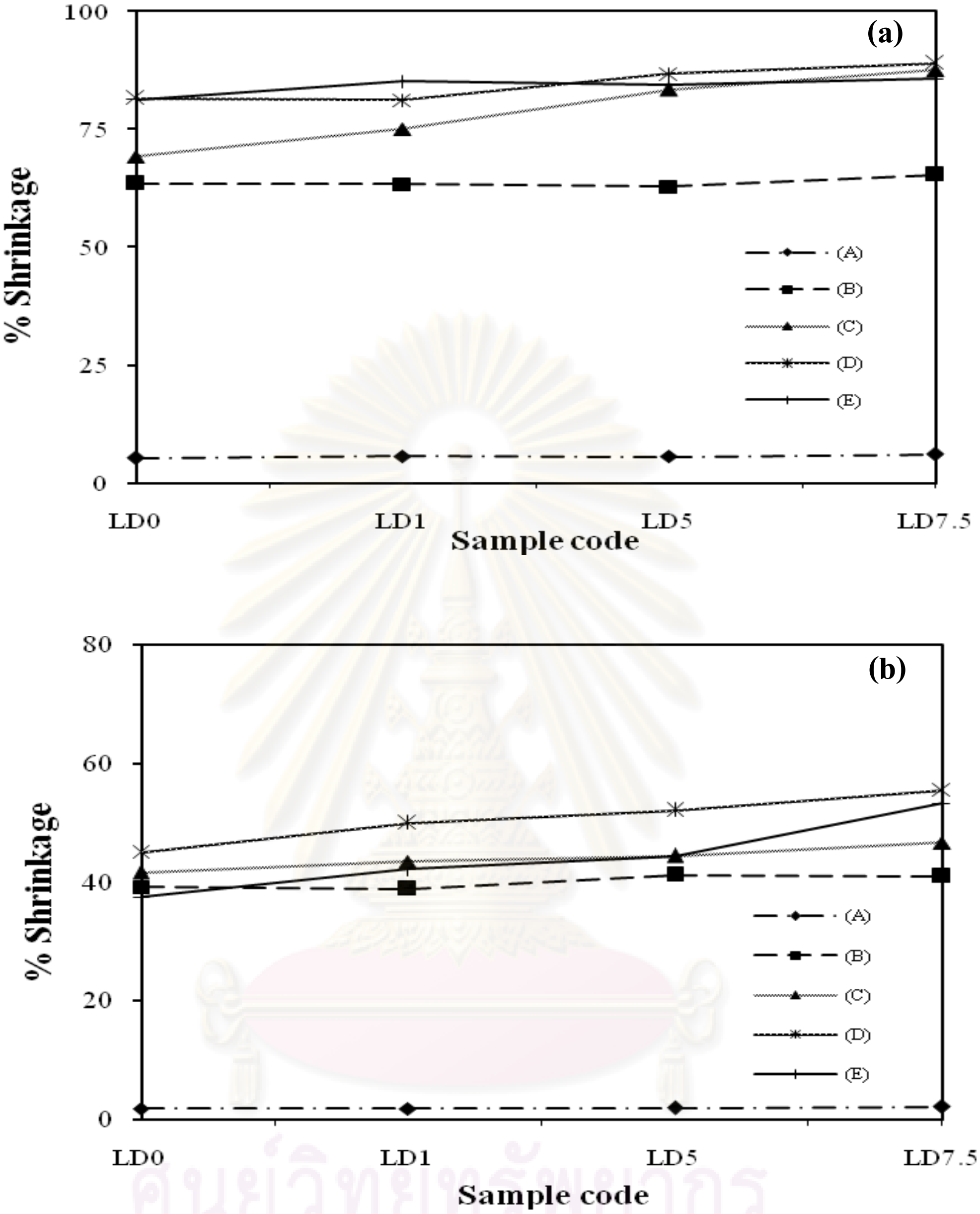

Figure 4.13 Variation of % shrinkage with NR content at various conditions: (a) MD direction and (b) TD direction (A) 100 °C 30 min, (B) 120 °C 30 min, (C) 150 °C 1 min, (D) 160 °C 1 min and (E) 170 °C 30 sec.

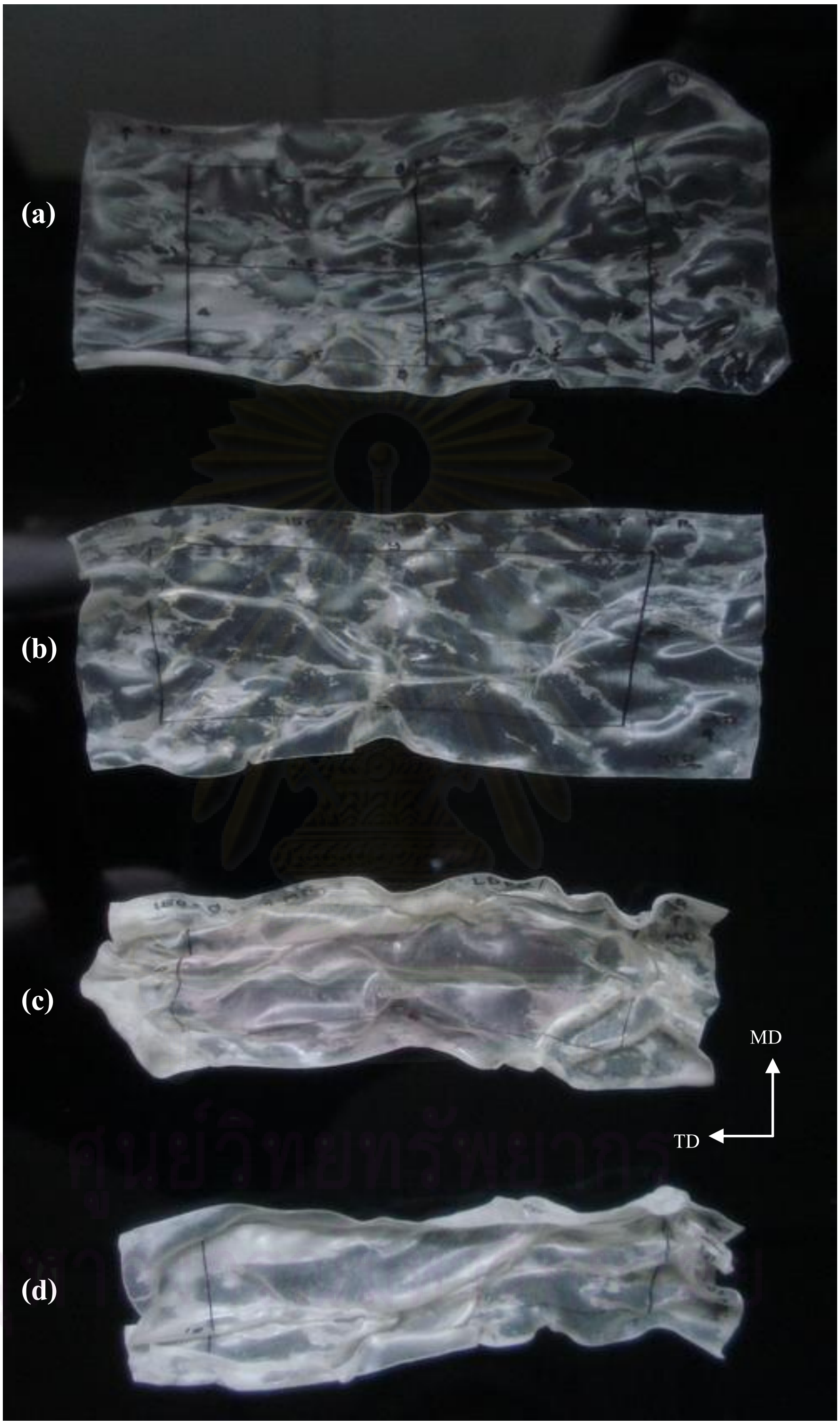

Figure 4.14 The appearance of neat LDPE and NR/LDPE films after heating at 150°C for 1 min: (a) LD0, (b) LD1, (c) LD5 and (d) LD7.5.

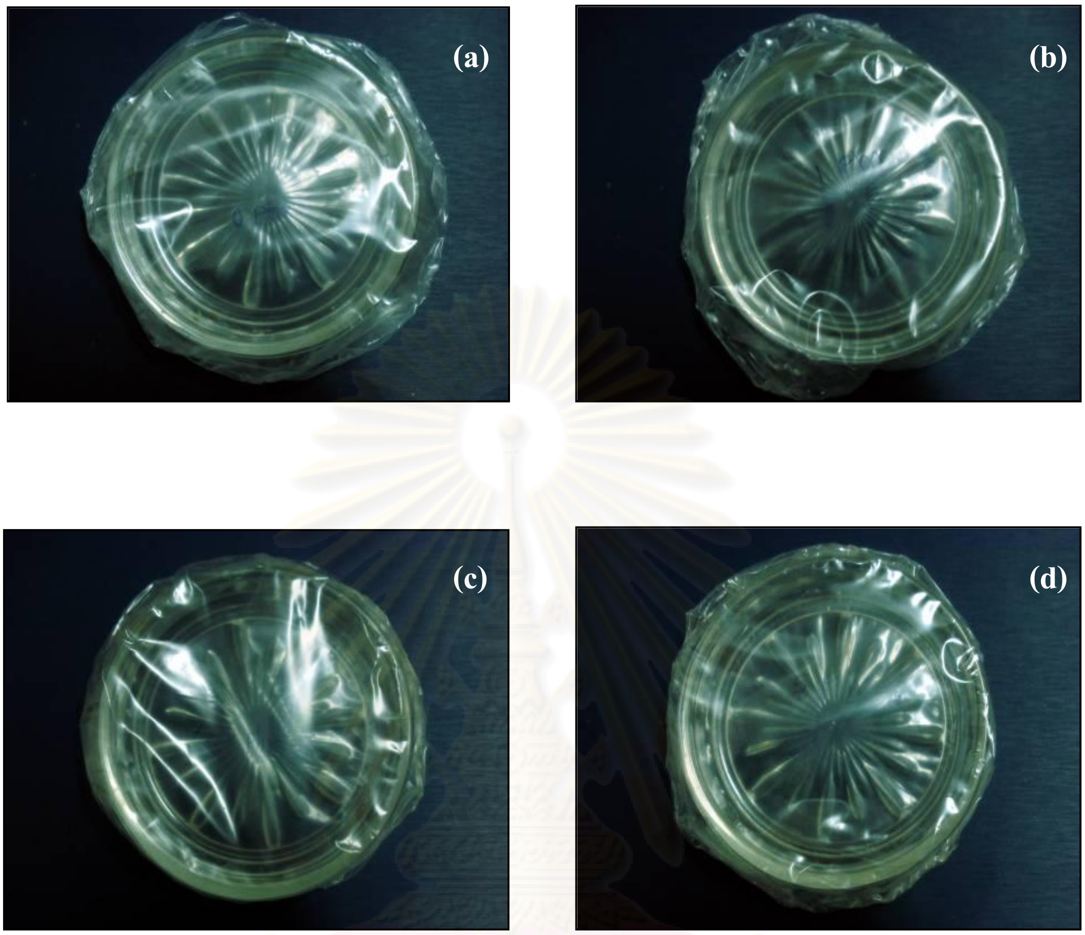

Figure 4.15 The neat LDPE and NR/LDPE film for packaging: (a) LD0, (b) LD1, (c) LD5, (d) LD7.5.

CHAPTER V

CONCLUSION AND FUTURE DIRECTION

5.1 Conclusion

In this study, we can be produced shrinkable film from LDPE blend with natural rubber (NR) latex by using blown film extrusion process. The influence of NR latex on the physical, thermal, dynamic mechanical, morphological, mechanical properties and shrinkability of NR/LDPE films were investigated. The main properties of NR/LDPE films are suitable to use in shrink film application. The NR/LDPE films were smooth surface and the addition of NR latex in LDPE matrix did not change the clarity of NR/LDPE films. The NR latex in the blend can improve some mechanical properties of LDPE film such as tear strength and impact resistance. However the tensile strength and hardness of NR/LDPE films were decreased with increasing NR content. The inferior mechanical properties could obtain when polymer blend with NR 7.5 phr due to the phase separation. This result was agreement with the DMA measurment, the loss modulus (E'') could be separated into 2 peaks. This result is indicating the immiscible blend. The SEM micrograph of NR/LDPE films were also confirmed the phase separation between LDPE matrix and NR latex. The NR latex is not too compatible it exists in droplets in continues LDPE matrix. Finally, the shrinkability of NR/LDPE films was increased with increasing NR content. Accordingly, NR has more entropy so after heated it preferred to recovery to the original form. These properties are benefit to use in shrink film application.

5.2 Future Direction

1. Study in more detail on the compatibility of NR/LDPE blend by using compatibilizer agent i.e., liquid natural rubber (LNR), phthalic anhydride (PA) and maleic anhydride grafted PE (MA-g-PE).
2. Explore the use of other rubber type i.e., deproteinized natural rubber (DPNR) and butadiene rubber (BR) in the blend with the aim to use appearance of film, compatibility and properties of the blend
3. Study in more detail about other product of thermoplastic/NR blends i.e., high density polyethylene (HDPE)/NR, polycarprolactone (PCL)/NR and polylactic acid (PLA)/NR

REFERENCES

[1] Hernandez, R.J. Plastics in packaging, Germany: Hanser-garder, 2000.

[2] Martin, Z. and Jiri, V. Modeling of the film blowing process by using variational principles. Journal of non-newtonian fluid mechanic. 123(2004): 201-213.

[3] Orville, J. Science and technology of polymer films, Vol. 1. New York: John wiley & sons, 1968.

[4] David, I. An introduction to polymer physics, Cambridge, 2002.

[5] Peacock, A. and Calhoun, A. Polymer chemistry: properties and applications, New York: Hanser, 2006.

[6] Calvart, K.O. Polymer lattices and their application, Germany: Hanser, 1982.

[7] Aziz, A. Advance in natural rubber production. Rubber chemical technology. 67(1994): 537-547.

[8] Maurice, M. and Vannostrand, R. Rubber technology, 3rd ed. New York: Hanser, 1987.

[9] Hans, E. An introduction to plastics, Germany: Wiley-vch, 2005.

[10] Paul, D.R. and Bucknall, C.B. Polymer blends vol.1: formulation, New York: Wiley, 2000.

[11] James, E.M., and Burak, E. Science and technology of rubber: elastomer blend, New York: Academic press, 1994.

[12] Sae-oui, P. Rubber chemicals, Bangkok: MTEC, 2005.

[13] Susan, E.M., Culter, J.D. and Hernandez, R.J. Plastics packaging, properties, processing, applications and regulations, 2nd ed., Munich: Hanser, 2004.

[14] Krick, C. Blow film extrusion, Munich: Hanser-gardner, 2006.

[15] Painter, P., and Coleman, M. Fundamentals of polymer science, New York: Technomic, 1994.

[16] Rauwendaal, C. Polymer extrusion, Munich: Carl hanser, 2001.

[17] Chung, C. Extrusion of polymers: theory and practice, Munich: Carl hanser, 2000.

[18] Tadmor, Z., and Klein, I. Engineering principles of plasticating extrusion, New York: Van nostrand reinhold, 1970.

[19] Levy, S., and Carley, J. Plastics extrusion technology handbook, New York: Industrial press, 1989.

[20] Rauwendaal, C. Understanding extrusion, Munich: Carl hanser, 1998.

[21] Wilson, D. Feeding technology for plastics processing, Munich: Carl hanser, 1998.

[22] Elias, H.G. An introduction to plastics, Wiley-vch, 2005.

[23] Kenton, R., Osborn, A., and Wilmer, A. Jenkins Plastic films technology and packaging applications. In cooperation with institute of packaging professionals, Technomic, 1992.

[24] Khonakdar, H.A., Morshedian, J., Mehrabzadeh, M., Wagenknecht, U., and Jafari, S.H. Thermal and shrinkage behaviour of stretched peroxide-crosslinked high-density polyethylene. European polymer journal. 39(2003): 1729-1734.

[25] Dahlan, H.M., Khairyl Zaman, M.D. and Ibrahim, A. The morphology and thermal properties of liquid natural rubber (LNR)-compatibilized 60/40 NR/LLDPE blends. Polymer testing. 21(2002): 905-911.

[26] Haijin Zhu, and *et al*. Influence of molecular architecture and melt rheological characteristic on the optical properties of LDPE blown films. Polymer. 48(2007): 5098-5106.

[27] Mishra, J.K., Raychowdhury, S. and Das, C.K. Effect of interchain crosslinking on the shrinkability of the blends consisting of grafted low-density polyethylene and carboxylated nitrile rubber. Material letters. 46(2000): 212-218.

[28] Mishra, J.K., Chang, Y.W., and Kim, D.K. Green thermoplastic elastomer based on polycaprolactone/epoxidized natural rubber blends as a heat shrinkable material. Material letters. 61(2007): 3551-3554.

[29] Ismail, H. and diansyah, S. Thermoplastic elastomer based on polypropylene/ natural rubber and polypropylene/recycle rubber blends. Polymer testing 21(2001): 389-395.

[30] Sirisinha, C., Saeoui, P. and Guaysomboon, J. Oil and thermal aging resistance in compatibilized and thermally stabilized chlorinated polyethylene/ natural rubber blends. Polymer. 45(2004): 4909-4916.

[31] Chowdhury, S.R., Mishra, J.K. and Das, C.K. Structure, shrinkability and thermal property correlations of ethylene vinyl acetate (EVA)/ carboxylated nitrile rubber (XNBR) polymer blends. Polymer degradation and stability. 70(2000): 199-204.

[32] Charoen, N., Krungjit, N., Azizo, K. and Suda, K. Dynamic vulcanization of natural rubber/high-density polyethylene blends: Effect to compatibilization, blend ratio and curing system. Polymer testing. 25(2006): 782-796.

[33] Radhesh Kumar, C., Fuhrmann, I. and Karger-Kocsis, J. LDPE-based thermoplastic elastomers containing ground tire rubber with and without dynamic curing. Polymer degradation and stability. 76(2002): 137-144.

[34] Vishu, S. Hand book of plastics testing technology, 2nd ed., New York: Wiley & sons, 1998.

[35] Sperling, L.H. Introduction to physical polymer science, 4th ed., New York: Wiley, 2006.

[36] David, I. An introduction to polymer physics, Cambridge, 2002.

[37] Geoff, A., Giles, R. and David, R.B. Materials and development of plastics packaging of the consumer market, Sheffield academic press, 2000.

[38] Dimensional stability website (Exxon) [online]

[39] Peter, S.J. Rubber processing an introduction, New York: Hanser, 2001.

[40] Azman, H., Mat U.W., and Ching, Y.C. Mechanical and morphological properties of PP/NR/LLDPE ternary blend-effect of HVA-2. Polymer testing 22(2003):281-290.

[41] Lavine, M.S., Waheed, N., and Rutledge, G.C. Molecular dynamics simulation of orientation and crystallization of polyethylene during uniaxial extension. Polymer 44(2003):1771-1779.

[42] Abdel-Hady, E.E. Positron annihilation lifetime study of irradiated and deformed low density polyethylene. Polymer degradable stability 80(2000):363-368.

[43] Goritz, D., Muller, F.H., and Sietz, W. Temperature induced and stress – induced crystallinzation in oriented polymers. Colloid & polymer science 62(1997):114-116.

[44] Tosaka, M., Murakami, S., Poompradub, S., and Kohjiya, S. Orientation and crystallinzation of natural rubber network as revealed by WAXD using synchrotron radiation. Macromolecules 37(2004):3299-3309.

[45] Luch, D., Yeh, G.S.Y. Morphology of strain-induced crystallization of NR I. electron microscopy on unvulcanize thin film. Journal apply physics 43(1972):4326-4338.

[46] Pedroso, A.G. and Rosa, D.S. Mechanical, thermal and morphological characterization of recycled LDPE/corn starch blends. Carbohydrate polymer 59(2005): 1-9.

[47] Peacock, A. and Calhoun, A. Polymer chemistry: Properties and applications, U.S.A.: Hanser, 2006.

[48] Roberts, A.D. Natural rubber science and technology, U.S.: Oxford,1988.

[49] Komalan, C., George, K.E., and Kunar, P.A.S. Dynamic mechanical analysis of binary and ternary polymer blends based on nylon copolymer/ EPDM rubber and EPM grafted maleic anhydride compatibilizer. Polymer letter 10(2007):641-653.

[50] Senna, M.H. Abdel-Fattah, A. and Abdel-Monem, Y.K. Spectroscopic analysis and mechanical properties of electron beam irradiated polypropylene/epoxidized natural rubber (PP/ENR) polymer blends. Nuclear instrument method B 266 (2008): 2599-2606

[51] Rattanasom, N., Poonsuk, A., and Makmoon, T. Effect of curing system on the mechanical properties and heat aging resistance of natural rubber/ tire tread reclaimed rubber blends. Polymer testing 24(2005): 728-732.

[52] Saleesung, T., Saeoui, P., and Sirisinha, C. Mechanical and thermal properties of thermoplastic elastomeric based on low density polyethylene and ultra-fine fully-vulcanized acrylonitrile butadiene rubber powder (UFNBRP). Polymer testing 29(2010): 977-983.

[53] Brydson, J.A. Plastics materials, 6th ed., New York: Butterworth Heinemann, 1995.

[54] Gedde, W. Polymer physics, Germany: Kluwer academic publishers, 1999.

[55] Chattopadhyay, S., Chaki, T.K., and Bhowmick, A.K. Heat shrinkability of electron beam modified thermoplastic elastomer film from blends of ethylene-vinyl acetate copolymer and polyethylene. Radiation physics chemistry 59(2000): 501-510.

APPENDICES

APPENDIX A

Table A-1 Calculated formulation of RR in LDPE blend

1 phr of RR = 1 g of RR (%Solid content = 100%)

Sample code	Weight of RR (phr)	Weight of LDPE (phr)
RR0.5	0.5	100
RR1	1	100
RR2	2	100
RR5	5	100

Table A-2 Calculated formulation of NR latex in LDPE blend

60% DRC of NR latex is 60% NR content and 40% water and other

1 phr NR = NR latex 1.67 g, LDPE 100 g

$$W_{wet} = \frac{(X * 100)}{\% DRC}$$

where W_{wet} is wet weight of NR latex (g), *X is* phr of NR in formula and *% DRC* of NR is constant value (60)

Sample code	Weight of NR latex (phr)	Weight of NR latex (g)	Weight of LDPE (phr)
LD1	1	1.67	100
LD5	5	8.33	100
LD7.5	7.5	12.50	100

APPENDIX B

Table B-1 Mechanical Properties of Neat LDPE and NR/LDPE Film

Sample	Tensile strength (MPa)	Elongation at break (%)	Tearing strength (MPa)	Impact resistance (gf)	Hardness (Shore D)
LD0	7.47	112.75	105.22	174.50	47
LD1	6.50	97.06	112.98	192.50	44
LD5	5.60	91.18	190.36	213.50	41
LD7.5	5.00	107.43	175.36	203.00	39

APPENDIX C

C-1: XRD measurement of LDPE film

Date : 15/3/2010
Sample : LDPE (pure)

Instrument : X-Ray Diffractometer ; Bruker AXS Model D8 Discover
Condition :

Target	Cu	
Voltage	40	kV
Current	40	mA
Angle	5-45	degree
Increment	0.02	degree/step
Scan speed	0.5	sec/step
Detecter	VÅNTEC-1 Detector (Super Speed Detector)	

Operator : Manop Tirarattanasompot
Memo :

Result :

Calculate Degree of crystallinity	
Crystalline area	538.46
Amorphous area	5100.60
Degree of crystallinity (%)	9.55

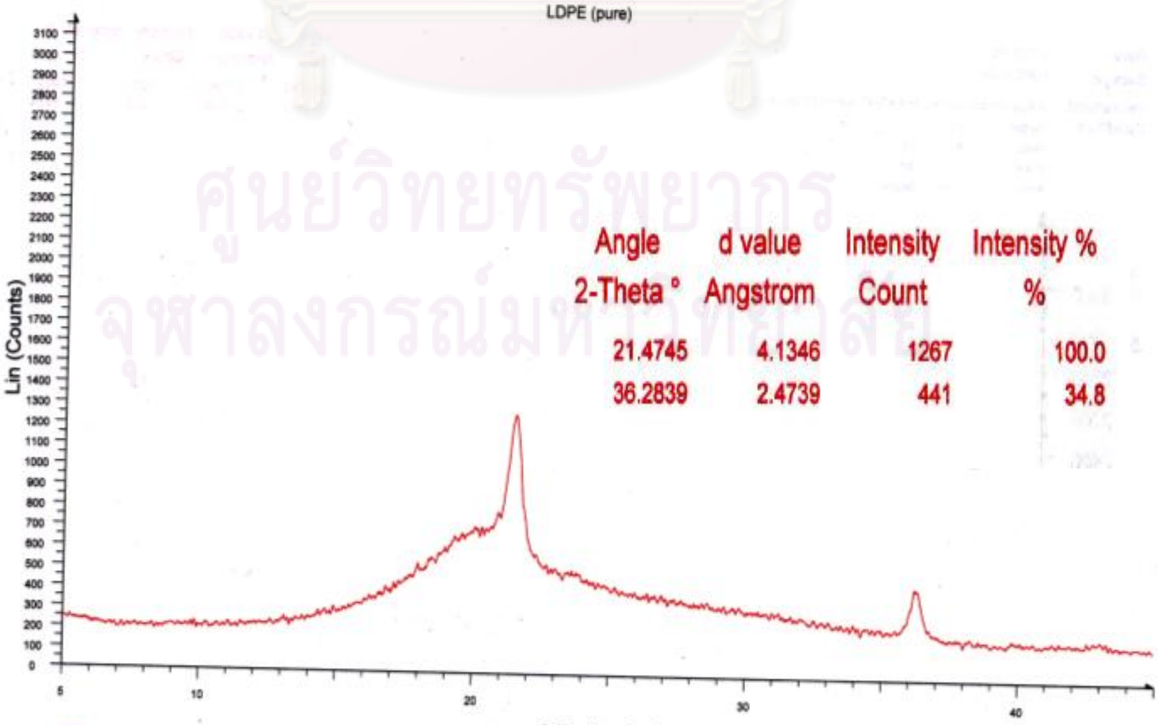

Angle 2-Theta °	d value Angstrom	Intensity Count	Intensity % %
21.4745	4.1346	1267	100.0
36.2839	2.4739	441	34.8

File: 530817-1.raw - Type: 2Th/Th locked - Start: 5.0000 ° - End: 44.9959 ° - Step: 0.0188 ° - Step time: 240. s - Temp.: 25 °C (Room)
Operations: Smooth 0.080 | Import

APPENDIX C

APPENDIX C-2: XRD measurement of LDPE/1phr

Date	: 15/3/2010		
Sample	: LDPE / 1 phr NR		
Instrument	: X-Ray Diffractometer ; Bruker AXS Model D8 Discover		
Condition	: Target	Cu	
	Voltage	40	kV
	Current	40	mA
	Angle	5-45	degree
	Increment	0.02	degree/step
	Scan speed	0.5	sec/step
	Detecter	VÅNTEC-1 Detector	(Super Speed Detector)
Operator	: Manop Tirarattanasompot		
Memo	:		

Result :

Calculate Degree of crystallinity	
Crystalline area	1687.10
Amorphous area	6698.21
Degree of crystallinity (%)	20.12

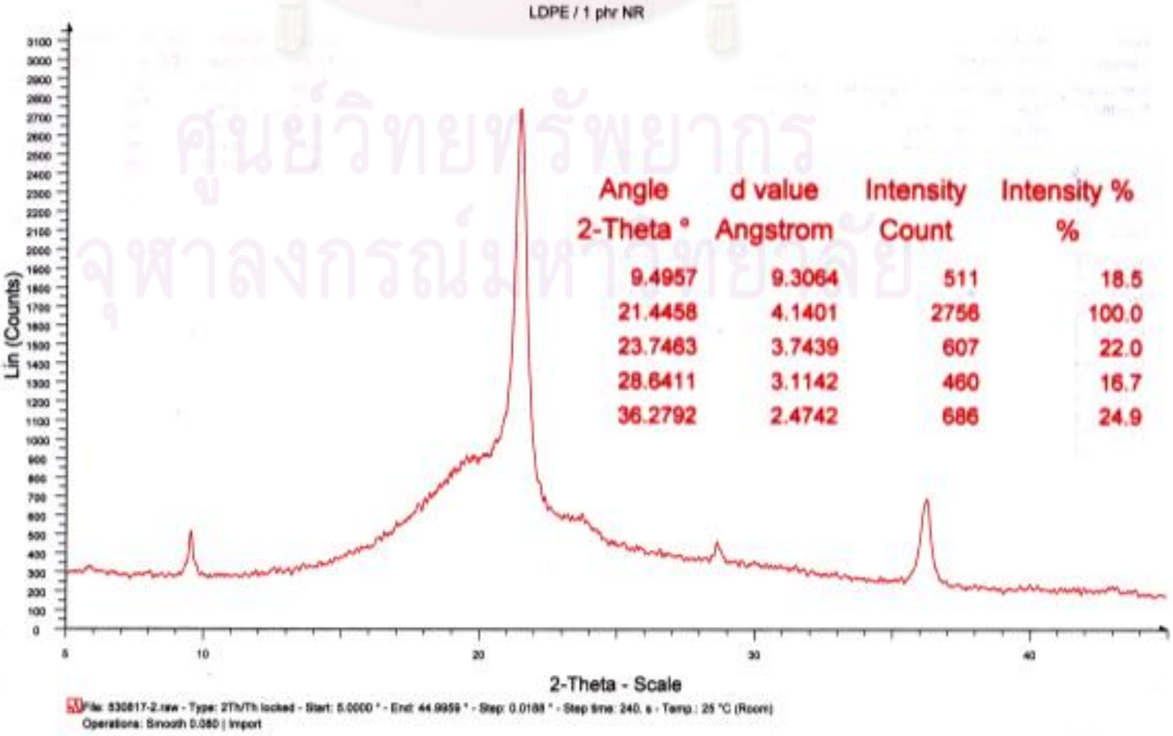

Angle 2-Theta °	d value Angstrom	Intensity Count	Intensity % %
9.4957	9.3064	511	18.5
21.4458	4.1401	2756	100.0
23.7463	3.7439	607	22.0
28.6411	3.1142	460	16.7
36.2792	2.4742	686	24.9

File: 530817-2.raw - Type: 2Th/Th locked - Start: 5.0000 ° - End: 44.9959 ° - Step: 0.0188 ° - Step time: 240. s - Temp.: 25 °C (Room)
Operations: Smooth 0.080 | Import

APPENDIX C

APPENDIX -3: XRD measurement of LDPE/5phr

Date : 2/6/2010
Sample : LDPE/5 phr NR Special
Instrument : X-Ray Diffractometer ; Bruker AXS Model D8 Discover
Condition : Target Cu

Target	Cu	
Voltage	40	kV
Current	40	mA
Angle	5-45	degree
Increment	0.02	degree/step
Scan speed	0.5	sec/step
Detecter	VÅNTEC-1 Detector (Super Speed Detector)	

Operator : Manop Tirarattanasompot
Memo :

Result :

Calculate Degree of crystallinity	
Crystalline area	3341.69
Amorphous area	10845.00
Degree of crystallinity (%)	23.56

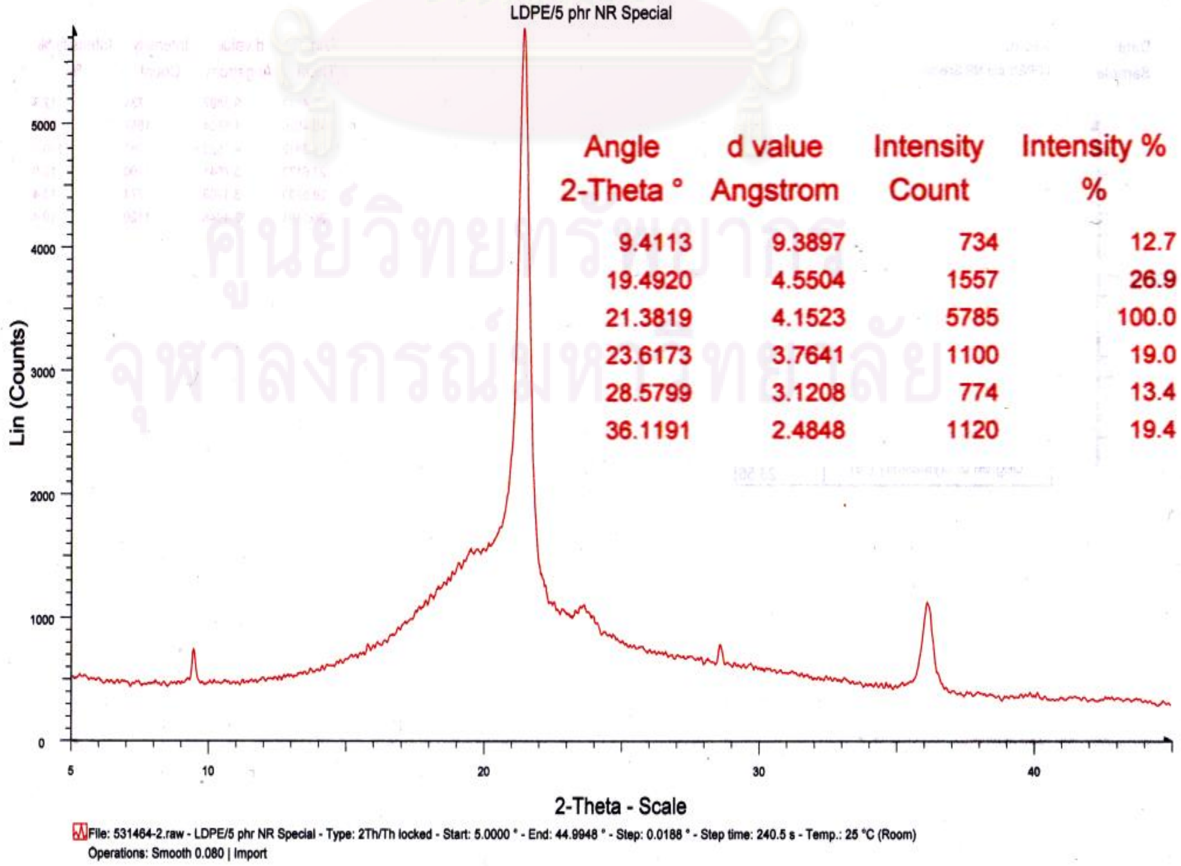

Angle 2-Theta °	d value Angstrom	Intensity Count	Intensity % %
9.4113	9.3897	734	12.7
19.4920	4.5504	1557	26.9
21.3819	4.1523	5785	100.0
23.6173	3.7641	1100	19.0
28.5799	3.1208	774	13.4
36.1191	2.4848	1120	19.4

APPENDIX C

APPENDIX -4: XRD measurement of LDPE/7.5phr

Date : 15/3/2010

Sample : LDPE / 7.5 phr NR

Instrument : X-Ray Diffractometer ; Bruker AXS Model D8 Discover

Condition :

Target	Cu	
Voltage	40	kV
Current	40	mA
Angle	5-45	degree
Increment	0.02	degree/step
Scan speed	0.5	sec/step
Detecter	VÅNTEC-1 Detector (Super Speed Detector)	

Operator : Manop Tirarattanasompot

Memo :

Result :

Calculate Degree of crystallinity	
Crystalline area	3419.79
Amorphous area	7539.69
Degree of crystallinity (%)	31.20

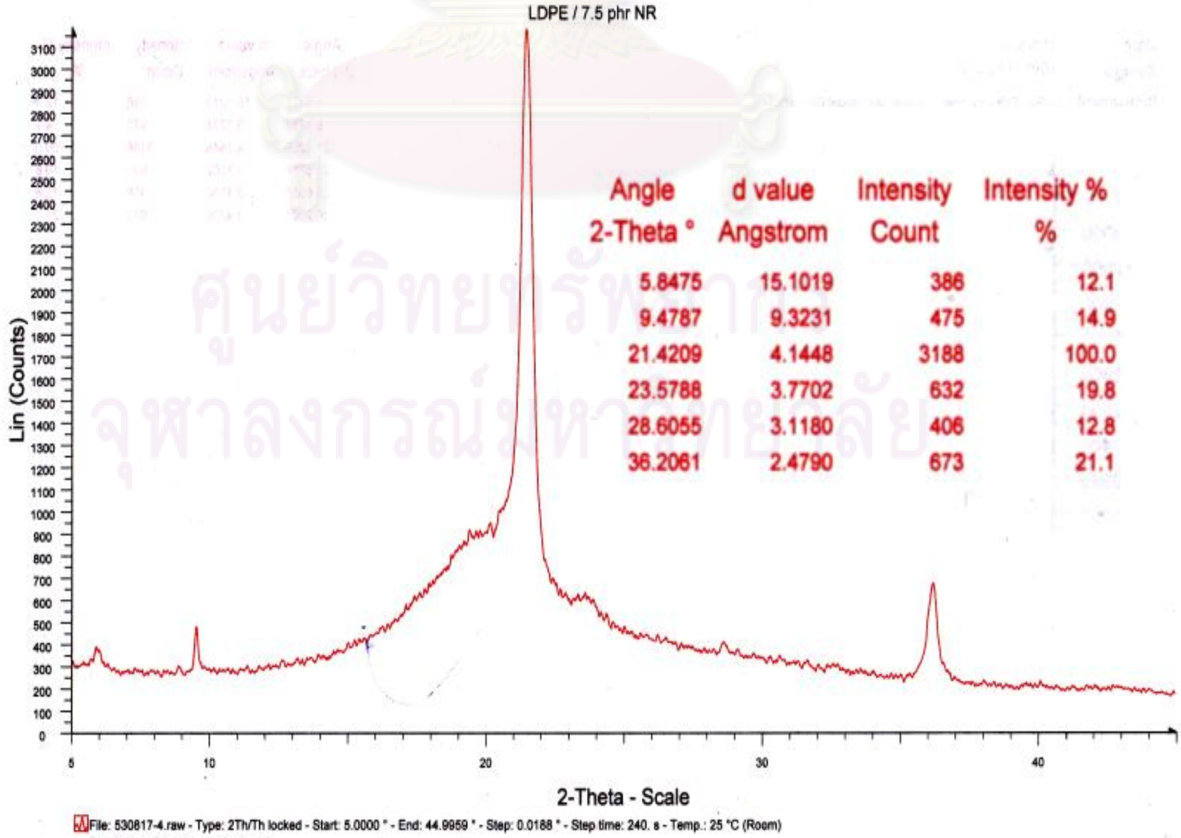

Angle 2-Theta °	d value Angstrom	Intensity Count	Intensity % %
5.8475	15.1019	386	12.1
9.4787	9.3231	475	14.9
21.4209	4.1448	3188	100.0
23.5788	3.7702	632	19.8
28.6055	3.1180	406	12.8
36.2061	2.4790	673	21.1

File: 530817-4.raw - Type: 2Th/Th locked - Start: 5.0000 ° - End: 44.9959 ° - Step: 0.0188 ° - Step time: 240. s - Temp.: 25 °C (Room)
Operations: Smooth 0.080 | Import

APPENDIX D

APPENDIX D-1: Stress-strain curve of LD0

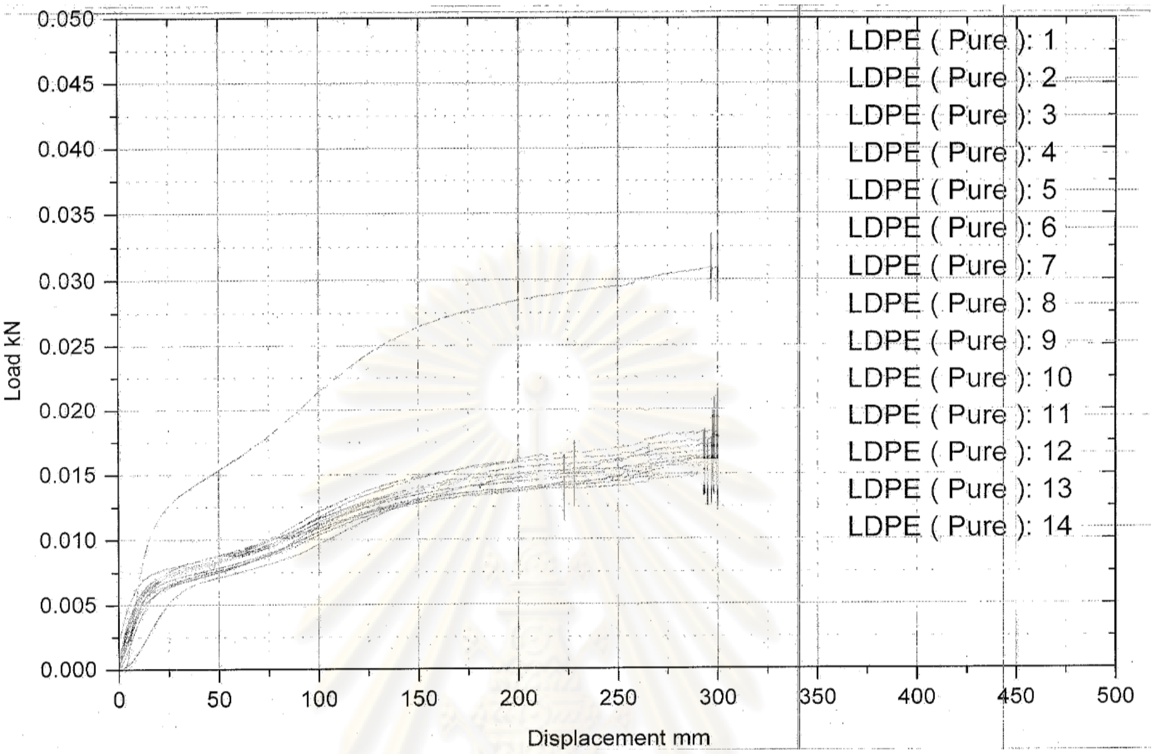

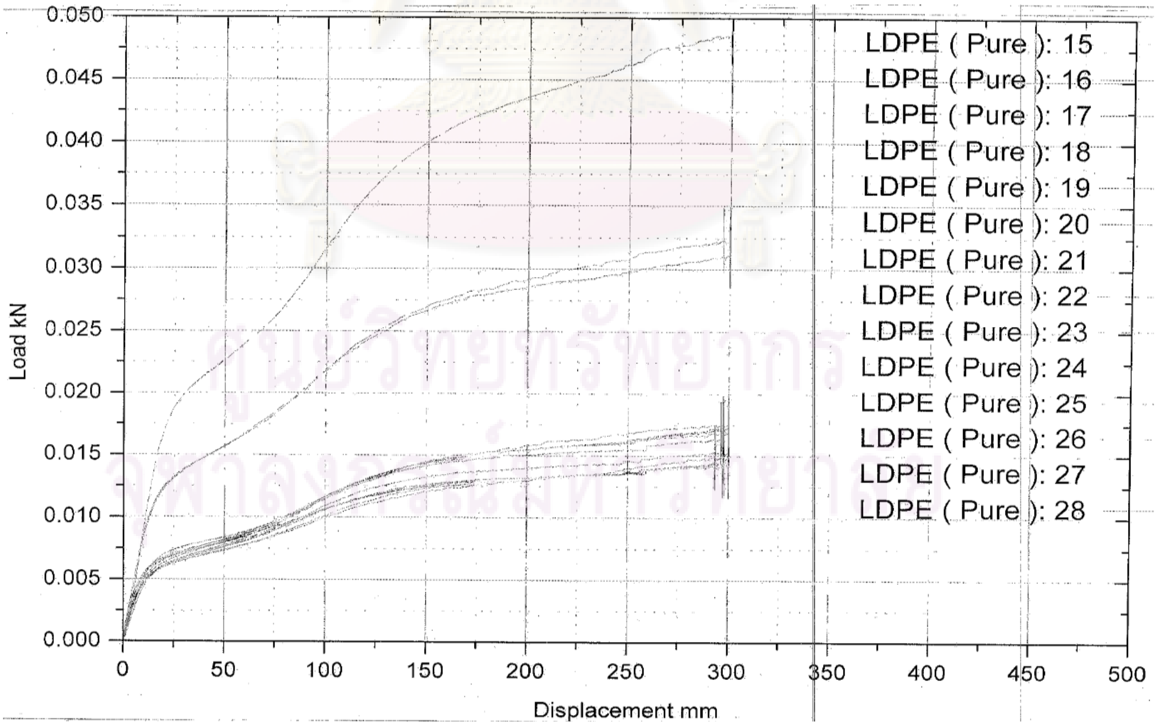

APPENDIX D

APPENDIX D-2: Stress-strain curve of LD1

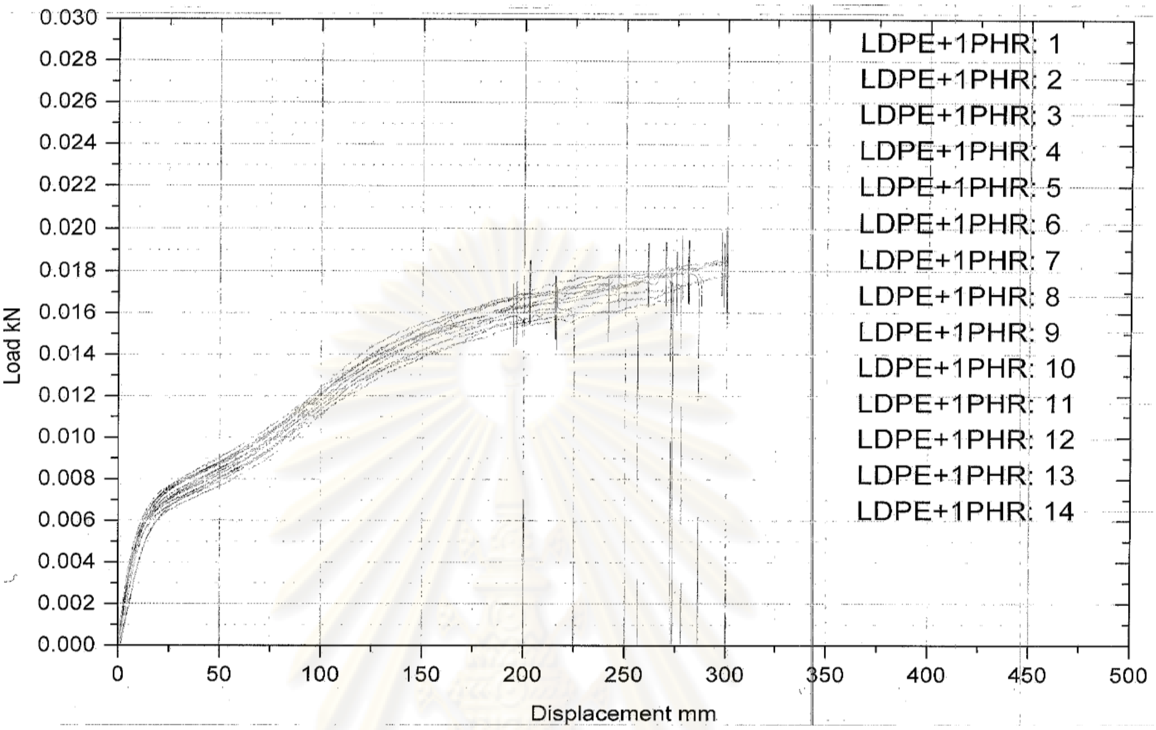

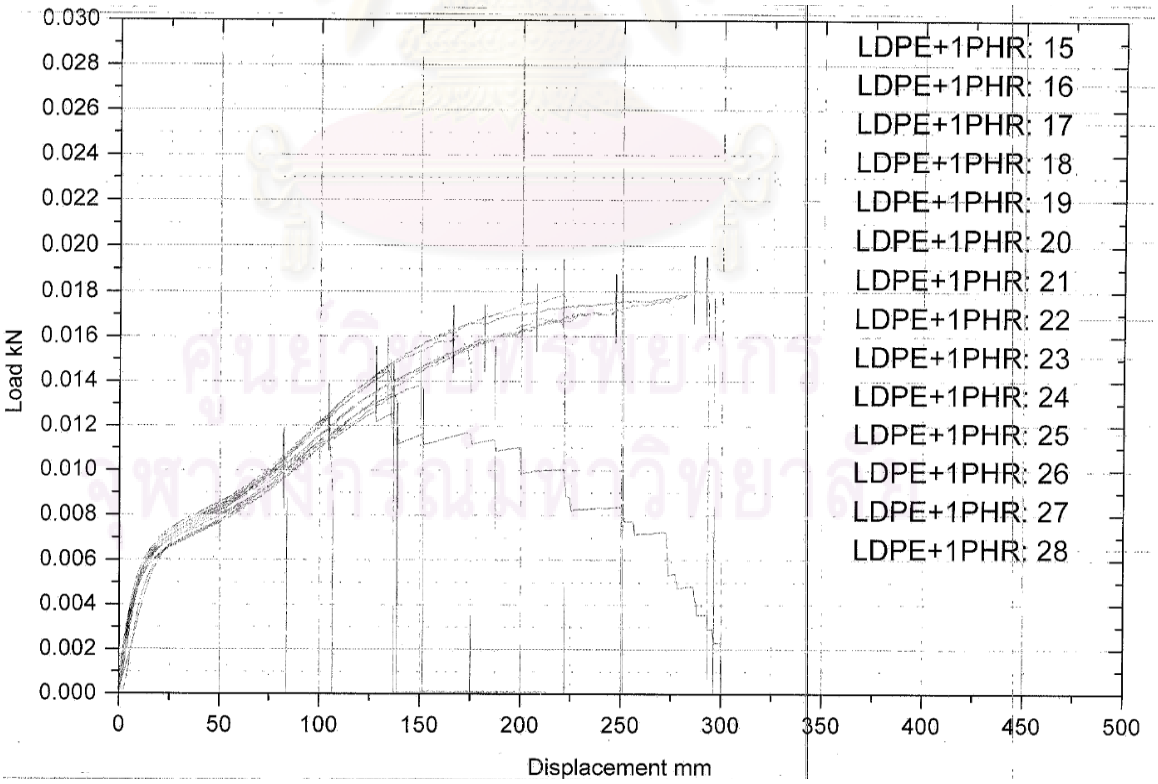

APPENDIX D

APPENDIX D-3: Stress-strain curve of LD5

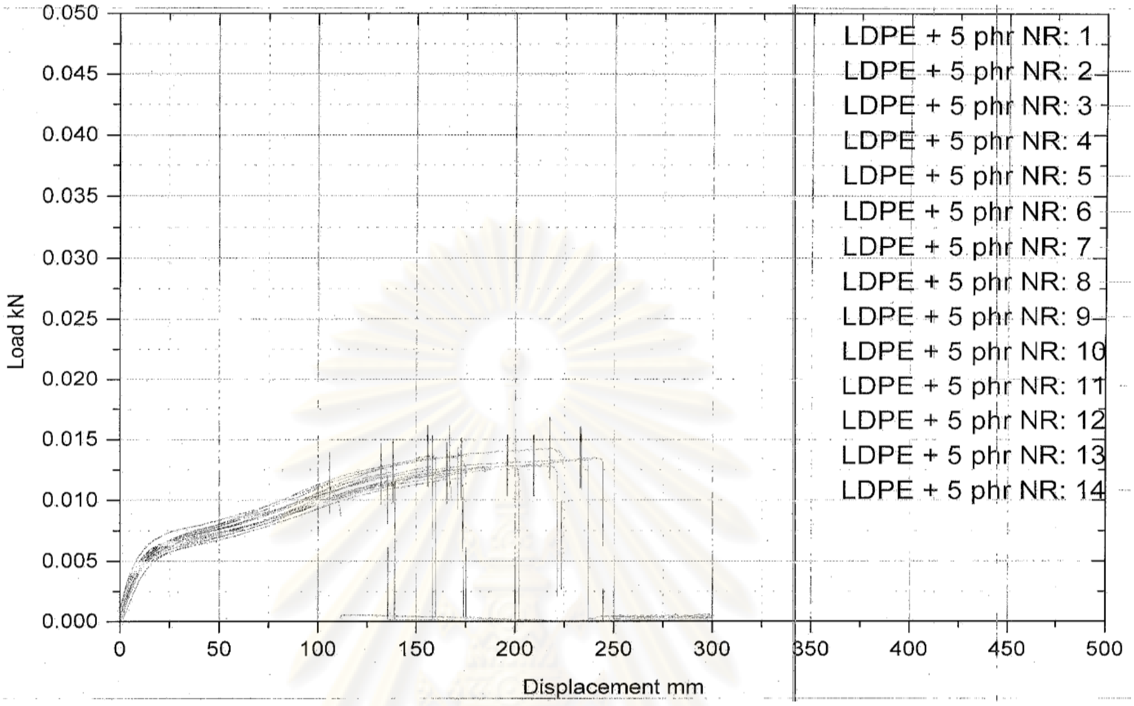

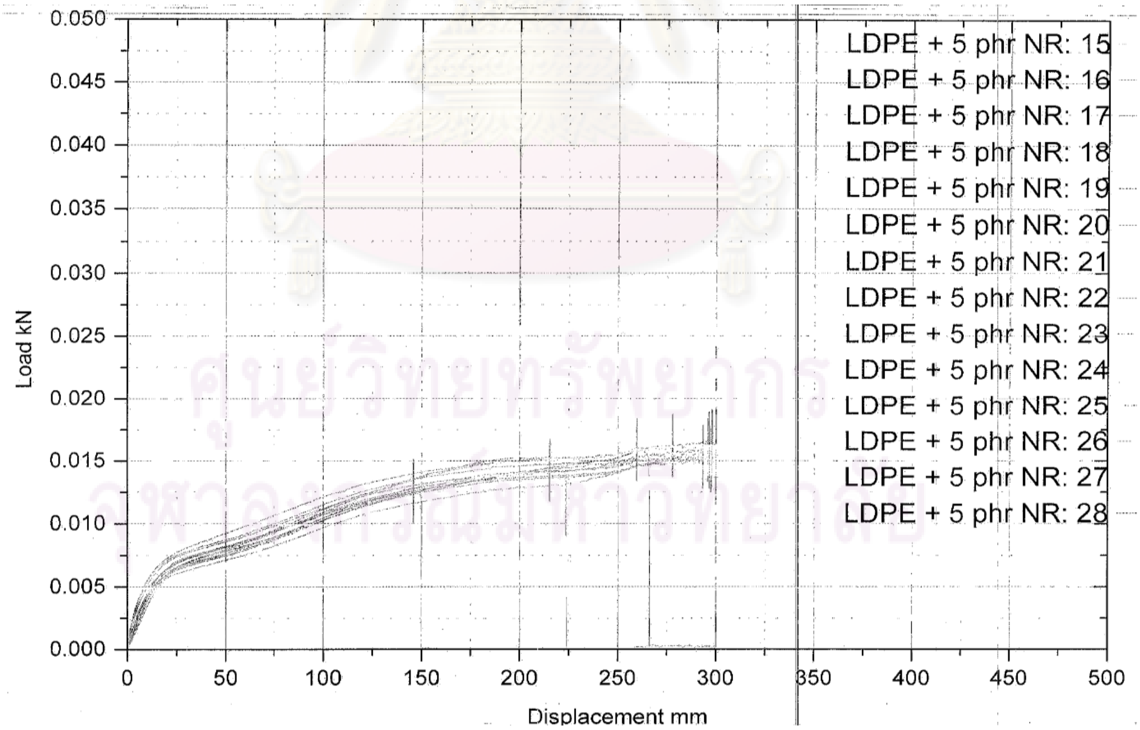

APPENDIX D

APPENDIX D-4: Stress-strain curve of LD7.5

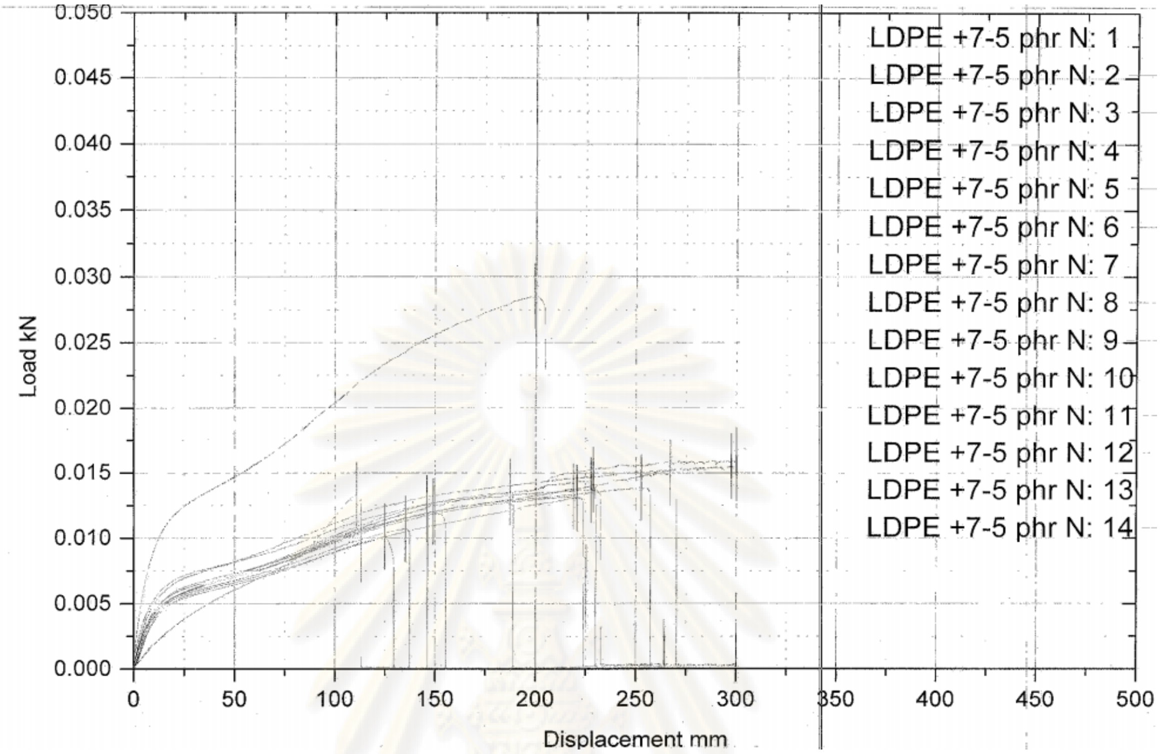

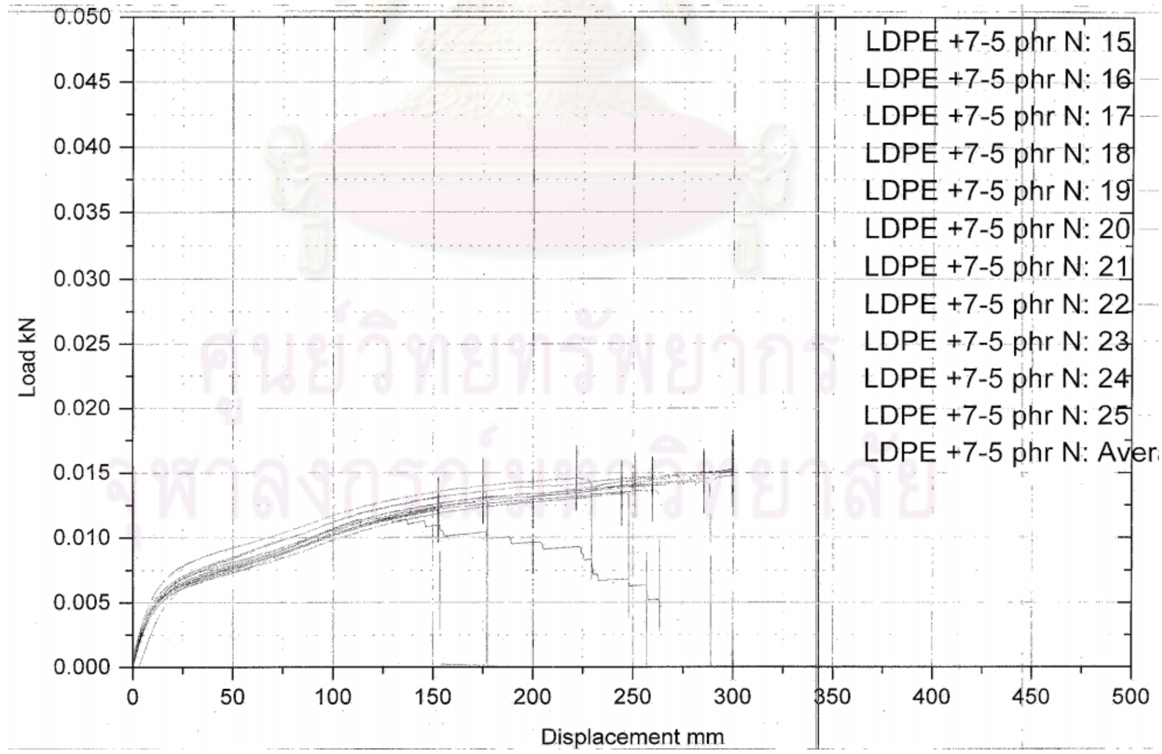

APPENDIX E

APPENDIX E-1: DSC thermogram of LD0

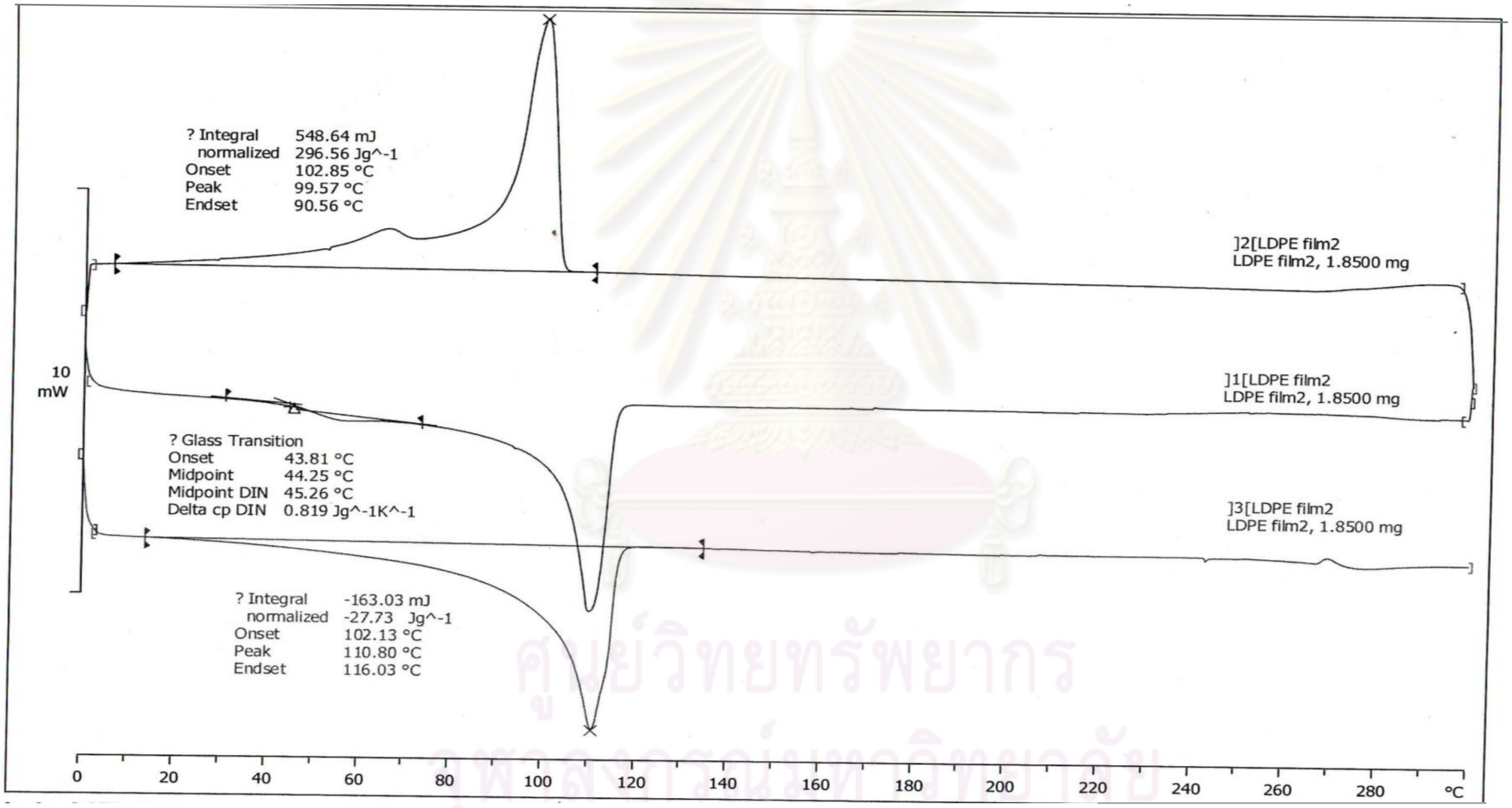

APPENDIX E

APPENDIX E-2: DSC thermogram of LD1

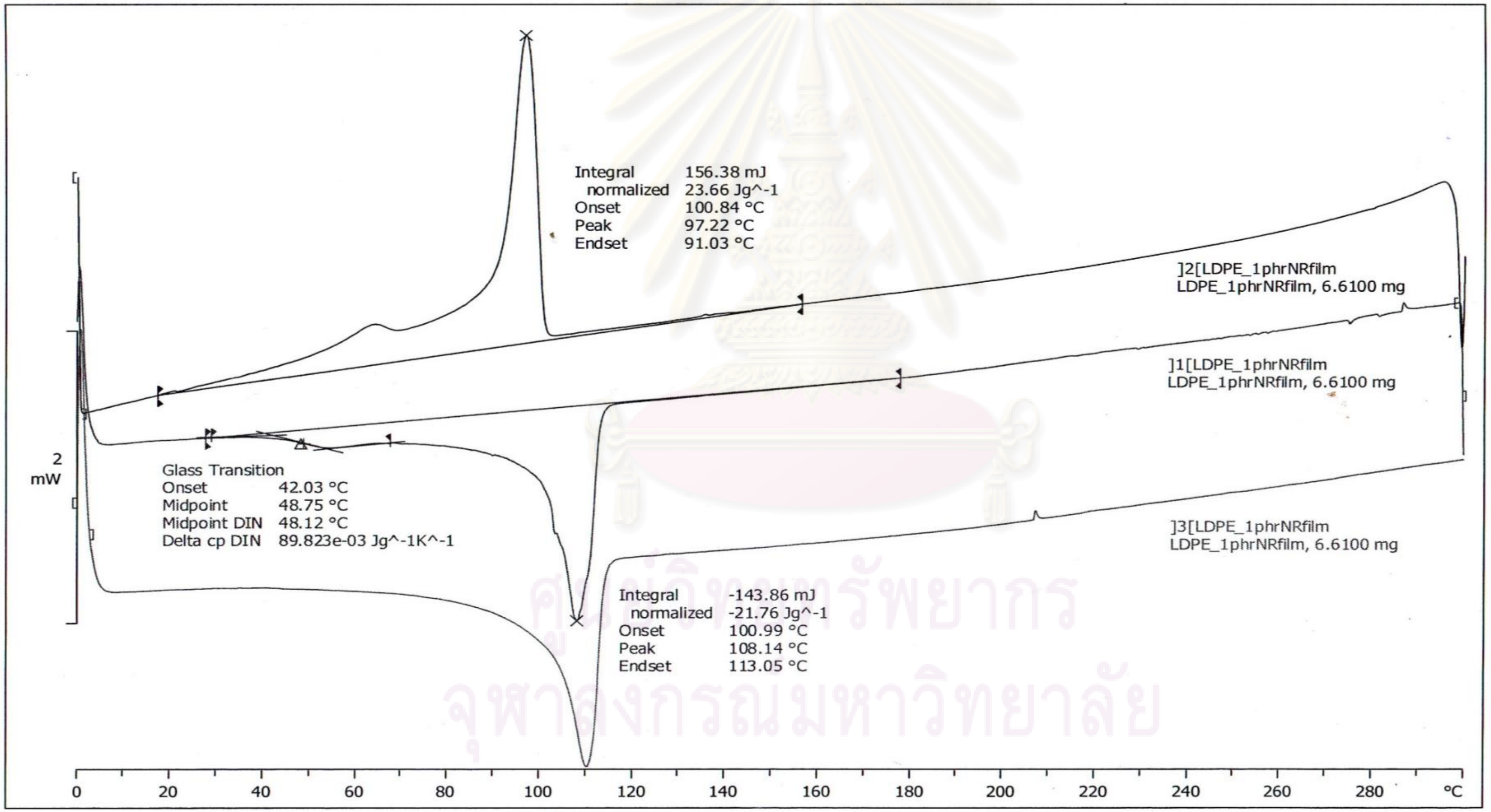

APPENDIX E

APPENDIX E-3: DSC thermogram of LD5

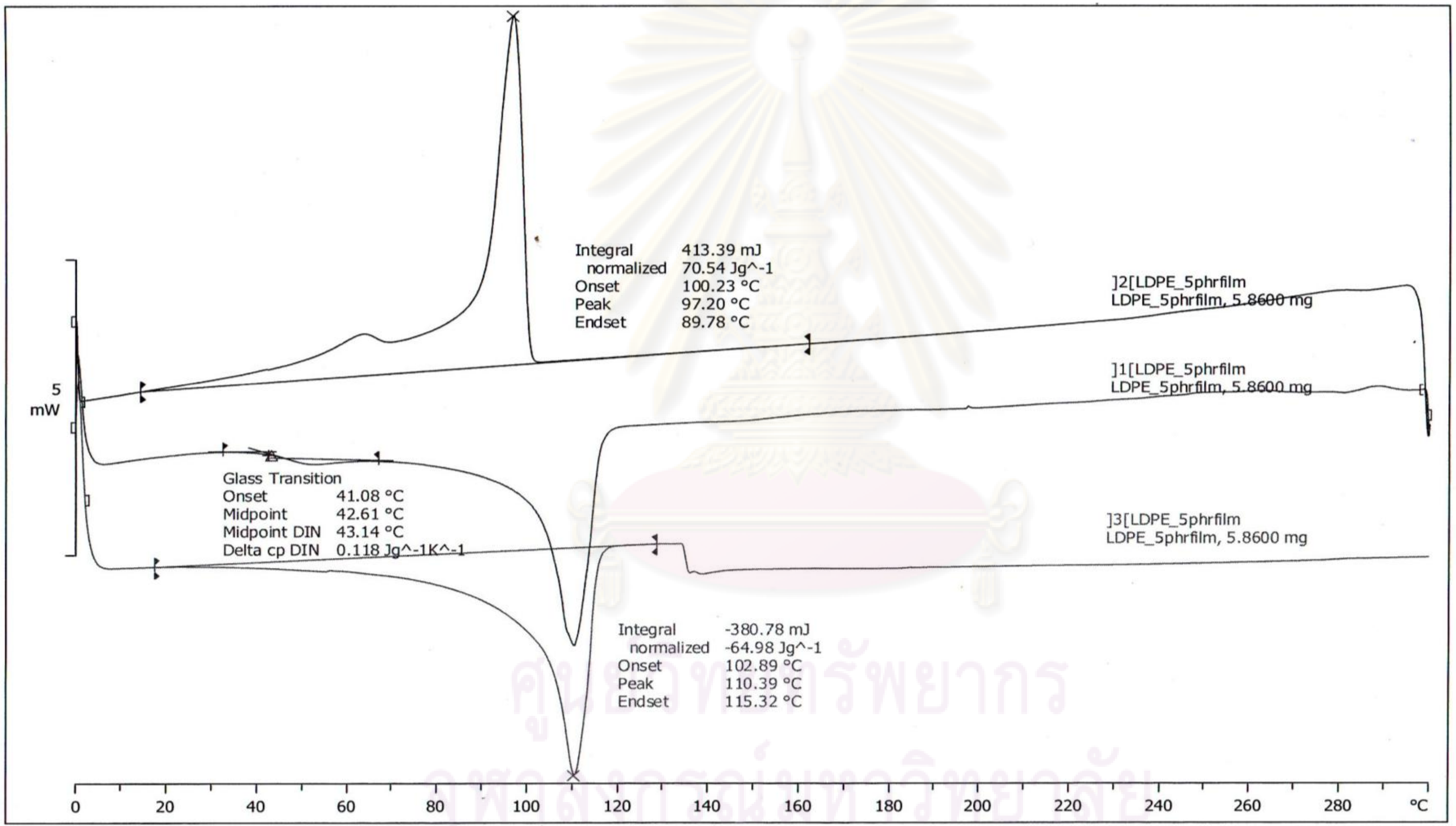

APPENDIX E

APPENDIX E-4: DSC thermogram of LD7.5

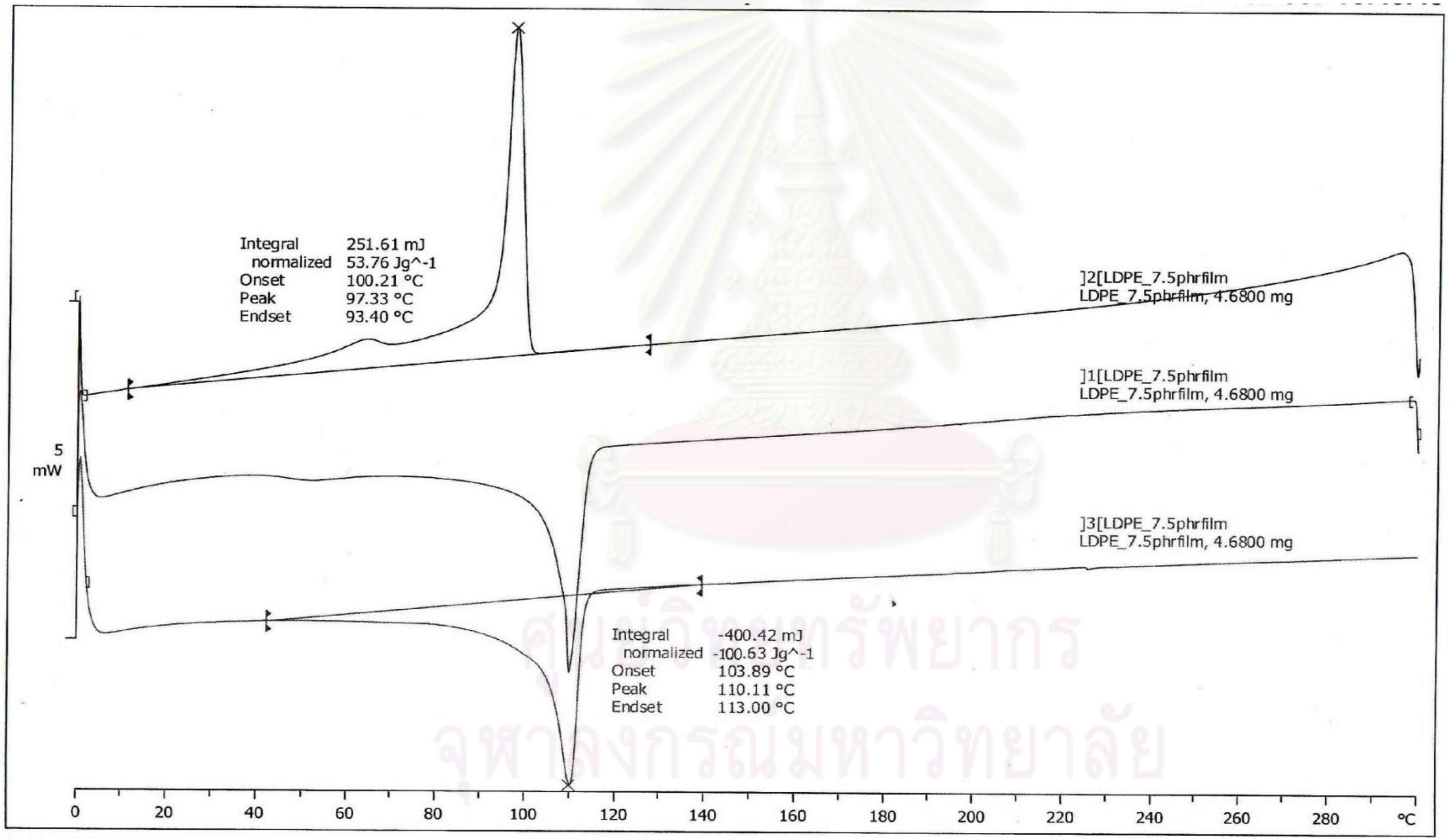

APPENDIX F

Table F-1 Heat shrinkability of the neat LDPE and NR/LDPE films

Sample	% Shrinkage															
	100 °C, 30 min		120 °C, 30 min		150 °C, 1 min		150 °C, 3 min		160 °C, 1 min		160 °C, 3 min		170 °C, 30 sec		180°C, 30 sec	
	MD[1]	TD[2]	MD	TD	MD	TD	MD	TD	MD	TD	MD	TD	MD	TD	MD	TD
LD0	5.28	1.89	63.38	39.22	69.14	41.67	83.33	50.00	81.48	45.12	81.11	50.00	81.25	37.50	81.25	43.75
LD1	5.64	1.82	63.25	38.86	75.00	43.49	87.50	50.50	81.11	50.00	87.50	55.00	85.00	42.22	86.25	47.25
LD5	5.59	2.00	62.69	41.21	83.33	44.44	87.50	52.50	86.67	52.13	87.05	55.06	84.44	44.44	86.67	54.02
LD7.5	6.02	2.16	65.32	41.00	87.50	46.67	88.89	55.56	88.89	55.56	88.89	59.33	85.56	53.33	87.50	58.24

[1] Machine direction, [2] Transverse direction

VITAE

Supak Mahapram was born on June 22, 1981 in Ranong, Thailand. She received a Bachelor's degree of Engineering, majoring in Petrochemicals and Polymeric Material from Silpakorn University in 2004. She has pursued Master's Degree in Petrochemistry and Polymer, Faculty of science, Chulalongkorn University, Bangkok, Thailand since 2007 and finished her study in 2011.

Presentations

1. 26-27 August 2010 Poster Presentation "Shrinkability and Thermal Property of Natural Rubber Latex/Low Density Polyethylene Blown Film" GMSTEC 2010 at the Imperial Queen's Park Hotel, Bangkok, Thailand.
2. 10-11 March 2011 Poster Presentation "Natural Rubber Latex/Low Density Polyethylene Blend for Production of Shrinkable Film" The Science Forum 2011 "Science-Energy of Creativity" at Chulalongkorn University, Bangkok, Thailand.